

BOOK OF ABSTRACTS – IMA12

12th Conference of the Internacional Marangoni Association

Interfacial Fluid Dynamics and Processes

9 - 12 June 2024, Madrid, Spain

ISBN: 979-13-990288-1-2



UNIVERSIDAD
NEBRIJA

BOOK OF ABSTRACTS – IMA12
12th Conference of the Internacional Marangoni Association
Interfacial Fluid Dynamics and Processes

© **Universidad Nebrija**
Madrid, 2025

Editorial direction/coordination:
Carolina Mendoza (Universidad Antonio de Nebrija) y
Santiago Madruga (Universidad Politécnica de Madrid)

ISBN: 979-13-990288-1-2

Welcome to IMA12

The International Marangoni Association coordinates the conferences of the International Marangoni Association (IMA). The objective of IMA12 is to foster the advancement and dissemination of knowledge on interfacial fluid dynamics and processes. IMA encourages scientists, engineers, students, postdoctoral researchers, and university faculty to share and discuss the latest developments in the field.

The 12th Conference of the International Marangoni Association in Madrid (2025) will continue the tradition of previous IMA conferences held in Gießen, Germany (2001); Brussels, Belgium (2004); Gainesville, FL (2006); Tokyo, Japan (2008); Florence, Italy (2010); Haifa, Israel (2012); Vienna, Austria (2014); Bad Honnef, Germany (2016); Guilin, China (2018); Iasi, Romania (2022); and Bordeaux, France (2023).

The Organizing Committee thanks Nebrija University for its support in organizing this International Conference.

Santiago Madruga
Conference Chair of IMA12

Committees

Organizing Committee

- Santiago Madruga (Conference Chair, Universidad Politécnica de Madrid, Spain)
- Carolina Mendoza (Universidad Nebrija, Spain)

Local Organizing Committee

- Carolina Mendoza Organizing (Universidad Nebrija, Spain)
- Santiago Madruga (Conference Chair, Universidad Politécnica de Madrid, Spain)
- Alia Baroudi (Universidad Nebrija, Spain)
- María Jesús Pioz (Universidad Nebrija, Spain)
- Bárbara Frade (Universidad Nebrija, Spain)
- Paula Narros (Universidad Nebrija, Spain)

Student Organizing Committee

- Sara Pineda-Pérez (Universidad Antonio de Nebrija, Spain)
- Daniel Felipe De Castro (Universidad Antonio de Nebrija, Spain)
- Mahmoud Roshdy (Universidad Antonio de Nebrija, Spain)

Advisory Committee

- H. Kuhlmann (Austria)
- R. Narayanan (USA)
- A. Oron (Israel)
- D. Schwabe (Germany)

Scientific Committee

- S. Amiroudine (France)
- E. Benilov (Ireland)
- M. Bestehorn (Germany)
- R. Borcia (Germany)
- K. Eckert (Germany)
- H. Kuhlmann (Austria)
- S. Kumar (USA)
- Q.-S. Liu (China)
- S. Madruga (Spain)
- M. Medale (France)
- A. Mizev (Russia)
- R. Narayanan (USA)
- A. Nepomnyashchy (Israel)
- A. Oron (Israel)
- D. Schwabe (Germany)
- V. Shevtsova (Spain)
- I. Ueno (Japan)

The order of the abstracts included in this collection fits that of the appearance of the corresponding oral talk or poster in the Conference program.

This PDF is fully searchable.

Session 1 – Evaporation and Condensation

Monday June 9, 10:00–11:00

Noncircular Deposition from Sessile Droplet Phase Change on Patterned Substrates

Fei Duan¹

¹*School of Mechanical and Aerospace Engineering, Nanyang Technological University, 50 Nanyang Avenue, 639798, Singapore, Singapore feiduan@ntu.edu.sg*

In the sessile droplet phase change, the abnormal wetting and deposition patterns can be formed. It can broadly be seen in nature and applications in printing, biomedical diagnose, coating, thermal management, etc. However, the mechanism has not fully been understood. Especially, noncircular wetting and drying are interesting phenomena with the more application of textured surface. The previous sessile droplets investigated on the wetting and drying were reported on the micropyramid structured substrates. The water-ethanol binary droplets on the substrate with the micropyramid cavities [1] showed that the droplets formed octagonal initial wetting areas on the substrate. With an increase of ethanol concentration increases, the side ratio of the initial wetting octagon increases. The increasing side ratio indicates that the wetting area transforms from an octagon to a square shape. The droplets demonstrate a pinning-depinning transition during the evaporation. The distinct spontaneous wetting transitions in surfactant solution droplets drying was demonstrated on the micropyramid patterned surface [2]. At low initial surfactant concentrations, the droplet maintains an octagonal shape to the end of drying. At intermediate initial surfactant concentrations, the early octagon first spreads to a square, and then evolves to a stretched rectangle. At high initial surfactant concentrations, the droplet exhibits the octagon-to-square transition, and the square shape is maintained to the end of evaporation. It is suggested that the surfactant deposition accumulates near the contact line could raise the local viscosity and enhance the pinning effect, leading to the great suppression of the “square-to-rectangle” transition. In the present study, we have experimentally investigated the wetting interface shape and evaporative dynamics of particle-laden droplets on the micropyramid substrates by changing the concentrations and sizes of microscale particles, which is found to modify the particle deposition with the octagonal shape. The small particles tend to create octagonal outer rings while the larger particles can produce more evenly distributed depositions. At a high particle concentration, the particles adsorbed at the droplet liquid–air interface form an agglomerate and deposit toward the centerline, leading to the crater-shaped patterns. The simulation with changing the particle concentrations and Marangoni numbers shows the similar trend with the experimental results. At the end, the wetting behaviors of sessile droplets are introduced in the special designed substrates to form the controlled noncircular deposition patterns. [The author thanks the support from MOE Tier 1 - RT16/22].

-
- [1]] H. Feng, K. S.L. Chong, K.S. Ong, and Fei Duan, “Octagon to square wetting area transition of water-ethanol droplets on a micropyramid substrate by increasing ethanol concentration”, *LANGMUIR* **33**, 1147-1154 (2017).
- [2]] X. Zhong, J. Ren, S.L. Chong, K.S. Ong, and Fei Duan, “Wetting transition at a threshold surfactant concentration of evaporating sessile droplets on a patterned surface”, *LANGMUIR*, **35**, 4509-4517 (2019).

Near-critical spreading and evaporation of droplets

Raphael Saiseau^{1,2,3}, Ulysse Delabre² and Jean-Pierre Delville³

¹Univ. Bordeaux, CNRS, LOMA, UMR 5798, Talence, F-33400, France ,
²Department of Physics, University of Konstanz, 78464, Konstanz, Germany,
³raphael.saiseau@uni-konstanz.de

The study of hydrodynamics at increasingly small scales raises fundamental questions about the validity of the classical hydrodynamics hypothesis as the system size approaches the interface thermal fluctuations length scale. More generally, for multi-scales systems, the interplay between macroscopic hydrodynamics and microscopic statistical physics is expected to play a role. For example, phase-field simulations have predicted that viscous dissipation singularities at moving contact lines can be regularised through evaporation-condensation mechanisms.

To explore this question, we use a two-phases liquid system close to a critical point of demixion showing diverging fluctuations of composition. Using the radiation pressure of a laser, a single liquid droplet of one phase is formed into the other and can be moved to coalesce on a substrate. We present an experimental and numerical investigation of this droplet spreading while varying the proximity to the critical point [1]. Surprisingly, the viscous spreading regime is robustly verified even close to the critical temperature but shows a diverging contribution to the viscous stress that is attributed to the vanishing of a prewetting layer thickness. The system also shows thermodynamic instability as the droplet simultaneously shrinks in size, analogous to evaporation. This shrinking behavior is then explored for spherical aerosols droplets and shows curvature but also a new unexpected gravity induced diffusion-limited regimes [2]. By unraveling new mechanisms on the coarsening and wetting of nucleated domains, characterised at the single domain scale, these results are of fundamental importance for phase separation processes.

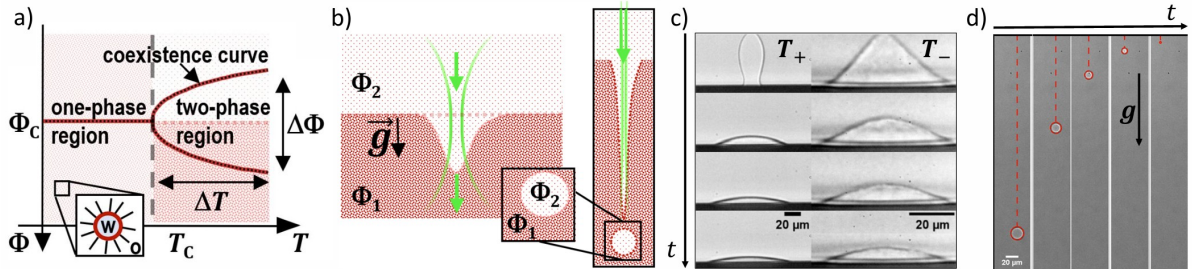


FIG. 1: a) Phase diagram in representation temperature and composition (T, ϕ) of a microemulsion close to a critical point at (T_C, ϕ_C) . The coexistence line fixes the composition difference $\Delta\phi$ for a temperature quench ΔT in the two-phases region. Here ϕ denotes the concentration in water micelles in oil. b) Near-critical demixed liquid phases 1 and 2 at a temperature $T = T_C + \Delta T$ with phase compositions ϕ_1 and $\phi_2 = \phi_1 - \Delta\phi$. The horizontal interface is deformed by the radiation pressure of a focused laser. For large enough power, an optical instability leads to a jet formation forming picoliters droplets. c) Images sequences of droplets of phase 1 surrounding by phase 2 spreading on a glass substrate for two different temperatures T_+ and T_- , with T_- being closer to T_C . d) Images sequence of a droplet of phase 1 decaying in phase 2 while rising towards the flat interface.

-
- [1] Saiseau, R., Pedersen, C., Benjana, A., Carlson, A., Delabre, U., Salez, T., & Delville, J. P., Near-critical spreading of droplets, *Nature Communications*, **13**(1), 7442 (2022).
[2] Saiseau, R., Truong, H., Guérin, T., Delabre, U., & Delville, J. P., Decay dynamics of a single spherical domain in near-critical phase-separated conditions. *Physical Review Letters*, **133**(1), 018201 (2024).

Vapor-mediated wetting and imbibition control on micropatterned surfaces

Ze Xu^{1,2}, Raphael Saiseau^{1,3} and Stefan Karpitschka^{1,4}

¹Department of Physics, University of Konstanz, 78464, Konstanz, Germany, ²ze.xu@uni-konstanz.de, ³raphael.saiseau@uni-konstanz.de, ⁴stefan.karpitschka@uni-konstanz.de

Wetting and evaporation of droplets on micropatterned surfaces is ubiquitous in nature and key to many technological applications, such as water/ice-proof coatings, spray cooling, inkjet printing, and semiconductor surface processing. Significant effort has been devoted to overcoming the intrinsic, chemistry- and topography-governed wetting behaviors of such surfaces, but most strategies require specific materials and/or patterns, thus limiting their practical use.

Here, we show that the spreading and wicking of water droplets on hydrophilic surface patterns can be controlled and even temporarily inhibited by the presence of the vapor of a low surface tension liquid (Fig. 1(a)(b)). We show that this delayed wicking arises from Marangoni forces due to vapor condensation at the droplet periphery, competing with the capillary wicking forces of the surface topography (Fig. 1(c)). Thereby, macroscopic droplets can be brought into an effective apparent wetting behavior that is independent of the surface topography, but coexists with a wicking film, playing the role of a wetting precursor, but on mesoscopic scales. Since the phenomenon emerges from physical effects like surface tension and fluid flow, it can be generalized to various material systems and surface patterns. We further demonstrate how modulating the vapor concentration in space and time can be used to guide droplets across patterns (Fig. 1(d)(e)) or even extract liquid from fully imbibed films, devising new strategies for coating, cleaning and drying of functional surface designs.

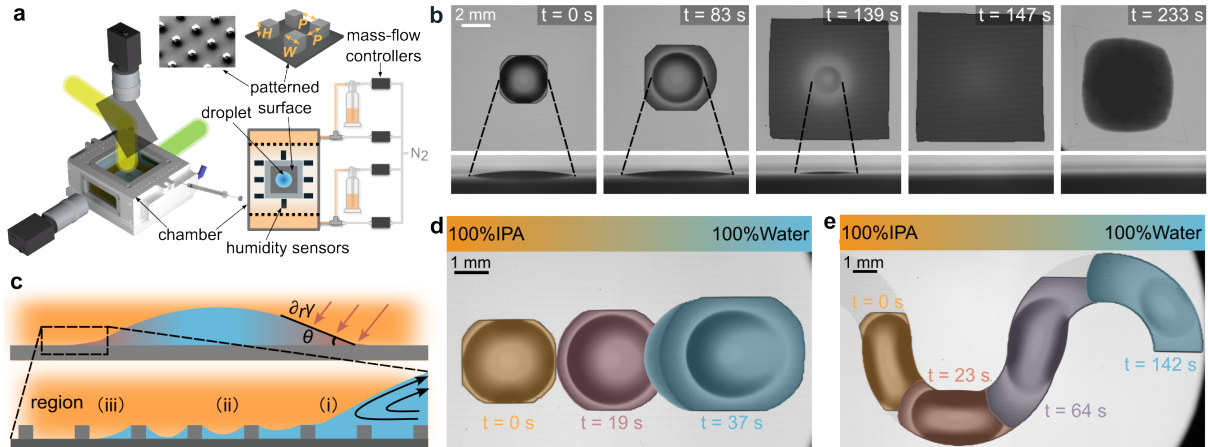


FIG. 1: **a**, Schematic of the experimental setup and SEM image of a micropillar decorated silicon wafer. **b**, Wicking of water into hydrophilic textures (images from top and side aspects) is delayed more than 100-fold in an isopropyl alcohol (IPA) vapor atmosphere. A Marangoni-contracted droplet, agnostic of the surface pattern, coexists on top of a wicking film. Only after ~ 80 s, the film expands gradually at the expense of the droplet, finally evaporating from the imbibed state after ~ 150 s. **c**, Schematic of the liquid conformation: a macroscopic droplet connected to a film that thins but remains pinned to the pillar caps. **d**, Droplet motion on a homogeneous square lattice with IPA vapor gradient. **e**, Droplet forced along a square pillar lattice within "S"-shaped bounds by a vapor gradient in x -direction.

Effect of Substrate Topography on Evaporating Film

Senthil Kumar Parimalanathan^{1,3}, Alexey Rednikov¹, Adam Chafai¹, Robin Maximilian Behle²,
Tatiana Gambaryan-Roisman^{2,4} and Pierre Colinet¹

¹TIPs Laboratory, Université libre de Bruxelles, Avenue F.D. Roosevelt 50, Brussels 1050, Belgium

³senthil.parimalanathan@ulb.be

²Institute for Technical Thermodynamics, Technical University of Darmstadt, Peter-Grünberg-Strasse 10,
Darmstadt, Germany ⁴gtatiana@ttd.tu-darmstadt.de

I. INTRODUCTION

Thin film evaporation plays a crucial role in industrial applications such as film coating, electronic cooling, and food processing. Temperature gradients in evaporating films can induce long-wave thermocapillary instabilities, leading to spontaneous rupture and dry-out [1], which can cause overheating and system failures. This issue is particularly important in microgravity, especially for capillary-driven thermal management systems, such as heat pipes and propellant storage devices. ESA has initiated research on thin film evaporation in microgravity to address these challenges. As part of the *Marangoni in Film* space project, we are investigating these instabilities on-ground conditions to enable meaningful comparisons with future space-based experiments. Here, we focus on controlling thermocapillary instabilities by modifying the substrate topography.

II. EXPERIMENTS AND DISCUSSION

Experiments were conducted using a small rectangular cell ($25 \times 25 \times 27 \text{ mm}^3$) with a $18 \times 18 \text{ mm}^2$ wide, and 0.5 mm deep square cavity at its base, similar to our recent work [2]. The cell comprises two aluminum walls and two plexiglass windows that enable laser interferometry observations. A vapor duct mounted above the cell directed evaporating vapor away from the windows, and the setup was placed on a high-precision scale to monitor mass loss. Vapor cloud was analyzed using laser interferometry, while an infrared camera captured thermocapillary-induced instabilities from above (see Fig. 1). Hydrofluoroether (HFE) 7100 served as the working fluid. This study investigates how substrate topography (plain and wavy) influences long-wave instabilities in the liquid, with potential supporting simulation results for comparison.

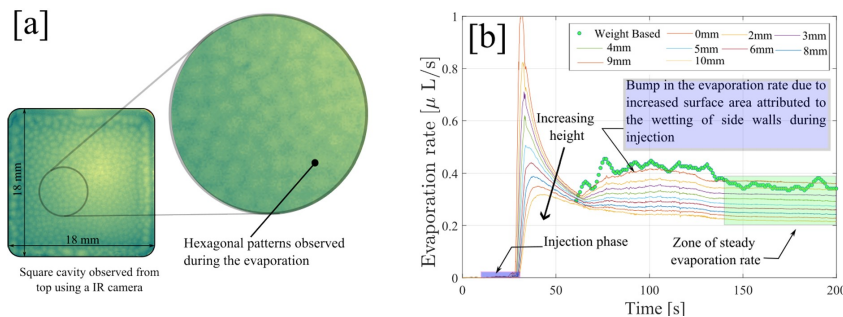


FIG. 1: [a] Thermocapillary instabilities on a plain substrate captured using an infrared (IR) camera. Hexagonal patterns are observed at $t = 2 \text{ s}$ after injection [b] Comparison of evaporation rates obtained from mass loss measurements and optical interferometry. The solid lines represent evaporation rates measured at different heights from the liquid interface (0 mm). A good agreement is observed between interferometric measurements and mass loss data.

III. ACKNOWLEDGEMENTS

The ULBteam acknowledges funding from BELSPO and ESA, while the TUD team is supported by DLR(grant no. 50WM2353). P.C. thanks FNRS for supporting his Research Director position.

- [1] Davis, S. H., Thermocapillary instabilities, *Annual Review of Fluid Mechanics*, 403-435 (1987).
- [2] Parimalanathan et al., Ground tests for a future space experiment: Evaporation rates through a centimetric square chimney by vapor interferometry and simulation. *Physics of Fluids*, **36**(11) (2024)

Session 2 – Phase field and multiphase systems

Monday June 9, 11:30–12:45

Compressible phase field model for investigating bubble rise near the liquid- vapor critical point

Deewakar Sharma¹, Arnaud Erriguible² and Sakir Amiroudine¹

¹*Université de Bordeaux, I2M, UMR CNRS 5295, Talence F-33400, France*

²*Bordeaux INP, ICMCB, UMR 5026, F-33600 Pessac, France.*

Recent technological advancements addressing some of the key global challenges such as, efficient energy processes for climate change, search for alternate fuels etc., have pushed the operating conditions in processes to high pressure and/or temperature conditions. The fluid in these systems is thus subjected to thermodynamic conditions which are close and sometimes, even cross the liquid-vapor critical point (termed as the critical point henceforth). The peculiarity of the critical point lies in the behavior of various thermophysical properties showing singularity at the critical point [1]. One such unusual behavior is the high isothermal compressibility of the liquid phase which becomes comparable to that of vapor phase when approaching the critical point. For understanding complex fluid dynamics near the liquid vapor critical point, the first step lies in understanding the two-phase flow with both phases being highly compressible yet being in subsonic regime and in isothermal conditions. This necessitates developing an appropriate model which can account for compressibility of both the phases. In this work, we address this gap in the literature by proposing a two-phase model based on phase-field modeling. The literature is abundant with studies using phase-field method for incompressible fluids while for compressible fluids, several studies have used diffuse interface method (similar to phase-field method but using density as a parameter to distinguish between the two phases). The model proposed in this work is based on using a scalar phase field parameter ϕ denoting mass fraction of phase 2 to distinguish between the two phases, the advantage being able to define interface thickness which is computationally realistic. Some previous works have demonstrated these models, primarily from mathematical aspects, and no attempt has been proposed to make practical demonstration of the physical test cases [2]. Further, as the proposed model can incorporate compressibility of both the phases independently, the model can also be used for a wide range of two-phase systems of varying compressibility, i.e. incompressible-incompressible, compressible-incompressible etc. We validate the model using various canonical cases –rise of lighter fluid bubble in a heavier fluid for density ratio of 10 and 1000 and present a comparison with the experimental studies for the rise of oxygen bubbles in the liquid oxygen at the thermodynamic conditions where the compressibility of both the phases cannot be neglected.

I. GOVERNING EQUATIONS

The phase field model considered in the present work uses mass fraction as the order parameter (ϕ) as described in [2] in conjunction with the compressible model as described in [3, 4]. The governing momentum equation for compressible fluid in terms of the scalar variable (ϕ) can be written as [2],

$$\frac{d\mathbf{V}}{dt} = -\nabla P + \nabla(\rho\bar{\alpha}|\phi|^2 - \rho\bar{\alpha}(\nabla\phi \otimes \nabla\phi)) + \nabla \cdot (\mu\nabla\mathbf{V}) + \nabla((\lambda + \mu)\nabla \cdot \mathbf{V}) \quad (1)$$

Here, the variables $\bar{\beta}$ and $\bar{\alpha}$ appear in the total free energy of the system given by, $\rho\bar{\beta}f_0(\phi) + \rho\frac{\bar{\alpha}}{2}|\nabla\phi|^2$ and are related to the surface tension and the interface thickness. Further, $f_0(\phi) = \phi^2(1 - \phi)^2$ defines the classical double-well potential form of the bulk free energy. For a compressible isothermal system, the equation of state defining the relation between pressure, order parameter, and density and can be described by $P = P(\rho, \phi)$. We can therefore write for small variations in P with ϕ and ρ with time as,

$$\frac{dP}{dt} = -\frac{1}{\chi_T}\nabla \cdot \mathbf{V} + \left(\frac{\partial P}{\partial \phi}\right)_{T,P} \frac{d\phi}{dt} \quad (2)$$

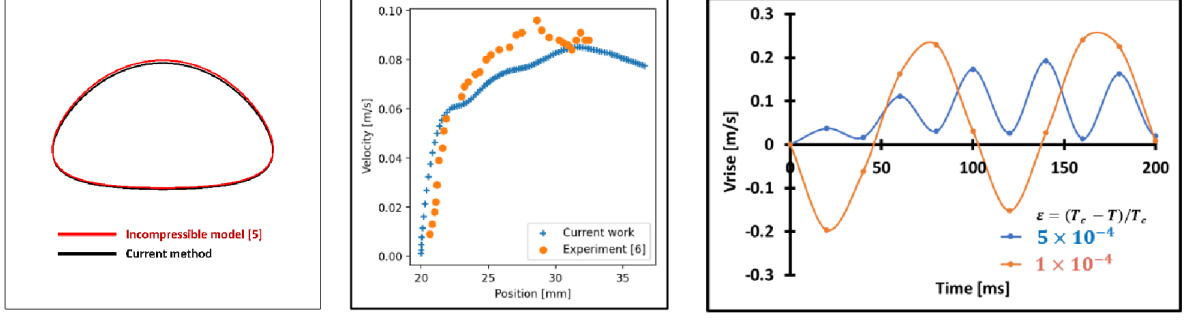


FIG. 1: Test cases comparing the bubble rise dynamics for: (from left to right)- density ratio 10 at $t = 3s$ | Comparison with experimental work for rise of oxygen bubble in liquid oxygen at 90.1K where compressibility of liquid phase is ~ 10 times that of water | Bubble rise velocity for two different proximities to the critical point.

Here, χ_T is the isothermal compressibility. Further, from thermodynamics, we know $P = \rho^2 \left(\frac{\partial f_b}{\partial \rho} \right)$ where $f_b = \rho \bar{\beta} f_0$ denoting the total free bulk energy. By integration of Eq. (2) over a small timestep, we get $P = P^0 - \nabla \cdot \mathbf{V} \delta t \frac{1}{\chi_T} + Y \delta t$, with $Y = \rho \bar{\beta} f'_0 \nabla \cdot (M \nabla \eta)$, $\eta = \frac{\delta F_V}{\delta \phi}$ denoting the chemical potential, and P^0 being the reference pressure. Substituting this expression of pressure in Eq. (1) we get,

$$\rho \frac{d\mathbf{V}}{dt} = -\nabla \left(P^0 - \nabla \cdot \mathbf{V} \frac{\delta t}{\chi_T} + Y \delta t \right) + \nabla (\rho \bar{\alpha} |\phi|^2 - \rho \bar{\alpha} (\nabla \phi \otimes \nabla \phi)) \quad (3)$$

$$+ \nabla \cdot \left(\mu \left(\nabla \mathbf{V} + \nabla^t \mathbf{V} - \frac{2}{3} \nabla \cdot \mathbf{V} \underline{\underline{\mathbf{I}}} \right) \right)$$

This momentum equation is solved with continuity equation to obtain density field while pressure is calculated using the expression presented above. The phase-field variable (ϕ) is evaluated from Cahn-Hilliard equation in order to complete the model and can be written as,

$$\frac{\partial \phi}{\partial t} + \mathbf{V} \cdot \nabla \phi = \frac{1}{\rho} \nabla \cdot (M \nabla \eta) \quad (4)$$

The mobility parameter M is evaluated based on adaptive thickness approach as described in [5].

II. RESULTS

The model has been tested for several test cases as mentioned previously. Here, we present results for the rise of a lighter incompressible fluid in heavier medium with density ratio 10 and experimental comparison where a bubble of oxygen rises in liquid oxygen [6]. In the former case, to account for incompressibility of both the phases, their compressibility was set to be very small value ($\chi_T = 10^{-14} Pa^{-1}$) rendering their behavior to be incompressible to the numerical precision. Figure. 1 compares the results obtained with the current model with those obtained from fully incompressible model [5]. Comparison for the rise of an oxygen bubble in the liquid oxygen at 90.1 K and pressure of 1 bar with gravity being 0.4g as described [6] shows also a good agreement with experimental data. Finally, we present a test case of the rise of a vapor bubble for two different proximities to the critical point and an unusual oscillating behavior while rising is observed. At this stage, we attribute this behavior to the stratified density profile in a liquid due to its high compressibility.

III. CONCLUSIONS

The presented work highlights a new model which permits to account for fluid compressibility of each phase separately and thus has been used to study bubble rise near the liquid-vapor critical point. An

interesting behaviour in bubble rise is observed where the bubble oscillates and is ascribed to dominance of stratification of density in liquid phase over the bubble rise. A further investigation of bubble rise in a stratified compressible near-critical liquid will be undertaken.

- [1] B. Zappoli, D. Beysens, Y. Garrabos, *Heat Transfers and Related Effects in Supercritical Fluids*, 1st ed., Springer Netherlands, 2014. <https://doi.org/10.1007/978-94-017-9187-8>.
- [2] Z. Guo, P. Lin, A thermodynamically consistent phase-field model for two-phase flows with thermocapillary effects, *J. Fluid Mech.* **766** (2015) 226–271. <https://doi.org/10.1017/jfm.2014.696>.
- [3] S. Amiroudine, J.P. Caltagirone, A. Erriguible, A Lagrangian–Eulerian compressible model for the trans-critical path of near-critical fluids, *Int. J. Multiph. Flow* **59** (2AD) 15–23. <https://doi.org/10.1016/j.ijmultiphaseflow.2013.10.008>.
- [4] D. Sharma, A. Erriguible, S. Amiroudine, Numerical modeling of the impact pressure in a compressible liquid medium: application to the slap phase of the locomotion of a basilisk lizard, *Theor. Comput. Fluid Dyn.* **31** (2017) 281–293. <https://doi.org/10.1007/s00162-017-0422-4>.
- [5] D. Sharma, M. Coquerelle, A. Erriguible, S. Amiroudine, Adaptive interface thickness based mobility—Phase-field method for incompressible fluids, *Int. J. Multiph. Flow* **142** (2021) 103687. <https://doi.org/10.1016/j.ijmultiphaseflow.2021.103687>.

Using a hybrid porous materials of a new generation in water purification process

Dominika Zabiega^{1,2,4}, Daniela Placha², Marcos Levi Cazaes³ and Fabio Dias de Sousa³

¹*Department of Mechanical and Construction Engineering, Faculty of Environment and Engineering, Northumbria University, NE1 8ST Newcastle upon Tyne, United Kingdom*

⁴*dominika.zabiegaj@northumbria.ac.uk*

²*CEET, VSB-Technical University of Ostrava, Nanotechnology Centre, Ostrava, Czech Republic*

³*Department of Industrial Chemistry, UFBA - Federal University of Bahia, Salvador de Bahia, Brazil*

Vermiculite (VMT) is known to have excellent antibacterial and sorption properties (removal of anti-inflammatory drugs, dyes, heavy metals, bio-recalcitrant compounds, nitrogen, and phosphate compounds). Organically modified vermiculites are also well-known nanostructured adsorbents of organic compounds from water or gaseous phases, similar to organically modified smectites or bentonites. The Activated Carbon (AC) famous for extraordinary antiseptic properties and very high specific surface area, therefore, by merging the properties of AC and VMT in the foam form, we can achieve a new generation of materials that have high multielement sorption capacities and antibacterial properties, capturing contaminants and preventing the bacteria colony formation in water storages/systems for a long time. Additionally, having a very high specific area and specifically tailored opened structure, allows fast penetration and treatment of a contaminated water through the large and highly selective area derived from porous structure of a foam itself and additional porosity given by mixed AC and VMT.

The presented work highlights the advancements in the sustainable materials that can be hired as filters/adsorbents actively capturing i.e. Uranium and other heavy metals, other pollutants providing antiseptic capacities of the filters with a wide industrial application such as hydrogen production, long term space missions, CO₂ capturing and waste management.



FIG. 1: Freestanding porous monoliths based on: VMT (a), AC (b), VMT-AC (c), AC-VMT (d)

-
- [1] D. Zabiegaj, D. Giuranno, M. T. Buscaglia, L. Liggieri, F. Ravera, Activated carbon monoliths from particle stabilized foams, *Microporous and Mesoporous Materials* **239** (2017), 45-53

Faraday Instability of an Isothermal Binary Mixture Described by a Phase Field

Michael Bestehorn^{1,3}, Rodica Borcia¹, Deewakar Sharma² and Sakir Amiroudine²

¹*Institut für Physik, BTU, 03044, Cottbus, Germany, ³bestehorn@b-tu.de*

²*I2M UMR Centre National de la Recherche Scientifique 5295, Université Bordeaux, Talence, F-33400 ,*

We study a binary fluid mixture using a phase field description. We consider a fluid pair that is immiscible for temperatures below a critical one (consolute temperature, T_c) and miscible above T_c . We derive an extended phase field equation that allows to move from the immiscible state (governed by a Cahn-Hilliard equation) to the miscible state (ruled by a species diffusion equation), where a uniform temperature serves as control parameter.

The whole system is mechanically excited showing Faraday instability of a flat interface. A linear stability analysis is performed for the stable case (interface waves) as well as for the unstable Faraday one. For the latter, a Floquet analysis shows the well-known Arnold's tongues as a function of the consolute temperature and the depth of the layer. Moreover, 2D finite difference simulations are performed allowing to model nonlinear flow patterns both in miscible and immiscible phases, see the figure below. Linear theory and non-linear simulations show interesting results such as the diminishing of wavelength of Faraday waves or a shift of the critical vibration amplitude when the consolute temperature is approached [1].

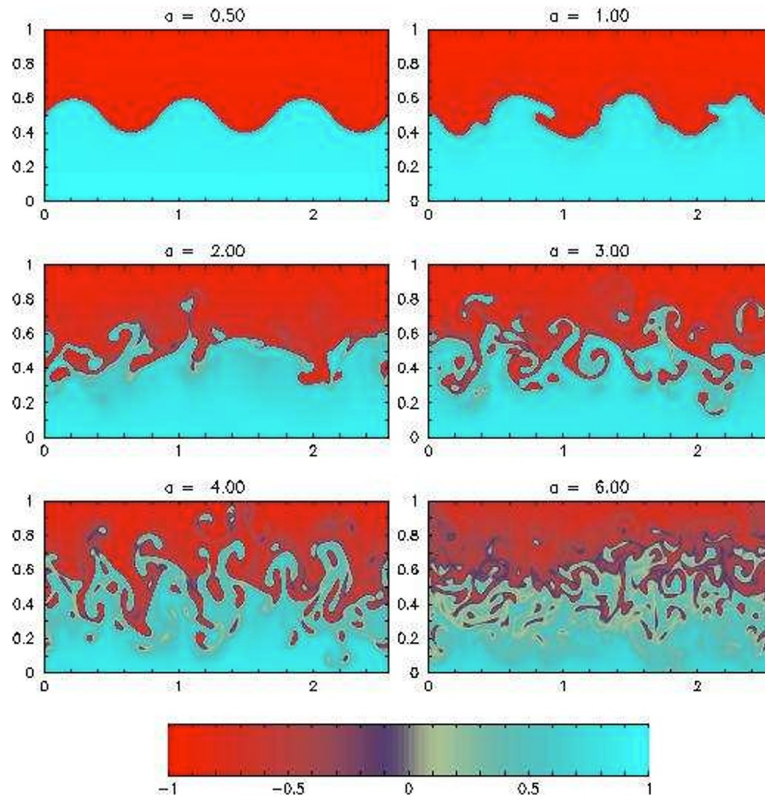


FIG. 1: Faraday instability of an immiscible fluid pair below T_c , from [1]

- [1] M. Bestehorn, D. Sharma, R. Borcia and S. Amiroudine, Faraday instability of binary miscible/immiscible fluids with phase field approach, *Phys. Rev. Fluids* **6**, 064002 (2021).

Electrolubrication and giant slip in flowing liquid mixtures

Roni Kroll¹ and Yoav Tsori²

^{1,2}Department of Chemical Physics, 84105 Beer Sheva, Israel, ¹krollr@post.bgu.ac.il,
²tsori@bgu.ac.il

We describe theoretically the “electrolubrication” occurring in liquid mixtures flowing in charged pores. For a mixture of two liquids, field-induced phase separation occurs near the solid surface. The electrostatic adsorption of a low viscosity liquid at the surfaces manifests as a giant effective slip length. These lubrication layers facilitate larger strain at a given stress. They reduce the total viscous drag in the pore, enhancing markedly the total flux. The thickness of the lubrication layers depends on the Debye length and the mixture correlation length. The effect is strong if the viscosities of the liquids are sufficiently different, the volume fraction of the less viscous liquid is small, the gap between the surfaces is small, and the applied potential is large. The maximum liquid velocity and flux are increased by a factor α . In most liquids, $\alpha \sim 1-10$, and in mixtures of water and glycerol $\alpha \sim 80-100$ under relatively small potentials.

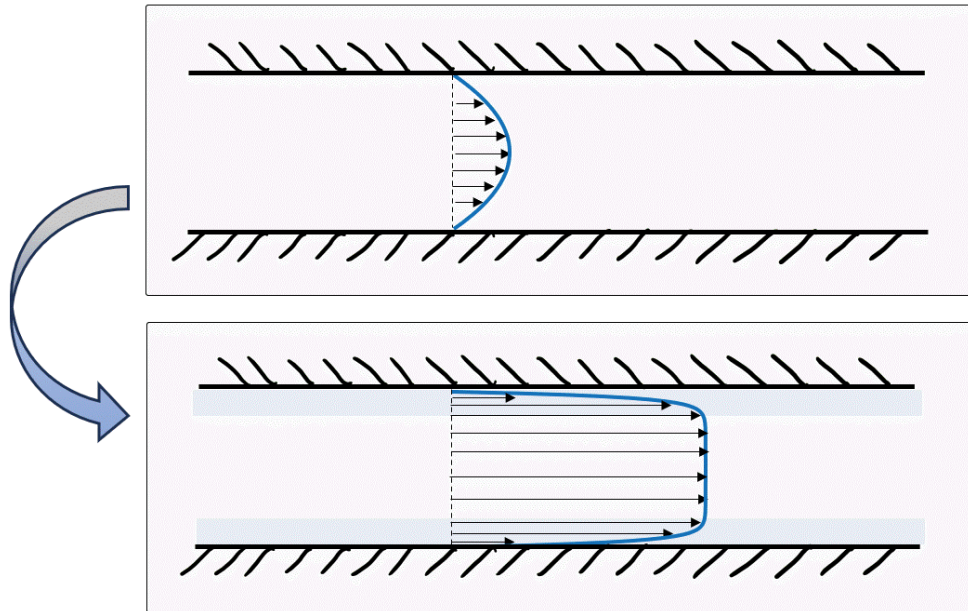


FIG. 1: Top: Flow of a homogeneous mixture between two solid walls driven by a pressure gradient. The flow profile is the classic Poiseuille (parabolic) one. Arrows indicate the liquid velocity. Right: The velocity profile when the surfaces are charged (e.g., when connected to an external potential). The mixtures demixes locally; faint blue color indicates the more polar liquid component. When the adsorbed liquid is the less viscous one, as in the case of water and glycerol, these lubrication layers change the flow profile drastically, and the flux is greatly increased compared to the no-field case (top). The apparent slip-length can be very large.

-
- [1] R. Kroll and Yoav Tsori, Electrolubrication of liquid mixtures between two parallel plates, *J. Fluid Mech.* **982**:A27 (2024).
[2] Y. Tsori, Electrolubrication in flowing liquid mixtures, *Phys. Fluids* **33**,073306 (2023).

Kinetic Theory of Coupled Binary-Fluid Surfactant System

Alexandra J. Hardy¹, Steven McDonald¹, Samuel Cameron^{1,2}, Abdallah Daddi-Moussa-Ider¹ and Elsen Tjhung¹

¹*School of Mathematics and Statistics, The Open University, Walton Hall, Kents Hill, Milton Keynes, MK7 6AA, United Kingdom* ²sam.cameron@open.ac.uk

We derive the hydrodynamic equations of coupled binary fluid and surfactant systems from microscopic forces and torques. At the microscopic level, the surfactant molecules are modeled as dumbbells, which can exert forces and torques on the fluid and the interface. By explicitly considering the molecular alignment, we then derive coarse-grained hydrodynamic variables, such as fluid density, fluid velocity, surfactant concentration, and surfactant polarization. The latter represents the average orientation of surfactants, which is crucial in preventing surfactant-laded droplets from coalescing with each other. Finally, we also derive the effective interfacial tension as a function of surfactant concentration.

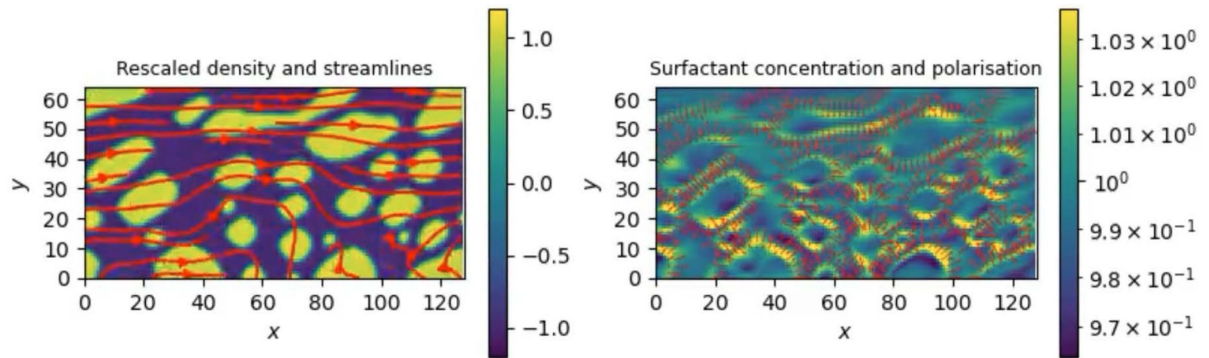


FIG. 1: Left panel shows the relative density of the binary fluid. Yellow represents fluid phase A (e.g. oil) and blue represents fluid phase B (e.g. water). Right panel shows the surfactant concentration (yellow) and polarization (red arrows). We may observe the surfactant molecules are concentrated mostly at the interfaces.

[1] A.J. Hardy, A. Daddi-Moussa-Ider and E. Tjhung, Hybrid particle-phase field model and renormalized surface tension in dilute suspensions of nanoparticles, *Phys. Rev. E* **110**, 044606 (2024)

Session 3 – Surfactants and particle suspensions I

Monday June 9, 14:15–15:45

Transition to the Stagnant Cap Regime in the System of a Solid Particle and a Bubble Covered by Insoluble Surfactant

Tatyana Lyubimova ¹, and Alexander Nepomnyashchy ²

¹*Institute of Continuous Media Mechanics UB RAS, 614013, Perm, Russia* lyubimova@icmm.ru

²*Technion - Israel Institute of Technology, 3200003, Haifa, Israel* nepom@technion.ac.il

Due to the low diffusion coefficient of the surfactant, the distribution of the surfactant adsorbed on the surface of a moving bubble is often highly non-uniform. The action of a sufficiently strong flow can create two zones: (i) a zone almost free of the surfactant in the front part of the bubble and (ii) a stagnant "cap" in the rear part of the bubble where the surfactant is concentrated. In the case of a weak flow, the distribution of the surfactant on the bubble surface is smooth and determined by the balance of the viscous stress tending to move the surfactant and the Marangoni stress tending to restore the uniform distribution of the surfactant. The transition between two regimes takes place at a certain critical velocity of the bubble.

In the present talk, we consider the system of a bubble covered by an insoluble surfactant and a solid particle rising along the same axis within a viscous liquid. This problem, which appears in the context of flotation, is studied in the framework of the Stokes equation under the assumption of a linear dependence between the surface tension and the surface concentration of the surfactant. Exact solutions for the flow and the distribution of the surfactant on the bubble surface are obtained.

The dependence of the critical velocity corresponding to the transition to the stagnant cap regime has been calculated. The generalizations of the problem are discussed.

I. ACKNOWLEDGEMENTS

The study was supported by Russian Science Foundation (Grant No. 24-11-00269).

Super diffusivity resolves anomalies in monolayer dilatation

Juan M. Lopez^{1,3}, Tyler J. Mucci², Jason Yalim,¹ Joe A. Adam² and Amir H. Hirs²

¹*School of Mathematical & Statistical Sci., Arizona State Univ., AZ 85281, Tempe, United States of America*

³*jmlopez@asu.edu*

²*Department of Mechanical, Aerospace and Nuclear Engineering, Rensselaer Polytechnic Inst., NY 12180, Troy, USA*

Hydrodynamics of surfactant monolayers are governed by surface tension, surface shear viscosity, surface dilatational viscosity and surface diffusivity. While the first two have been studied comprehensively with consistent results, surface dilatational viscosity is plagued with anomalies, including apparent negative values. Here, full-field interfacial velocity measurements together with simulations of the Navier-Stokes equations reveal that a source of these anomalies is the use of equilibrium surface diffusivity for systems far from equilibrium. Our results provide, perhaps for the first time, a consistent realization of the Boussinesq–Scriven surface model applied to a monolayer of DPPC under periodic compression and expansion that results in monolayer concentration gradients. The parameter regime considered (scale of the channel, along with the frequency Ω and amplitude Re of the floor oscillation) was sufficient to establish that the Boussinesq number Bq (non-dimensional sum of the surface viscosities) is indeed positive when surface diffusivity is taken to be much larger than the generally used equilibrium value (as shown in figure 1). Using the equilibrium surface diffusivity within the Boussinesq–Scriven surface model results in negative Bq being needed to obtain surface velocities of the same magnitude as in experiments. A possible explanation is that the co-existing liquid expanded and liquid condensed domains of the DPPC monolayer phase act as pockets of condensed matter resulting in the larger non-equilibrium surface diffusivity. This resolves a long-standing issue where the surface viscosity was misinterpreted to be negative.

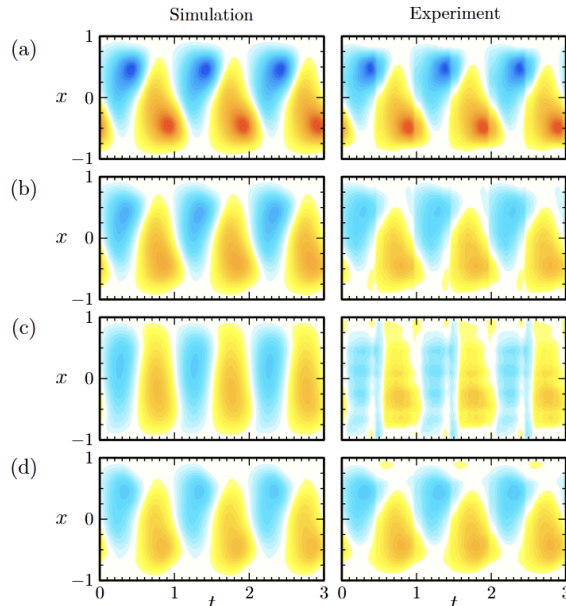


FIG. 1: Space-time plots of the interfacial velocity u^s from simulations and experiments at initial monolayer concentration $c_0 = 1.5 \text{ mg/m}^2$, $Bq = 1$, Schmidt number $Sc = 0.0023$ and various (Re, Ω) : (a) (200, 1/3), (b) (200, 1/2), (c) (200, 1), and (d) (400, 1/2). For $Re = 200$ and 400 , capillary numbers are $Ca = 5.483 \times 10^{-4}$ and 8.225×10^{-4} respectively.

Self-similarity in the viscous Marangoni spreading of surfactant on a deep subphase

Fernando Temprano-Coletto^{1,2} and Howard A. Stone¹

¹*Department of Mechanical and Aerospace Engineering, Princeton University, NJ 08544, Princeton, United States of America*

²*Andlinger Center for Energy and the Environment, Princeton University, NJ 08544, Princeton, United States of America*

The spreading of an insoluble surfactant on a fluid interface through Marangoni flow is a fundamental problem relevant for colloid science, biology, and the environment. While many different spreading regimes have been studied theoretically, analytical progress has proven challenging in the limit of a deep subphase at low Reynolds number, due to the non-local coupling between the fluid flow and the surfactant concentration [1]. Recently, the problem was shown to be equivalent to the complex Burgers equation [2], leading to exact solutions obtained through mathematical methods [2–5] from which it is nevertheless challenging to infer general properties. Here, we analyze the self-similarity of the problem, providing insights into its structure and revealing its universal features [6]. Three different similarity regimes are identified using a combination of a phase-plane formalism and stability arguments. Surfactant ‘pulses’ with a locally high concentration exhibit a surfactant front whose position x spreads outward as $x \propto t^{1/2}$ (Figure 1a). Conversely, distributions that are locally depleted and flow inwards display two distinct similarity behaviors near a critical time t_* when the surfactant gradients become singular. On one hand, ‘dimple’ distributions with a quadratic minimum flow as $x \propto |t - t_*|^2$ (Figure 1b). On the other hand, ‘hole’ distributions with flatter minima exhibit a power law $x \propto |t - t_*|^{3/2}$ (Figure 1c). Overall, we obtain six similarity solutions in closed form, and discuss the implications of these results.

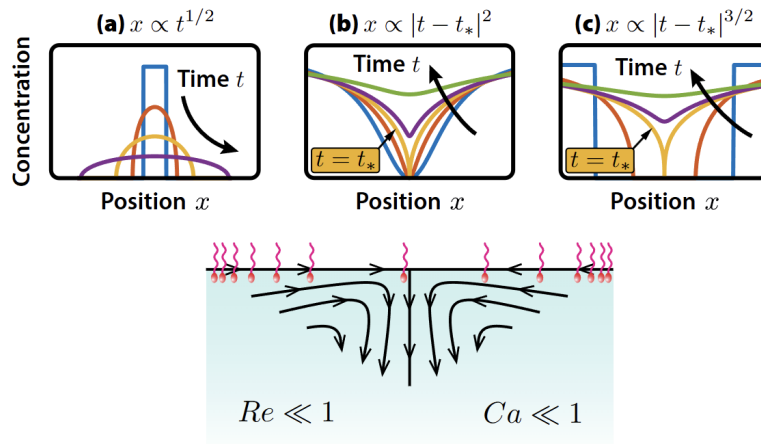


FIG. 1: Self-similarity of viscous Marangoni spreading on a deep fluid subphase. (a) Surfactant ‘pulses’ spread outward as $x \propto t^{1/2}$. (b) ‘Dimples’ with a quadratic minimum flow inwards as $x \propto t^2$, with t_* a critical time where gradients become singular. (c) ‘Holes’ with flatter minima exhibit $x \propto t^{3/2}$ power-law behavior.

-
- [1] A. Thess, D. Spirn, and B. Jüttner, *Phys. Rev. Lett.* **75**, 4614 (1995).
 - [2] D. G. Crowdy, *SIAM J. Appl. Math.* **81**, 2526 (2021).
 - [3] D. G. Crowdy, *J. Eng. Math.* **131**, 10 (2021).
 - [4] T. Bickel and F. Detcheverry, *Phys. Rev. E* **106**, 045107 (2022).
 - [5] D. G. Crowdy, A. E. Curran, and D. T. Papageorgiou, *J. Fluid Mech.* **969**, A8 (2023).
 - [6] F. Temprano-Coletto and H. A. Stone, *J. Fluid Mech.* **997**, A45 (2024).

Thermosolutal instabilities in a moderately dense nanoparticle suspension: Effect of interfacial nanoparticle kinetics

Raj Gandhi^{1,3}, Alexander Nepomnyashchy^{1,4} and Alexander Oron²

¹*Department of Mathematics, Technion - Israel Institute of Technology, 3200003, Haifa, Israel*

³*raj.gandhi@campus.technion.ac.il*, ⁴*nepom@technion.ac.il*

²*Department of Mechanical Engineering, Technion - Israel Institute of Technology, 3200003, Haifa, Israel*
meroron@technion.ac.il

A nanoparticle suspension (a nanofluid) in a layer of a Newtonian carrier fluid open to the gas phase is prone to strongly adsorb particles at the free interface, thereby affecting the local surface tension and leading to the *Marangoni* instability. A nanofluid layer cooled at the solid substrate exhibits the emergence of solutocapillary instability because of the concentration gradient created within the layer by the Soret effect. Furthermore, we note that the nanoparticle adsorption/desorption kinetics at the layer interface profoundly alter the already complex thermosolutal instability because of an additional inhomogeneity at the interface. This inhomogeneity of the nanoparticle concentration at the interface strongly couples the temperature and concentration fields in the bulk and at the interface. Generally, in a quiescent pure liquid layer and in a nanofluid layer cooled at the substrate, the thermocapillarity is a stabilizing mechanism. However, remarkably, in the same setting we find that the onset of both thermocapillary and solutocapillary instabilities when interfacial kinetics at the free nondeformable interface takes place. These instabilities are found to be both monotonic. Figure 1 presents the stability boundary for the system under the joint action of the thermocapillary and solutocapillary. We identify that the thermocapillary instability threshold linearly decreases if solutocapillarity is active, and hence, both surface tension-driven mechanisms are destabilizing. Interestingly, we observe that the relationship between the solutal M_S and thermal Marangoni numbers M_T at the instability threshold of the system is linear and expressed by $M_T/M_{TC} + M_S/M_{SC} = 1$, where M_{TC} and M_{SC} represent the critical values of the thermal and solutal Marangoni numbers in the case of pure thermocapillary and solutocapillary instabilities, respectively.

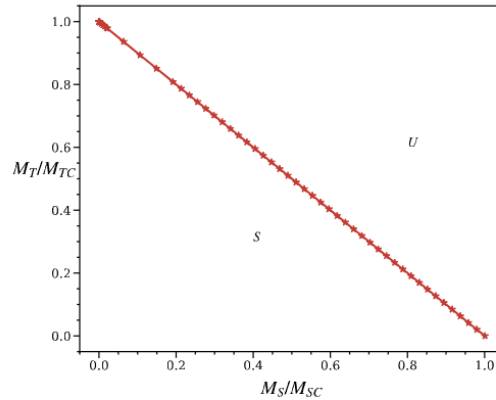


FIG. 1: Monotonic thermosolutal instability threshold in the $M_S/M_{SC} - M_T/M_{TC}$ plane in the case of cooling at the substrate for a given set of the problem parameters. The threshold values of MT and MS are normalized with M_{TC} and M_{SC} . The symbols U and S represent the unstable and stable domains of the system, respectively

I. ACKNOWLEDGEMENTS

This work is supported by the Grant from the European Union's Horizon 2020 research and innovation program under the Marie Skłodowska-Curie Grant # 955612 (NanoPaInt).

Asynchrony-driven chaotic mixing in two-dimensional viscous flows

Prabhash Kumar^{1,2}, Prahallada Jutur¹, Anubhab Roy¹ and Mahesh Pachagnula¹

¹Department of Applied Mechanics, Indian Institute of Technology Madras, 600036, Chennai, India

²prabhash@cacs.iitm.ac.in

We use experimental and numerical methods to explore the effects of asynchronous oscillations on mixing within a microchannel and the subsequent transition to chaotic behaviour. Our findings indicate that asynchronous oscillations in viscous flows at low Reynolds numbers are pivotal in initiating mixing, which can evolve into chaos depending on specific values of asymmetry parameter ϕ and the normalized oscillation frequency Sr. The mixing process is driven by stretch-and-fold mechanisms, with periodic transitions between closed streamlines (Moffatt eddies [1]) and open streamlines, further enhancing the mixing. We have developed a regime map within the parameter space of Sr and ϕ that delineates a region of chaotic mixing. This chaotic behaviour occurs when Sr is low and ϕ is closer to $\pi/2$, as illustrated in FIG. 1. The figure showcases typical experimental visuals related to both chaotic and non-chaotic scenarios. Notably, our numerical analysis reveals that an increase in the line element, expressed as $\alpha = (1/L)(\Delta L/\Delta N)$, follows an exponential trend in chaotic cases while exhibiting power-law behaviour in non-chaotic situations. In this equation, L denotes the length of the line element, and N represents the number of oscillation cycles. These findings underscore the critical role of asynchrony in wall-bounded, time-periodic viscous flows, with significant implications for particle transport across various physical, biological, and industrial systems.

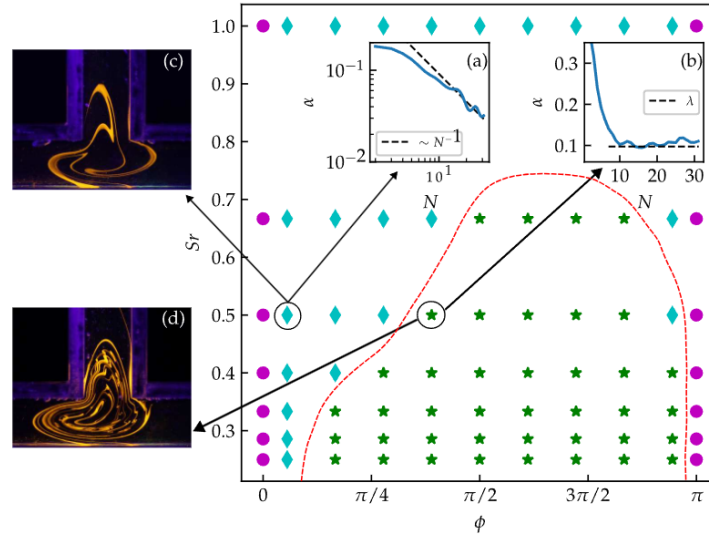


FIG. 1: The regime plot of Sr Vs ϕ indicates the regions of non-chaotic and chaotic fluid trajectories. Here, the ● symbol represents the time-periodic trajectories, the ◆ symbol represents non-chaotic trajectories, and ★ indicates chaotic trajectories. The red dashed line is the separating boundary of chaotic and nonchaotic regions. (a) Evolution of α with N for a non-chaotic case ($\phi = 10^\circ$, Sr = 0.5), (b) Evolution of α with N for a chaotic case ($\phi = 70^\circ$, Sr = 0.5), (c) Experimental visuals of non-chaotic case ($\phi = 10^\circ$, Sr = 0.5) at N = 10 and (d) Experimental visuals of chaotic case ($\phi = 70^\circ$, Sr = 0.5) at N = 10.

[1] . K. Moffatt, Viscous and resistive eddies near a sharp corner, J. Fluid Mech. **18**, 1–18 (1964).

Self-lubricated spreading of surfactant-laden droplets

Yotam Stern^{1,2}, Victor Multanen¹, Rafael Tadmor¹ and Roiy Sayag¹

¹Dept. of Mechanical Engineering, Ben Gurion University of the Negev, Beer Sheva, Israel

²sternyo@post.bgu.ac.il

While surfactants are known to affect fluid-fluid interfaces, their impact on solid-liquid interfaces is an open problem. We model the spreading of a non-volatile droplet by lubrication theory [1] and perform experiments on surfactant-laden droplets at various surfactant concentrations, c_0 , for ten different surfactant/substrate combinations. At low concentrations, spreading conforms to Tanner's law [2] where the base radius scales as $r_B \sim t^{1/10}$, which is confirmed experimentally. However, as c_0 increases, we observe a transition to a new power law of $r_B \sim t^{1/7}$, with a dependence on c_0 itself, as well as a crossover in time at intermediate surfactant concentrations from $t^{1/10}$ to $t^{1/7}$. To explain this behavior, we experimentally demonstrate the existence of a gradient in γ_{SL} owing to surfactant adsorption at the solid-liquid interface [3], and include it in our model through the reduction of the solid-liquid interfacial tangential stress, leading to a slip velocity [4]. Subsequently, we arrive at a new lubrication equation with an additional term accounting for the γ_{SL} gradient. We obtain a new dimensionless number, the Israelachvili number, I_J , analogous to the Marangoni number [5]. Upon analyzing I_J , we recover the time and concentration dependent crossover between the two spreading regimes. Additionally, we find that the new $t^{1/7}$ spreading includes a $c_0^{1/7}$ scaling, which we confirm across all our experimental settings.

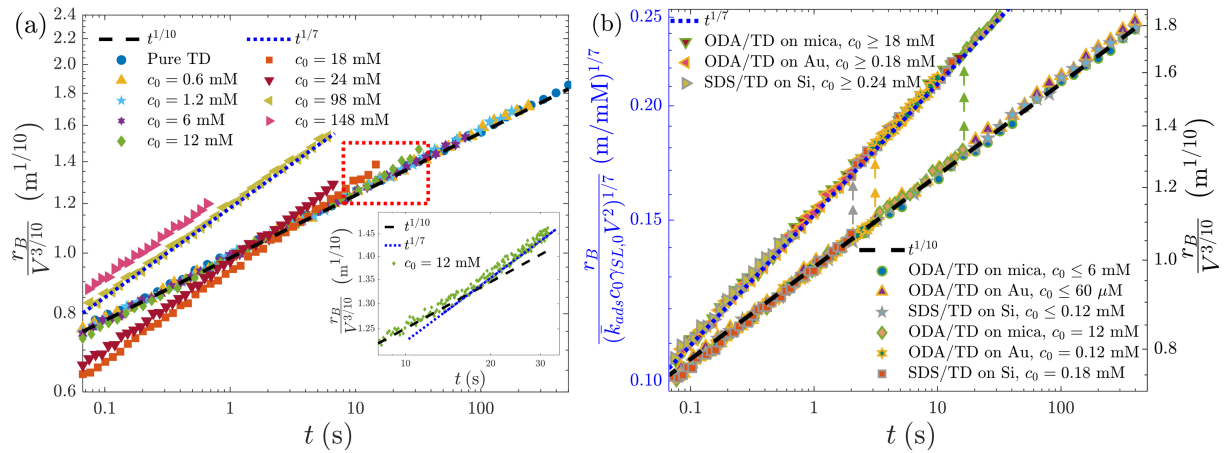


FIG. 1: (a) Results of spreading experiments for ODA/TD on mica, showing Tanner's law spreading and the crossover to a faster, concentration-dependent spreading rate. (b) Summary of spreading results for three experimental settings on two axes for the two power laws with arrows at crossovers, showing the two spreading regimes with data reduction.

Our findings expand on the present understanding of interfacial phenomena, providing a quantitative picture of interfacial energy gradients at solid-liquid interfaces in motion for the first time, and are central to predicting and controlling surfactant adsorption and the behavior of surfactant-laden droplets.

-
- [1] L.M. Hocking and A.D. Rivers, *Journal of Fluid Mechanics* **121**, 425 (1982).
 [2] L. H. Tanner, *J. Phys. D: Appl. Phys.* **12**, 1473 (1979).
 [3] R. Tadmor, V. Multanen, Y. Stern, and Y. B. Yakir, *Journal of Colloid and Interface Science* **581**, 496 (2021).
 [4] M. Wörner, X. Cai, H. Alla, and P. Yue, *Fluid Dyn. Res.* **50**, 035501 (2018).
 [5] C. Marangoni, *Nuovo Cim* **5**, 239 (1871).

Session 4 – Instabilities

Monday June 9, 16:15–17:00

Model for the nonlinear Rayleigh-Taylor instability in ideal media

A. R. Piriz,^{1,4} S. A. Piriz,^{2,5} and N. A. Tahir^{3,6}

¹*Instituto de Investigaciones Energéticas (INEI), E.T.S.I.I., and CYTEMA, Universidad de Castilla-La Mancha, 13071 Ciudad Real, Spain* ⁴*roberto.piriz@uclm.es*

²*Instituto de Investigaciones Energéticas (INEI), E.I.I.A., and CYTEMA, Universidad de Castilla-La Mancha, 45071 Toledo, Spain* ⁵*sofiaayelen.piriz@uclm.es*

³*GSI Helmholtzzentrum für Schwerionenforschung Darmstadt, Planckstrasse 1, 64291 Darmstadt, Germany*

⁶*n.tahir@gsi.de*

A model for the single mode, two-dimensional Rayleigh-Taylor instability in ideal, incompressible, immiscible and inviscid fluids is developed as an extension of a previous linear model based on the Newton's second law [1]. It describes the transition from linear to nonlinear regimes, and takes into account the mass of fluids participating in the motion during the instability evolution, including the laterally displaced mass. This latter feature naturally leads to the bubble and spike velocity saturation without requiring the usual drag term necessary in the well known buoyancy-drag model (BDM). In addition, it also provides an explanation to the latter phase of bubble reacceleration without appealing to the vorticity generation due to the Kelvin-Helmholtz instability. The model is in perfect agreement with the BDM buoyancy-drag model, but apart from extending its range of application, it solves many of its issues of concern and provides a more consistent physical picture.

-
- [1] A. R. Piriz, O. D. Cortázar, J. J. López Cela, O. D. Cortázar, and N. A. Tahir, The Rayleigh-Taylor instability, *Am. J. Phys.* **74**, 1095 (2006)

Rayleigh-Taylor instability in binary fluids with miscibility gap

Anubhav Dubey¹, Constantin Habes², Holger Marschall² and Sakir Amiroudine¹

¹Université de Bordeaux, I2M, UMR CNRS 5295, 33400, Talence, France

²Department of Mathematics, Computational Multiphase Flow, Technical University Darmstadt, 64289, Darmstadt, Germany

A pair of partially miscible liquids, exhibiting an upper-critical solution temperature (UCST) is considered to investigate the effect of miscibility on the Rayleigh-Taylor (RT) instability. The dynamic nature of the ratio of thermophysical properties and the interfacial tension in binary fluids with UCST renders them applicable to a wide variety of industrial and medical applications such as protein extraction [1] and targeted drug delivery [2] to name a few. Thus, a thorough understanding of the flow features associated with such fluids is necessary. We propose a novel modified phase-field approach [3] to track the continuous evolution of the smearing interface from the state of immiscibility to miscibility via partially miscible states. The numerical methodology accurately captures the Korteweg stresses above the UCST as long as the concentration gradient is non-trivial. The proximity to the UCST (T_c) is characterized by a parameter r , where $r = \frac{T_c - T}{T_c}$. This parameter is incorporated while defining the bulk free energy as a function of temperature. The interface between the two fluids is disturbed with finite amplitude perturbation to provoke the RT instability. To begin with, we performed a linear stability analysis employing Boussinesq approximation to derive the dispersion relations [3] for the RT instability and gravity capillary waves, while accounting for the partial miscibility of the fluids. Subsequently, the complete Cahn-Hilliard-Navier-Stokes equations are numerically solved to investigate the late-time behaviour of the diffusing fluid-fluid interface. The results quantify the perturbation growth behaviour as a function of Atwood and Weber numbers. Finally, the study concludes with a brief account of the role played by the parameter " r " in the emanation of secondary instability in the form of Kelvin-Helmholtz rolls as shown in Fig. 1.

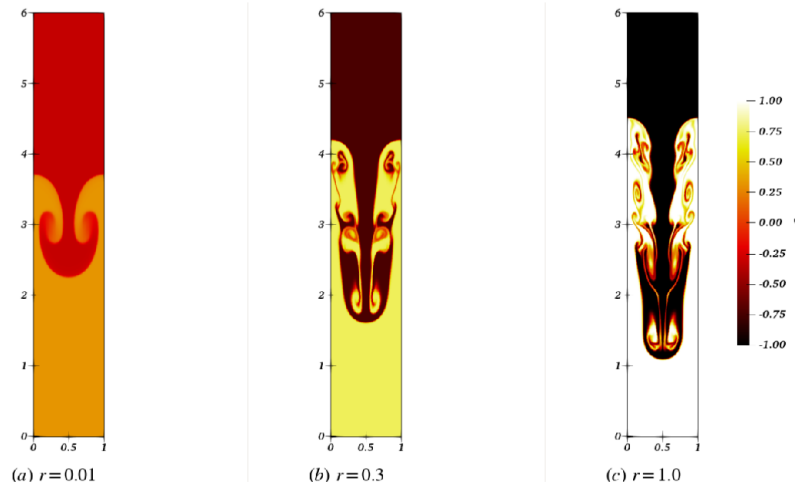


FIG. 1: Interface topology at $t = 9$, for $A = 0.2$, $We = 10000$, $Re = 5000$ as a function of miscibility parameter - (a) $r = 0.01$, (b) $r = 0.3$ and (c) $r = 1$

-
- [1] Kohno et al., "Extraction of protein with temperature sensitive and reversible phase change of IL/Water mixture", Polym. Chem., 2, 862, (2011).
 [2] Schmaljohann, D., "Thermo- and pH- responsive polymers in drug delivery" Adv. Drug Delivery Rev., 58, 1655-1670 (2006).
 [3] Dubey et al., "Rayleigh-Taylor instability in binary fluids with miscibility gap", Submitted to Phys. of Fluids (The arxiv version can be found at <https://arxiv.org/abs/2411.16292>)

Convective-absolute and dripping-jetting transitions in core-annular flow within fuel cells

Matthieu Rykner^{1,5}, Georg Dietze², Adrie Bruneton¹, Elie Saikali¹, Benoît Mathieu³ and Vadim Nikolayev^{4,6},

¹Université Paris-Saclay, CEA, Service de Génie Logiciel pour la Simulation, 91191, Gif-sur-Yvette, France
⁵matthieu.rykner@cea.fr

²Université Paris-Saclay, CNRS, FAST, 91405, Orsay, France

³Université Grenoble Alpes, CEA Liten, 38054 Grenoble, France

⁴Université Paris-Saclay, CEA, CNRS, Service de Physique de l'Etat Condensé, 91191 Gif-sur-Yvette Cedex, France ⁶vadim.nikolayev@cea.fr

Liquid/vapour water flows are encountered in a variety of fields, such as in Proton Exchange Membrane Fuel Cell (PEMFC), an emerging technology for energy decarbonation. In PEMFC, two-phase core-annular water flows are observed in the gas fuel channels (GFC) used to supply the reactive species to the cell. Formation of liquid plugs may occur via the Plateau-Rayleigh instability in these millimeter-size GFC [1]. This instability is however modified by the presence of an imposed core gas flow which may non-linearly saturate its development and prevent the formation of plugs [3]. Both convective and absolute instabilities are observed under these conditions.

A 2D-axisymmetrical two-phase lubrication model is developed to investigate this instability transition. It is solved numerically for two configurations: (1) in an open domain with a finite-difference scheme allowing to simulate the spatio-temporal evolution of the flow; (2) in a periodic domain using the continuation software *Auto-07p* which allows to track nonlinear travelling-wave solutions corresponding to the most dangerous instability mode. By comparing these approaches, it is observed that, while both methods predict similar results for a convective instability, significant differences in the predicted wavelength are observed for an absolute instability. Notably, a transition from dripping to jetting is observed; in the dripping regime, the wavelength is selected by the boundary condition. Similar results are also obtained when inertial effects are accounted for by using a WRIBL model [2] implemented in *Auto-07p* and an open-domain Direct Numerical Simulation solved with *TRUST/TrioCFD*.

The goal of the current work is to understand the dripping regime under the conditions of the absolute instability in order to obtain correlations between the input parameters (liquid/gas flow rates $Q_{l,g}$ and inlet film thickness) and the travelling-wave variables (celerity, maximum/minimum film thickness, wavelength, plug width, etc.). Ultimately, the global pressure drop over a full channel length shall be predicted by this model, enabling the construction of a macroscopic 1D channel model to be coupled to electrochemical and transport models in an integrative model of the fuel cell.

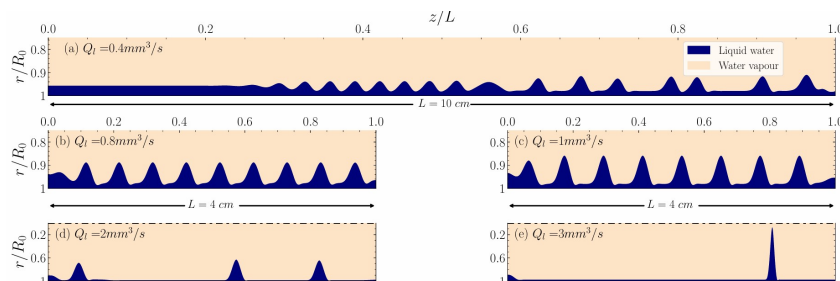


FIG. 1: Travelling waves in a 0.5 mm-radius tube for $Q_g = 1000 \text{ mm}^3 \text{ s}^{-1}$ and Q_l increasing from (a) to (e). Only half of the tube is illustrated in (d)-(e) and one eighth in (a)-(c). (a) Convective instability. (b)-(c) Absolute instability with increasing wavelength. (d) Period doubling of the absolute instability. (e) Apparition of plugs.

-
- [1] M. Rykner, E. Saikali, A. Bruneton, B. Mathieu and V. S. Nikolayev, Plateau–Rayleigh instability in a capillary: assessing the importance of inertia, *J. Fluid Mech.* **1001**, A15 (2024).
- [2] G. F. Dietze and C. Ruyer-Quil, Films in narrow tubes, *J. Fluid Mech.* **762**, 68–109 (2015).
- [3] A. L. Frenkel, A. J. Babchin, B. G. Levich, T. Shlang and G. I. Sivashinsky, Annular flows can keep unstable films from breakup: Nonlinear saturation of capillary instability, *J. Colloid Interface Sci.* **115**, 225-233 (1987).

Session 5 – Vibrated systems

Tuesday June 10, 9:00–11:15

Boundary layer flow induced electrokinetic effects at the glass/electrolyte and (piezoelectric) lithium niobate/electrolyte interfaces under the excitation of a mega-Hertz-level mechanical wave in the solid substrates

Ofer Manor^{1,2}, Yifan Li¹, Gideon Onuh¹ and Sudeepti Aremanda¹

¹Department of Chemical Engineering, Technion-Israel Institute of Technology, Haifa, Israel

²manoro@technion.ac.il

I will discuss the theory [1] and measurement of the dynamic electrical properties of a spontaneously charged glass and lithium niobate surfaces in an electrolyte solution by exciting spatiotemporal periodic boundary layer flow using a MHz-level surface acoustic wave (SAW) actuator. [2] The boundary layer flow vibrates ions at the nanometer-thick electrical double layer to appear at the glass / electrolyte and lithium niobate / electrolyte interfaces. The out-of-equilibrium EDL leaks electrical field, which is modulated by ion vibration frequency, revealing the ion dynamics. A previous study [3] directly excited EDLs on the piezoelectric lithium niobate substrate of a SAW actuator; it remained unclear whether the mechanical or electrical components of the SAW in the piezoelectric substrate dominated the EDL excitation. We isolate the mechanical component of the SAW as a same frequency mechanical vibration in glass and show that it introduces the expected ion electrokinetic vibration in the excited EDL at the glass/electrolyte interface. The measured electrical field leakage spectra exhibit a non-monotonic behavior, taking local maxima where the SAW frequency matches the ion relaxation time in the EDL. At these frequencies, the synchronization maximizes ion vibration displacement, thereby amplifying the electrical field leakage in agreement with the theory. Our findings may be used to study the electrokinetic properties of arbitrary solid surfaces and further suggest that SAW-actuated nano-fluidic platforms may be associated with out-of-equilibrium EDL systems of consequence to membranes and liquid films that rely on EDLs to screen ion species and for stability, respectively.

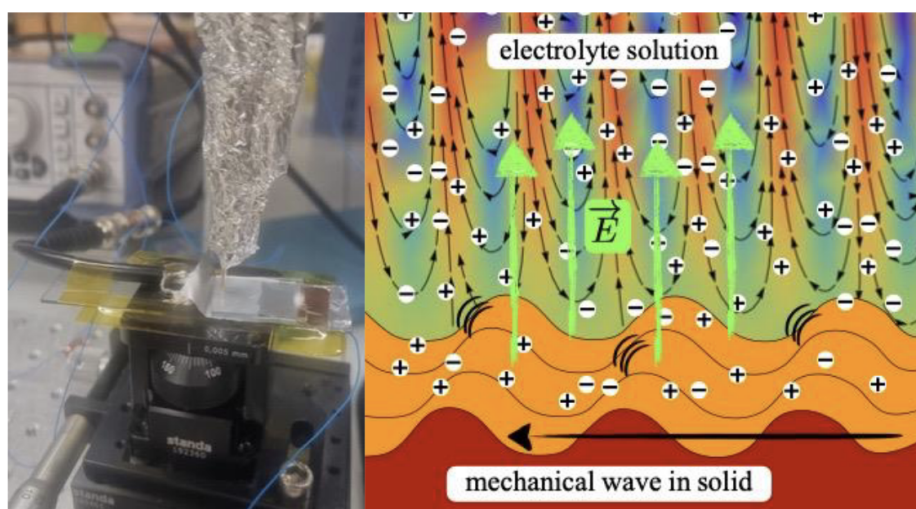


FIG. 1: (right) Illustration of a surface acoustic wave (SAW) in solid, interacting with ions in an electrical double layer (EDL) via a spatiotemporal periodic boundary layer flow (essentially, a mechanical evanescent wave) in the neighboring electrolyte. This results in an electrical field leakage, \vec{E} , that we measure (left).

[1] O. Dubrovski and O. Manor. *Langmuir* 2021, **37**, 14679–14687 (2021)

[2] O. Manor, L. Y. Yeo, J. R. Friend, *J. Fluid Mech.* **707**, 482–495 (2012)

[3] S. Aremanda and O. Manor. *J. Phys. Chem. C*, **127**, 20911–20918 (2023)

Drop behavior on a heterogeneous ratchet-structured substrate vibrated harmonically in lateral direction

Rodica Borcia^{1,2}, Ion Dan Borcia¹ and Michael Bestehorn¹

¹*Institut für Physik, BTU, 03046, Cottbus, Germany* ²*borciar@b-tu.de*

We analyze numerically a new ratchet system: a liquid drop is sitting on a heterogeneous ratchet-structured solid plate. The heterogeneous ratchet-structured solid plate is realized by varying the contact angle periodically along the x axis at the bottom boundary – asymmetrically along one period. The coated plate is subject to a lateral harmonic oscillation (see Figure 1). The systematic investigation performed in the frame of a phase field model shows the possibility to realize a long-distance net driven motion for isolated domains of the forcing parameters [1]. The studied problem might be of considerable interest for controlled motion in micro- and nano-fluidics.

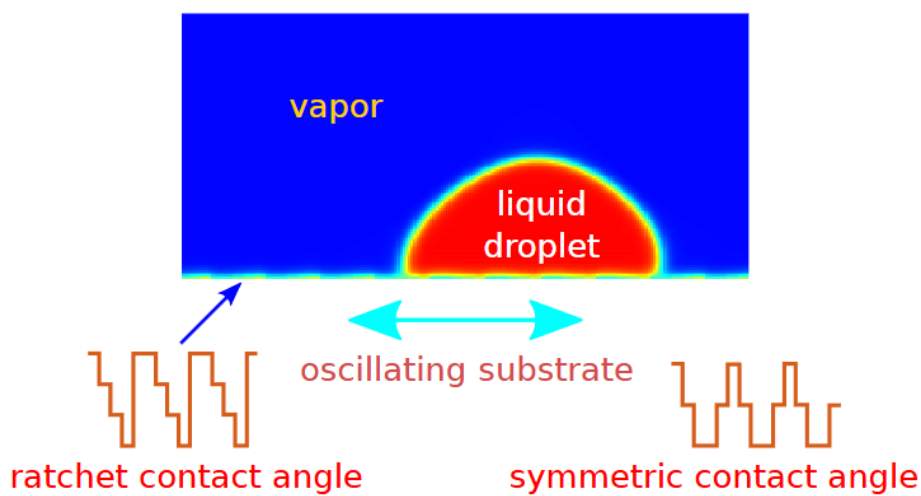


FIG. 1: Heterogeneous substrate subject to horizontal harmonic oscillation.

-
- [1] R. Borcia, I.D. Borcia, M. Bestehorn, Drop behavior on heterogeneous ratchet-structured substrate vibrated harmonically in lateral direction. *Langmuir* **40**, 13709 (2024).

Faraday waves at the surfactant-covered free surface of the vertically vibrated non isothermal liquid

Alexander A. Mikishev^{1,3} and Alexander A. Nepomnyashchy^{2,4}

¹*Department of Eng. Technology, Sam Houston State University, TX 77341, Huntsville, Texas, United States of America* ³*amik@shsu.edu*

²*Department of Mathematics, Technion, 32000, Haifa, Israel* ⁴*nepom@technion.ac.il*

The stability of liquid partially filling a vibrated container and heated from above is considered. The surface of the liquid is covered by an insoluble surfactant.

There exist two kinds of surface waves in a liquid heated from above, transverse capillary-gravity waves and longitudinal waves caused by Marangoni stresses. In the absence of vibration, their resonant mixing creates an oscillatory instability above a certain critical value of the Marangoni number. The action of vibration is twofold. Below the critical value of the Marangoni number, the vibration creates subharmonic (the frequency is half the driving frequency) or harmonic (the frequency equals the driving frequency) parametric (Faraday) waves. Also, the vibration acts on the oscillatory Marangoni instability, creating the excitation of subharmonic, harmonic and quasiperiodic modes.

We consider both cases, taking into account the dependence of the surface wave frequency on the thermocapillary Marangoni number and the elasticity number characterizing the action of the surfactant. The influence of the surfactant concentration on the instability threshold is investigated in detail.

Translational Instability of an Oscillating Bubble under the Effect of an Acoustic Field

S. İlke Kaykanat^{1,2} and A. Kerem Uğuz^{1,3}

¹Department of Chemical Engineering, Bogazici University, 34342, Istanbul, Turkey

²seymenilke.kaykanat@std.bogazici.edu.tr, ³kerem.uguz@bogazici.edu.tr

Bubble oscillations induced by an external acoustic field play a crucial role in biomedical applications, such as targeted drug and gene delivery, as well as their use as contrast agents in medical imaging. Controlling shape stability is critical for effective drug delivery, as it helps regulate microbubble break up and estimate collapse pressure during tissue ablation. The onset of bubble break-up is directly related to the loss of spherical shape due to the growing shape instabilities at the interface. This study examines the behavior of a bubble in blood, with an emphasis on its translational instability under acoustic excitation. When a spherical bubble undergoing volume oscillations becomes unstable, it develops shape deformations in two adjacent modes [1, 2, 3]. The interaction between the translational mode and these shape oscillations leads to translational instability. In the present work we describe how the translational motion of a bubble affects the shape oscillations. The translational motion of a bubble is investigated by adding the effect of primary Bjerknes force. The system consists of a single bubble in an unbounded liquid as depicted in FIG. 1. Blood is represented by a power-law constitutive model. An external acoustic field is applied to induce volume oscillations. For small perturbations, the dispersion relation is obtained from the Rayleigh and energy equations. This study explores the influence of frequency, power-law index, and apparent viscosity on the critical acoustic pressure amplitude, above which the bubble becomes unstable.

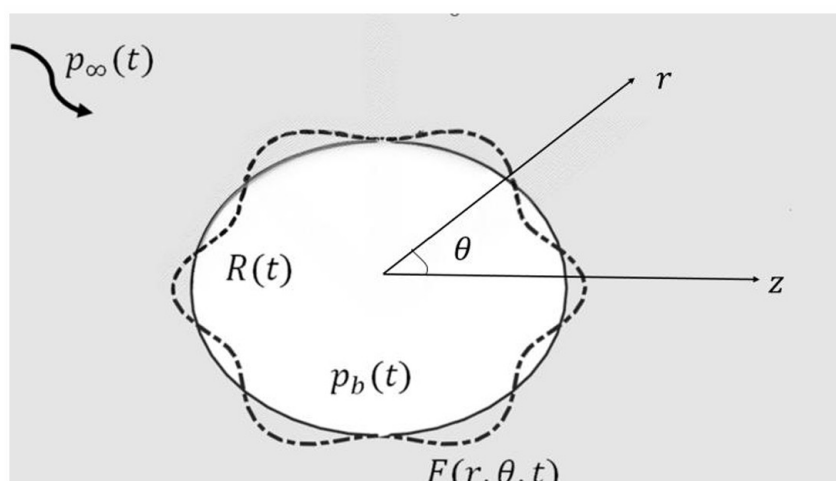


FIG. 1: Sketch of a non-spherical bubble geometry in spherical coordinates. The solid and dashed lines show the spherical and non-spherical oscillations.

-
- [1] Doinikov, A. A. (2004). Translational motion of a bubble undergoing shape oscillations. *Journal of Fluid Mechanics*, **501**, 1-24.
 - [2] Feng, Z. C., & Leal, L. G. (1995). Translational instability of a bubble undergoing shape oscillations. *Physics of Fluids*, **7**(6), 1325-1336
 - [3] Mettin, R., & Doinikov, A. A. (2009). Translational instability of a spherical bubble in a standing ultrasound wave. *Applied Acoustics*, **70**(10), 1330-1339.

Surface Acoustic Wave (SAW) Streaming Through Porous Media

Jinan P^{1,2} and Ofer Manor^{1,3}

¹Department of Chemical Engineering, Technion-Israel Institute of Technology, Haifa, Israel

²jinanparathi@campus.technion.ac.il, ³manoro@technion.ac.il

The transport of fluids through porous media has long been a subject of scientific inquiry, with applications ranging from geological processes and unit operations to cutting-edge technologies like lab-on-a-chip devices. Traditional approaches to enhance fluid flow often encounter challenges, such as limited directional control or inefficiencies in manipulating flows in complex geometries. Surface Acoustic Waves (SAWs), characterized by their ability to generate intense, localized acoustic fields, offer transformative potential in this domain. SAW streaming enables the generation of precise, controlled, and directional flows, addressing limitations inherent in conventional techniques. Moreover, the non-invasive nature of SAW-induced streaming ensures compatibility with delicate or intricate systems, making it highly applicable to emerging technologies and microfluidic platforms. We present an investigation of surface acoustic wave (SAW) streaming through porous media, with a focus on understanding mass transport mechanisms and deriving a macroscopic flow model. This study builds on the framework established for acoustic streaming in porous media by Ofer Manor [1]. Instead of planar acoustic waves, we focus on the dynamics introduced by SAW streaming. The analysis is conducted by detailed calculation of mass transport through individual cylindrical pores with different orientations using Navier Stokes equation with a spatially averaged acoustic forcing. The analysis includes different cases such as the acoustic impedance of both liquid and pore surface being the same and streaming in rigid porous media where there is a large difference in acoustic impedance. We consider large, medium and small pore diameter limits relative to the viscous penetration length of the acoustic wave near the pore surface.

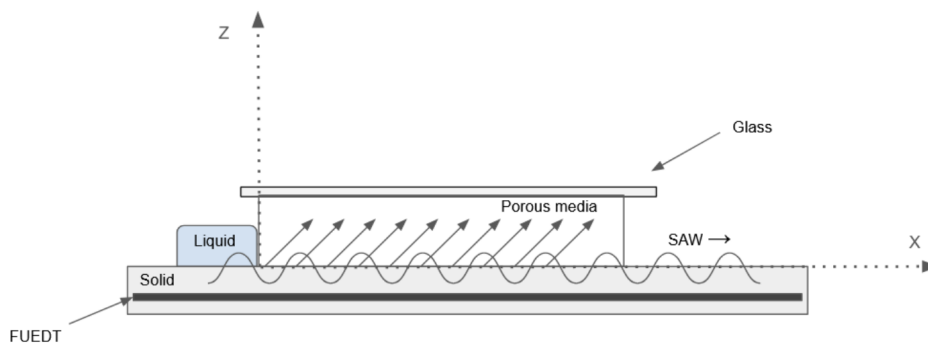


FIG. 1: Schematic diagram of Surface Acoustic Wave (SAW) propagating through piezoelectric solid on top of which porous media is placed

-
- [1] O. Manor, Acoustic flow in porous media, *J. Fluid Mech.*, **920**, A11 (2021). [10.1017/jfm.2021.436](https://doi.org/10.1017/jfm.2021.436)

Free-surface flows in a water filled parametrically excited circular channel with a submerged hill

Ion Dan Borcia^{1,3}, Franz-Theo Schön^{2,6}, Uwe Harlander^{2,7}, Rodica Borcia^{1,4} and Michael Bestehorn^{1,5}

¹*Institute of Physics, BTU, 03046, Cottbus, Germany*

³borciai@b-tu.de, ⁴borciar@b-tu.de, ⁵bestehorn@b-tu.de

²*Department of Fluid Mechanics, BTU, 03044, Cottbus, Germany*

⁶shoefra@b-tu.de, ⁷haruwe@b-tu.de

We investigated surface waves in an oscillating ring channel with the mean radius of 0.76 m. The ring is placed on a rotating table that can oscillate symmetrically (harmonic oscillation of the rotation velocity) or non-symmetrically (ratchet excitation) [1-3]. On the bottom of the periodic boundary channel we placed a symmetrical (SM) or asymmetrical (with higher asymmetry HA or lower asymmetry LA) mountain (see Fig. 1).

Two combination of the spatial/temporal setups were studied: symmetrical mountain with ratchet excitation and ratchet mountain with symmetrical excitation. The effects of temporal and spatial asymmetry are compared. The resonance curves in terms of wave amplitude and induced mean flow are plotted for each case. For frequency values close to the resonance, bore like waves moving in one direction have much boarder elevation. At these frequencies the transport effect is important and it will be studied in both experiment (using floating tracers and PIV) and simulation. An interesting result is that the direction of the induced mean flow appears in the opposite direction for the HA and LA cases. We attribute this result to the appearance of a vortex at high fluid velocities relative to the bottom elevation in the HA case, which blocks the flow through the channel. The vortex didn't appear in LA case.

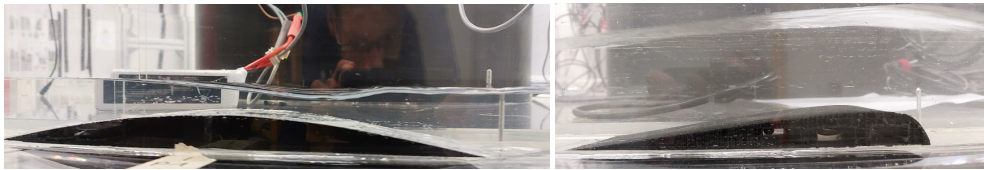


FIG. 1: Left: Symmetric hill (SM), right: highly asymmetrical hill (HA)

-
- [1] I. D. Borcia, F.-T. Schön, U. Harlander, R. Borcia, and M. Bestehorn, “Mean flow generated by asymmetric periodic excitation in an annular channel”, *Eur. Phys. J. Special Topics* **233**, 2024.
 - [2] F.-T. Schön, I. D. Borcia, U. Harlander, R. Borcia, S. Richter, and M. Bestehorn, “Resonant surface waves in an oscillating periodic tank with a submerged hill”, *Journal of Fluid Mechanics* **999**, 2024.
 - [3] I. D. Borcia, S. Richter, R. Borcia, F.-T. Schön, U. Harlander, and M. Bestehorn, “Wave propagation in a circular channel - sloshing and resonance”, *Eur. Phys. J. Special Topics* **232**, 2023.

Resonance-induced stabilization of Marangoni instability in viscoelastic fluids

I. B. Ignatius^{1,4}, B. Dinesh^{2,6}, Georg Dietze^{3,7} and R. Narayanan^{1,5}

¹*Department of Chemical Engineering, University of Florida, Gainesville, FL 32601, United States of America*

⁴*iginbenny@gmail.com*, ⁵*ranga@ufl.edu*

²*IIT BHU, Varanasi, UP, 221005, India* ⁶*dineshbh6@gmail.com*

³*Université Paris-Saclay, CNRS, FAST, 91405 Orsay, France* ⁷*georg.dietze@cnrs.fr*

A long-wave Marangoni instability, leading to film dry-out [1], can occur when a thin fluid layer in a container is heated from below beyond a critical temperature gradient. In the absence of fluid elasticity, a vertical mechanical oscillation raises the threshold for the long-wave Marangoni instability mode, thereby stabilizing the system and preventing dry-out via resonant effects. Linear stability calculations by Ignatius et al. [2] showed that a stable quiescent state can be achieved within a finite range of forcing amplitudes, provided the forcing frequency is below a critical value. Outside this parameter range, the system becomes unstable due to either a Marangoni instability at lower forcing amplitudes or a Faraday instability at higher forcing amplitudes. In the present study, we extend our earlier work to investigate the influence of elasticity on the stabilization of an inherently Marangoni-unstable thin viscoelastic film.

Our study reveals that the behavior of a viscoelastic fluid differs significantly from that of a Newtonian fluid in two significant ways due to the memory effect imparted by fluid elasticity. First, the forcing amplitude range for complete stabilization is bounded by an upper and a lower forcing frequency, unlike the Newtonian case, which is bounded by only an upper frequency. Second, fluid elasticity reduces the forcing amplitude for both the stabilization of Marangoni instability and the onset of Faraday instability, with a more significant reduction in the latter. This leads to the lowering of both the threshold amplitude and the amplitude range for full stabilization of the viscoelastic thin-film system, a result attributed to the spring-like behavior introduced by the fluid's elasticity. Suppressing dry-out in viscoelastic thin films, such as polymeric films, is important due to its relevance in coating industries, especially in the manufacture of thin optical films.

I. ACKNOWLEDGEMENTS

The authors gratefully acknowledge funding from NSF via grant CBET-2422919 and NASA via grants NNX17AL27G and 80NSSC23K0457. I.B.I. acknowledges support from a Chateaubriand fellowship.

-
- [1] S. J. VanHook, M. F. Schatz, J. B. Swift, W. D. McCormick, and H. L. Swinney, "Long-wavelength surface tension-driven Bénard convection: experiment and theory," *Journal of Fluid Mechanics*, vol. **345**, p. 45–78, 1997.
- [2] Ignatius, I. B., Dinesh, B., Dietze, G. F. & Narayanan, R. 2024 Influence of parametric forcing on Marangoni instability. *J. Fluid Mech.* **981**, A8.

Session 6 – Solid-liquid phase change I

Tuesday June 10, 11:15–12:15

The combined effect of natural and thermocapillary convection on the melting of PCMs in rectangular and cylindrical domains

Andriy Borshchak Kachalov¹, Pablo Salgado Sánchez¹, Jeff Porter^{1,2}, Jose Miguel Ezquerro¹ and Jacobo Rodríguez¹

¹*E-USOC, Center for Computational Simulation, E. T. S. de Ingeniería Aeronáutica y del Espacio, Universidad Politécnica de Madrid, 28040, Madrid, Spain* ²*jeff.porter@upm.es*

The results of numerical simulations investigating the influence of natural and thermocapillary convection on the liquid-solid phase transition of n-octadecane in rectangular [1] and cylindrical [3] domains are presented. A systematic analysis is performed by varying key parameters including the aspect ratio of the domain (Γ), the Rayleigh (Ra) and Marangoni (Ma) numbers, and the dynamic Bond number ($Bo_{\text{dyn}} = Ra/Ma$), which measures the relative importance of natural and thermocapillary convection. In rectangular containers with $\Gamma \gg 1$ and $Bo_{\text{dyn}} \ll 1$, thermocapillary convection is shown to significantly accelerate the melting process while, with $\Gamma \sim Bo_{\text{dyn}} \sim O(1)$, the thermocapillary effect is detrimental on average and increases the total melting time; see Fig.1(left). The presence of gravity stabilises the dynamics of the flow, delaying the appearance of oscillatory convection. In (quasi-) cylindrical domains, where the PCM is held between two circular supports maintained at different temperatures, the results depend crucially on whether the system is heated from below or above; see Fig.1(right). In the former case, natural convection acts in the same sense as thermocapillary convection and the total heat transfer rate is increased. When heating from above, the thermocapillary-driven flow is opposed by the buoyancy force, which decreases total heat transport.

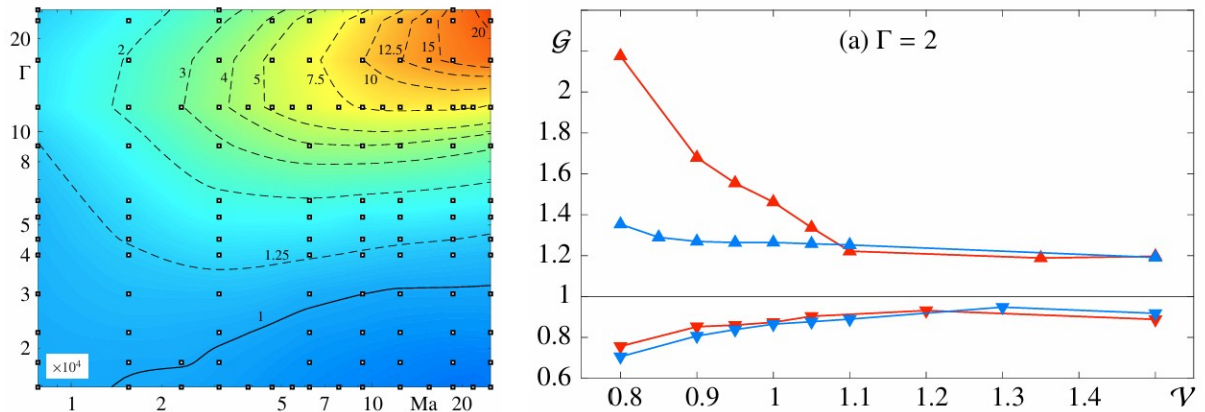


FIG. 1: (left) Contours of the Marangoni enhancement factor \mathcal{G} for varying Ma and Γ in rectangular domains. The (neutral) curve $\mathcal{G} = 1$ is distinguished by a thicker solid curve. (right) Natural convection enhancement factor \mathcal{G} versus the dimensionless volume \mathcal{V} for selected $Ma = 15519$ (blue), 155186 (red), in a (quasi-) cylindrical domain with $\Gamma = 2$. The horizontal line indicates the microgravity case $\mathcal{G} = 1$. Configurations with heating from below (above) are shown with upright (inverted) triangles.

-
- [1] A. Borshchak Kachalov, P. Salgado Sánchez, J. Porter and J. M. Ezquerro, The combined effect of natural and thermocapillary convection on the melting of phase change materials in rectangular containers, *Int. J. Heat Mass Transf.* **168**, 120864 (2021).
 [2] R. Varas, U. Martínez, K. Olfe, P. Salgado Sánchez, J. Porter and J. M. Ezquerro, Effects of thermocapillary and natural convection during the melting of PCMs with a liquid bridge geometry, *Microg. Sci. Technol.* **35**, 17 (2023).

Flexible microfluidic thermal emitter - Irrevesibility analysis

Fikret Alic¹

¹*Department of Thermal and Fluid technique, Faculty of Mechanical Engineering, University of Tuzla, Bosnia and Herzegovina* `fikret.alic@untz.ba`

I. ABSTRACT

Heating of microchannels and microfluidic devices today is primarily done using standard microheaters. Fluid flow occurs inside microchannels of different shapes and sizes in microfluidic devices, measurement equipment, and cooling microsystems. Enhancing heat transfer within microfluidic channels can be achieved by using various nanofluids. As a result, some researchers are studying heat transfer of different nanofluids inside channels and microchannels, [1], [2]. Heat transfer between microchannels and nanofluids also results in thermal irreversibilities. Various research teams have investigated and analyzed of the total thermal entropy, [3-6]. Based on previous research and analysis, the concept of directly heating nanofluids inside microtube with an outer diameter of 0.5mm using an electro-resistant heating wire with a diameter of 0.15mm was developed. An electrically resistant wire is positioned in the center of the microtube causing that the nanofluid to flow through the annular cross-section. In this analysis, the nanofluid was created by dispersing Al_2O_3 nanoparticles within the base fluid (water) at volumetric fraction ratios of 3% and 6%. The nanofluid flows inside the microtube in a spiral around a central Nano-enhanced Phase Change Material (NePCM) cylindrical cartridge. In this analysis nanoparticles (TiO_2) are dispersed in various volume fractions into the base PCM, which in this study is sodium acetate trihydrate ($\text{C}_2\text{H}_3\text{O}_2\text{Na}$). Through mixing, the nanoparticles are evenly homogeneously distributed within the base PCM, creating a nano-enhanced phase change material (NePCM). A flexible microfluidic emitter in the form of a spiral microtube can adjust the distance between its coils using an external magnetic actuator. This adjustment directly impacts the heat transfer between the nanofluid and the NePCM cylindrical cartridge. The thermal irreversibility of the nanofluid and NePCM is analyzed analytically and experimentally tested in this study. The methodology established can serve as a foundation for optimization by minimizing total thermal entropy of nanofluid. The geometric and process parameters of the optimization enable indirect automatic control of the flexible microfluidic emitter simultaneously in accordance with the established optimization criteria.

II. METHODOLOGY

The flow and direction of the nanofluid are controlled by software that supports a microfluidic peristaltic pump (see Figure 1). This pump enables multiple variations of the process parameters covered in this work, based on changes in nanofluid flow within it. A flexible microfluidic thermal emitter can adjust the spacing between its spiral coils, allowing them to partially or fully cover a NePCM cylindrical cartridge. The controlled movement of the spiral microtube coils is achieved using an external magnetic actuator. In the analysis conducted, the total thermal entropy of the nanofluid is determined using analytical modeling, and the results obtained are verified through experimental testing. The volumetric flow rate of the nanofluid, the ratio of Al_2O_3 and TiO_2 nanoparticles, the temperature of the electroresistive heating wire, and the geometric parameters of the flexible spiral emitter are all varied simultaneously.

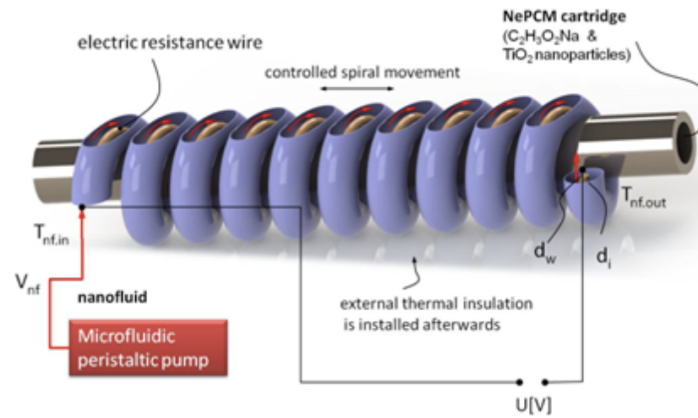


FIG. 1: A flexible microfluidic emitter accumulates heat within the NePCM cartridge.

By using the control software, it is possible to switch on and off the high-precision microfluidic peristaltic pumps (CPP1 1000-2M) on and off using their shared driver, Figure 2. These pumps are plug-and-play, USB powered, and compatible with computers. The flow range of pump is from $2 \mu\text{l}/\text{min}$ to $1700 \mu\text{l}/\text{min}$.

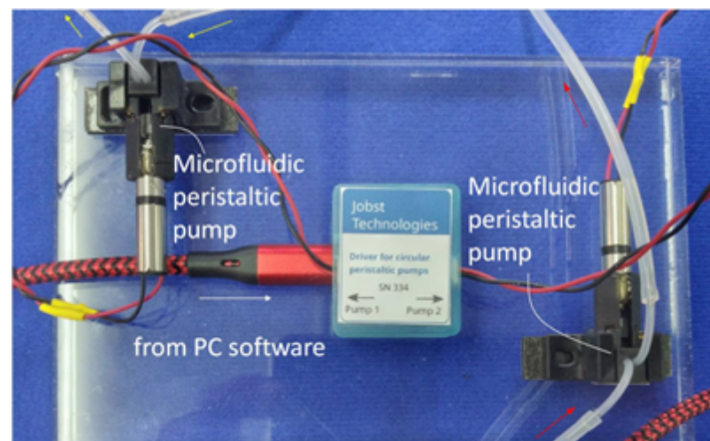


FIG. 2: Part of the experimental set-up for ensuring the flow of nanofluid.

- [1] Mebarek-Oudina, F. Convective heat transfer of titania nanofluids of different base fluids in cylindrical annulus with discrete heat source. *Heat Transf.-Asian Res.* **48**(1), 135–147 (2019).
- [2] Jung SY, Park H. Experimental investigation of heat transfer of Al₂O₃ nanofluid in a microchannel heat sink. *Int J Heat Mass Tran.* **179**, 121729 (2021).
- [3] F.Alic. The non-dimensional analysis of nanofluid irreversibility within novel adaptive process electric heaters *Applied Thermal Engineering.* **152**, 13-23 (2019).
- [4] Sheikhzadeh G, Aghaei A, Ehteram H, et al. Analytical study of parameters affecting entropy generation of fluid turbulent flow in channel and micro-channel. *Therm Sci.* **20**, 2037–2050. (2016).
- [5] Alic, F. (2020). Entropy dissipation analysis and new irreversibility dimension ratio of nanofluid flow through adaptive heating element, *Energies.* **13**,114 (2020).
- [6] X. Cheng, Q. Zhang, X. Liang. Analyses of entropy dissipation, entropy generation and entropy-dissipation-based thermal resistance on heat exchanger optimization. *Applied Thermal Engineering.* **38**, 31- 39 (2012).

Thermocapillary effects during the melting of phase change materials subjected to isothermal or heat flux boundary conditions

Andriy Borshchak Kachalov¹, Pablo Salgado Sánchez¹, Ali Arshadi¹, Álvaro Bello¹, Jose Ezquerro¹, and Úrsula Martínez^{1,2}

¹*E-USOC, Center for Computational Simulation, E. T. S. de Ingeniería Aeronáutica y del Espacio, Universidad Politécnica de Madrid, 28040, Madrid, Spain* ²*ursula.martinez.alvarez@upm.es*

We numerically investigate the melting dynamics of n-octadecane in a rectangular container that is subjected to either isothermal [1] or heat flux boundary conditions [2], and is open to air in microgravity. As the melting progresses, the temperature gradient existing at the open boundary drives thermocapillary flow within the liquid phase and modifies the phase change dynamics. We conduct a parametric study varying the container aspect ratio, and the Marangoni and Stefan numbers, and compare the associated temporal dynamics with those observed in the (so-called) reference case, where heat is transferred solely by conduction. In the isothermal case, the overall effect of thermocapillary flows is to accelerate melting by a factor up to 20. Under constant heat flux, the analogous contribution is about one order of magnitude smaller. Finally, we analyze the oscillatory flows that eventually appear during melting and investigate other scenarios of potential interest for microgravity applications [3].

-
- [1] P. Salgado Sánchez, J. M. Ezquerro, J. Fernández and J. Rodríguez, Thermocapillary effects during the melting of phase change materials in microgravity: heat transport enhancement, *Int. J. Heat Mass Transf.* **163**, 120478 (2020).
 - [2] A. Borshchak Kachalov, R. García-Roco, P. Salgado Sánchez, K. Olfe and A. Bello, Thermocapillary effects during the melting of phase change materials subjected to lateral heat flux in microgravity, *Int. J. Heat Mass Transf.* **218**, 124806 (2024).
 - [3] R. García-Roco, P. Salgado Sánchez, A. Bello, K. Olfe and J. Rodríguez, Dynamics of PCM melting driven by a constant heat flux at the free surface in microgravity, *Therm. Sci. Eng. Progress* **48**, 102370 (2024)

Design, testing, and initial ground results of the “Effect of Marangoni Convection on Heat Transfer in Phase Change Materials” experiment

Úrsula Martínez^{1,2}, Jose Miguel Ezquerro¹, Ignacio Tinao¹, Dan Gligor¹ and Jose Fernández¹

¹*E-USOC, Center for Computational Simulation, E. T. S. de Ingeniería Aeronáutica y del Espacio, Universidad Politécnica de Madrid, 28040, Madrid, Spain* ²*ursula.martinez.alvarez@upm.es*

The experiment “Effect of Marangoni Convection on Heat Transfer in Phase Change Materials” (MarPCM) [1] aims to investigate the efficacy of thermal Marangoni convection in increasing the heat transfer rate of passive phase change materials (PCMs) that incorporate a free surface in microgravity; the (so-called) thermocapillary-enhanced PCMs (TePCMs). Compared to thermal conduction, thermocapillary flows can increase heat transport by a significant factor [2]. In addition to advancing scientific understanding, the experiment seeks to evaluate the practical feasibility of using TePCMs as passive thermal control devices for space missions and assess possible implementation challenges. We revise here the recent work published in Ref. [3], which presented the design and testing of the MarPCM cuboidal cell prototype; see Fig. 1(left). In particular, the comprehensive approach towards developing space experiments is illustrated, adhering to rigorous and demanding scientific and technical requirements. Along with the validation of the initial experiment prototype, the evaluation of ground tests is also addressed; see Fig. 1(right). Overall, the hardware developed demonstrates an adequate performance, while the obtained results are coherent and compliant with the established scientific requirements.

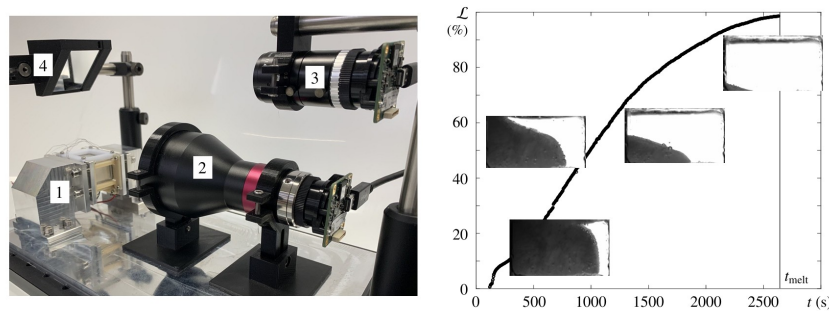


FIG. 1: (left) Prototype of the cuboidal cell experiment set-up: (1) cell assembly, (2) primary and (3) secondary cameras, (4) angular prism. (right) Evolution of the liquid PCM fraction \mathcal{L} (in %) during a ground test of a Marangoni experiment.

-
- [1] J. Porter, A. Laverón-Simavilla, M. M. Bou-Ali, X. Ruiz, F. Gavalda et al., The “Effect of Marangoni Convection on Heat Transfer in Phase Change Materials” experiment, *Acta Astron.* **210**, 212–223 (2023).
 - [2] P. Salgado Sánchez, J. M. Ezquerro, J. Fernández and J. Rodríguez, Thermocapillary effects during the melting of phase change materials in microgravity: heat transport enhancement, *Int. J. Heat Mass Transf.* **163**, 120478 (2020).
 - [3] U. Martínez, J. M. Ezquerro, J. Fernández and K. Olfe, The “Effect of Marangoni Convection on Heat Transfer in Phase Change Materials” experiment: Design and performance of the cuboidal cell, *Acta Astron.* **216**, 152-162 (2024).

Session 7 – Films and waves

Tuesday June 10, 13:45–15:15

Laser heating and melting of metals on nanoscale: Breakup of metal filaments & thermal crowding

Lou Kondic^{1,4}, Ryan H. Allaire^{2,5} and Linda J. Cummings^{3,6}

¹*Department of Mathematical Sciences, NJIT, NJ 07103, Newark, New Jersey, United States of America*
⁴*kondic@njit.edu*

²*Department of Mathematical Sciences, United States Military Academy, West Point, New York, United States of America*
⁵*ryan.allaire@westpoint.edu*

³*Department of Mathematical Sciences, NJIT, NJ 07103, Newark, New Jersey, United States of America*
⁶*linda.cummings@njit.edu*

We apply our recently developed asymptotic model [1, 2] to study the instability and breakup of metal filaments exposed to heating by laser pulses and placed on thermally conductive substrates. One particular aspect of this setup is that the heating is volumetric since the absorption length of the laser pulse is comparable to a typical filament thickness. In such a setup, absorption of thermal energy and filament evolution are coupled and must be considered self-consistently. The asymptotic model that we use allows for significant simplification, which is crucial both for understanding the main physical effects (including the relevance of Marangoni effect and of temperature dependence of fluid viscosity and thermal conductivity) and for developing efficient simulations of the filament evolution and subsequent nanoparticle formation. We focus in particular on the influence of thermal crowding, meaning that the evolution of the filaments depends on their size and number; Fig. 1 shows an example, see [3] for more details. This finding opens the door to considerations of self- and directed-assembly of metal nanoparticles via a suitable choice of the initial metal geometry on the nanoscale.

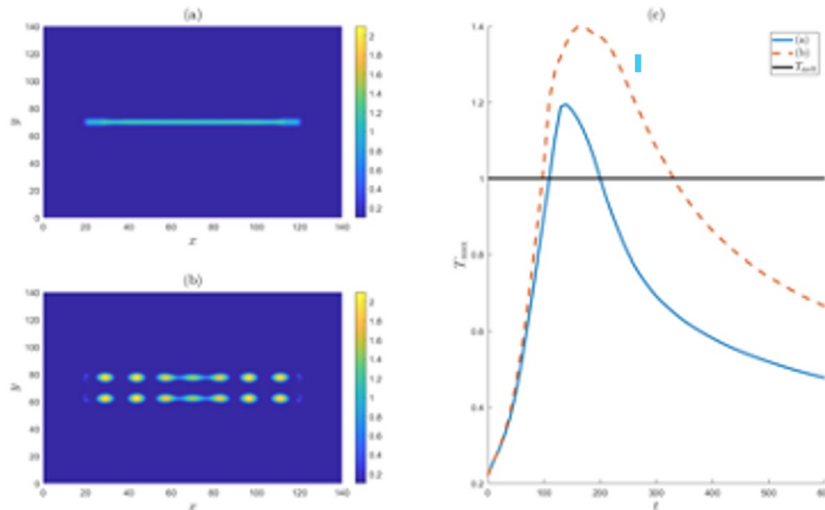


FIG. 1: Final configuration of one (a) and two (b) metal filaments placed on a thermally conductive substrate and exposed to the same laser pulse. (c) Maximum metal temperature as a function of time. Adopted from [3].

-
- [1] R. H. Allaire, L. J. Cummings, and L. Kondic, On efficient asymptotic modelling of thin films on thermally conductive substrates, *J. Fluid Mech.* **915**, A133 (2021).
 - [2] R. H. Allaire, L. J. Cummings, and L. Kondic, Influence of thermal effects on the breakup of thin films of nanometric thickness, *Phys. Rev. Fluids* **7**, 064001 (2022).
 - [3] R. H. Allaire, L. J. Cummings, and L. Kondic, Using Thermal Crowding to Direct Pattern Formation on the Nanoscale, *Phys. Rev. Lett.* **133**, 214003 (2024).

On the influence of the heat transfer at the free surface of a thermally-driven rotating annulus

Gabriel Meletti¹, Stéphane Abide², Uwe Harlander^{3,5}, Isabelle Raspo⁴ and Stéphane Viazzo⁴

¹Universitat Politècnica de Catalunya, Departament de Matemàtiques, 08028, Barcelona, Spain

²Université Côte d'Azur, CNRS, Laboratoire Jean Alexandre Dieudonné (LJAD), 06108 Nice Cedex 2, France

³Brandenburg University of Technology (BTU) Cottbus-Senftenberg, Department of Aerodynamics and Fluid Mechanics, 03046, Cottbus, Germany ⁵uwe.harlander@b-tu.de

⁴Aix Marseille Université, CNRS, Centrale Med, M2P2, 13451 Marseille Cedex 20, France

Experiments on rotating annuli that are differentially heated in the radial direction have largely contributed to a better understanding of baroclinic instabilities [1]. This configuration creates waves at a laboratory scale that are related to atmospheric circulations. Pioneer studies in baroclinic tanks have shown that experiments with low aspect ratios are more suitable to reproduce small-scale inertia gravity waves, but these tanks have a larger free surface, which leads to higher interactions with their surrounding environment. Considering the heat transferred through the free surface, the present work investigates its impacts on the baroclinic instability using direct numerical simulations (DNS) [2]

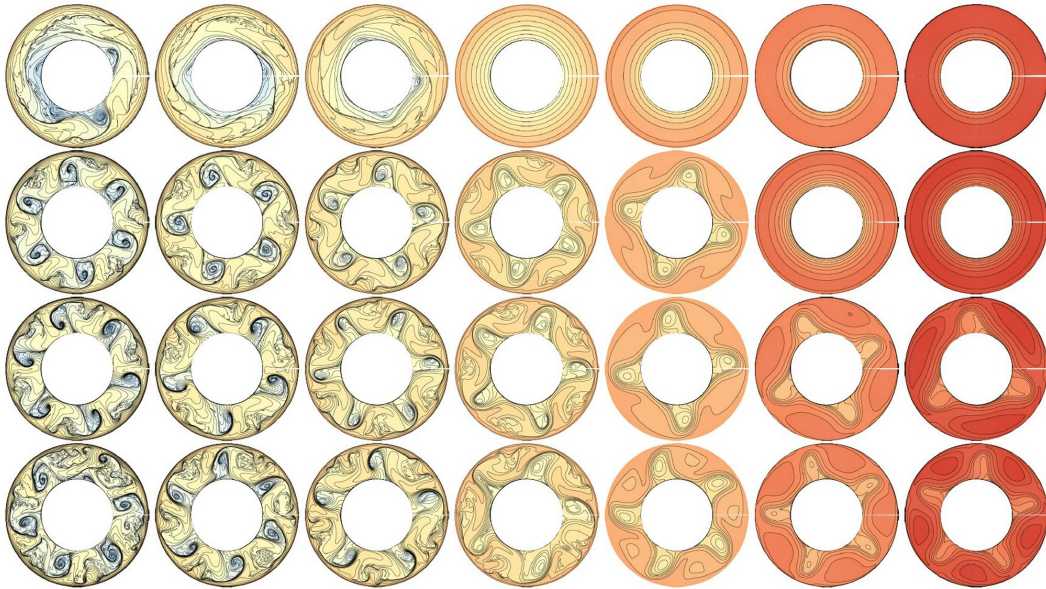


FIG. 1: Snapshots of the temperature surface highlighting the influence of the quiescent temperature on the baroclinic instability features. From left to right, the quiescent temperature systematically increased in increments of 1 within the interval $-3 \leq \Theta_q \leq +3$. From top to bottom, the rotation rates are incrementally raised by 0.1, spanning from $0.3 \leq \Omega \leq 0.6$ rpm.

-
- [1] U. Harlander, M. V. Kurgansky, K. Speer and M. Vincze, Baroclinic instability from an experimental perspective, *Comptes Rendus. Physique* **Online first**, 1–48 (2024).
[2] G. Meletti, S. Abide, U. Harlander, I. Raspo and S. Viazzo, On the influence of the heat transfer at the free surface of a thermally-driven rotating annulus, *Physics of Fluids* **accepted**, 1–25 (2025). (2011)

Cascading Sawtooth Patterns from Evaporating Salt-Surfactant Thin Films

Greg Paris^{1,3}, Kripa K. Varanasi^{2,5} and Samantha A. McBride^{1,4}

¹*Department of Mechanical Engineering and Applied Mechanics, University of Pennsylvania, PA 19104, Philadelphia, United States of America* ³*parisig@seas.upenn.edu*; ⁴*sammcb@seas.upenn.edu*
²*Department of Mechanical Engineering, Massachusetts Institute of Technology, MA 02139, Cambridge, United States of America* ⁵*varanasi@mit.edu*

Instabilities arising during evaporation of drops can enable self-assembly of a number of ordered micro- and nanoscale patterns through the controlled deposition of particles or solutes. Marangoni forces, in particular, become dominant at small length scales and can give rise to ordered array patterns due to pinch-off of regularly spaced microdroplets from a dewetting front [1–3]. In recent work, we demonstrated that such patterns can form from evaporating drops of water with saturated calcium sulfate on hydrophilic substrates due to solutal Marangoni forces [3]. Upon complete evaporation of the microdroplets and crystallization of the salt inside, ordered hexagonal array patterns composed of salt clusters are left behind (Fig. 1(i)). That same investigation found that when contact angles are lowered further, triangular/sawtooth structures emerge from the drying salt structures rather than ordered arrays (Fig. 1(ii)). However, all available evidence suggests that these triangular patterns, unlike the periodic arrays, are not controlled by Marangoni forces. For instance, seminal work by Deegan discovered remarkably similar triangular patterns emerging from drying drops of colloidal solution; where solutal effects should not be present [4]. In our experiments, addition of surfactant to salt solution disrupted array patterning, but did not disrupt sawtooth patterning. Triangular patterns were also observed to be invariant to salt chemistry and will appear for a variety of sparingly-soluble salts. A key feature of these sawtooth patterns, from both our work and others, is a sharp step-change in height of the deposited layer. For example, for colloidal deposition, deposition of a uniform monolayer of particles exhibited a step-change to a bilayer in a sawtooth fashion [4].

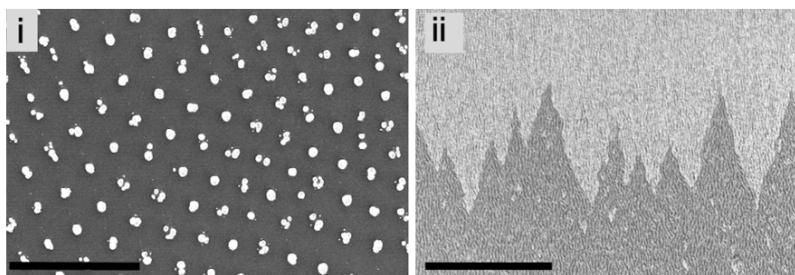


FIG. 1: SEM images of (i) hexagonal array pattern formed by solutal Marangoni forces in an evaporating drop of water with saturated calcium sulfate on a hydrophilic substrate, (ii) sawtooth patterns exhibiting a sharp step-change in height between the lighter phase and darker phase from the same system on a superhydrophilic substrate. Scale bar is $50 \mu\text{m}$. Adapted from [3].

If the thin-film instability giving rise to sawtooth patterns does not rely on Marangoni forces, how do these patterns form, and why are they so persistent across different chemical and colloidal systems? To probe these questions, we investigate the changes in the appearance and contact line motion associated with triangular patterns when surfactant is added to solution. In particular, at high surfactant concentrations we observe a cascading structure of triangle patterns that are almost reminiscent of a Sierpinski triangle (Fig. 2). Here, we present results from experiments in which evaporation temperature and surfactant concentration are systematically varied to probe the physics of this unusual thin film phenomena that gives rise to these patterns.

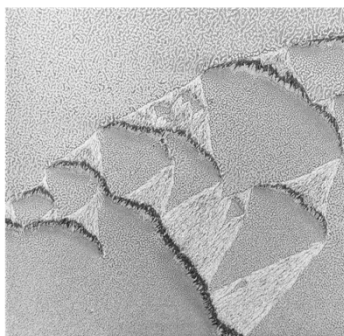


FIG. 2: SEM image of cascading triangle structure formed from evaporating films of saturated calcium sulfate solution and surfactant.

-
- [1] Y. Cai and B. Zhang Newby, Marangoni Flow-Induced Self-Assembly of Hexagonal and Stripelike Nanoparticle Patterns, *J. Am. Chem. Soc.* **130**, 6076 (2008).
 - [2] X. Fanton and A. M. Cazabat, Spreading and Instabilities Induced by a Solutal Marangoni Effect, *Langmuir* **14**, 2554 (1998).
 - [3] S. A. McBride, S. Atis, A. A. Pahlavan, and K. K. Varanasi, Crystal Patterning from Aqueous Solutions via Solutal Instabilities, *ACS Appl. Mater. Interfaces* **16**, 70980 (2024).
 - [4] R. D. Deegan, Pattern formation in drying drops, *Phys. Rev. E* **61**, 475 (2000).
 - [5] C. S. Bretherton and E. A. Spiegel, Intermittency through modulational instability, *Physics Letters A* **96**, 152 (1983).

Free surface flows over and inside a porous microtube

Phillipe Beltrame^{1,3}, and Florian Cajot^{2,4}

¹UMR1114 EMMAH INRAE-AU, Avignon Université, F-84194 Avignon, France

³*philippe.beltrame@univ-avignon.fr*

²ISTO, UMR 7327, Université d'Orléans, CNRS BRGM, F-45071 Orléans, France

⁴*florian.cajot@univ-orleans.fr*

The issue of flow along porous microtubes arises in many industrial contexts, particularly in the case of hollow fiber membranes. These can be made of organic material (cellulose) which has an amphiphilic character. Flow in a microtube has been the subject of many studies in the case of an impermeable wall. Recently, we focused on the wettability effect by studying microtube with thin film in inertialess limit [1, 2]. We have highlighted many flow regimes specific to partial wetting. Notably, traveling waves of drop train that consists of a clustering of drops without coalescence. However, little has been done in the case of a porous wall. The objective of this article is the modelling and the simulation of film flow dynamics inside and over a narrow tube of a porous wall and driven by a longitudinal force as the gravity. Due to amphiphilic properties of the hollow fiber, Darcy's model no longer yields and a free energy based model as to be considered in the wall [3]. Moreover, according to [4], flows are not only hydrodynamically but also thermodynamically coupled. We propose to combine the hydrodynamic model of [1] for the free surface flows over the fiber with the approach developed in [3, 4] for water exchange between thin films and the porous wall. We associate to each medium a free energy functional depending on the order parameter in each medium (thin liquid films and porous medium). Evolution equations are written in the form of a gradient dynamics for non conserved order fields [5, 6].

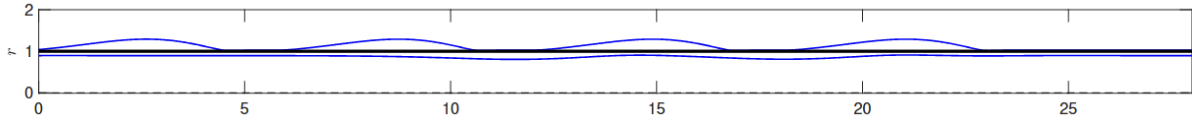


FIG. 1: Radial profiles (blue line) of axisymmetric flow over and through the porous wall of a hollow fiber. The bold black line represents the porous wall. The driving force is horizontal.

The simulation of axisymmetric thin film flows highlights complex interactions between the inside and outside flows notably due to the amphiphilic properties of the porous wall (Fig. 1). This rich behavior is analyzed using time integration, path-following methods, and numerical bifurcation analysis.

-
- [1] P. Beltrame, Partial and complete wetting in a microtube, *EPL* **121**:64002 (2018).
 - [2] P. Beltrame, Drop train flow in a microtube, *Eur. Phys. J. Spec. Top.*, **232**(4), 435–442 (2023).
 - [3] P. Beltrame and F. Cajot, Model of hydrophobic porous media applied to stratified media: Water trapping, intermittent flow and fingering instability, *EPL* **138**:53004 (2022).
 - [4] F. Cajot, C. Doussan, S. Hartmann and P. Beltrame, Model of drop infiltration into a thin amphiphilic porous medium, *J. Colloid Interface Sci.* **684**, 35–46 (2025).

Reduced equations for a thin liquid film subjected to solar radiation

Omar A. A. Mohamed^{1,4}, Christian Ruyer-Quil^{2,5} and Luca Biancofiore^{3,6}

¹Department of Mechanical Engineering, Bilkent University, 06800, Ankara, Türkiye,

⁴omair.mohamed@bilkent.edu.tr

²CNRS, LOCIE, Université Savoie Mont Blanc, 73000 Chambéry, France, ⁵ruyerquc@univ-smb.fr

³Department of Industrial and Information Engineering and Economics, University of L'Aquila, 67100 L'Aquila, Italy, ⁶luca.biancofiore@univaq.it

The operating temperature of a photovoltaic (PV) cell can be drastically reduced by the introduction of a thin film of fluid flowing over its surface, which has been shown to result in increased electrical output [1], extended operating lifetime [2], as well as preventing the soiling its surface. Moreover, studies have indicated that the heat transfer across a wavy liquid film can be up to 10 – 100% larger than that of a flat film [3], and therefore, investigating the complex relationship between the dynamic behavior of the wavy liquid film and the temperature profile across it can yield valuable insights towards optimizing such a system. Typically, dealing with this problem requires the numerical solution of the Fourier heat problem coupled with the Navier-Stokes equations, which is prohibitively expensive for the parametric studies required for a comprehensive understanding of the physical phenomena involved.

Therefore, we tackle this complex problem by employing the Weighted Integral Boundary Layer [4] (WIBL) method to model the hydrodynamics of the film in conjunction with an asymptotic decomposition of the temperature variable [5]. The system of equations governing the temperature field is then truncated consistently in line with the *least-degeneracy principle*, such that all physical effects are retained at leading order. We varied the complexity of this decomposition to produce a hierarchy of models of increasing sophistication, each facilitated by an appropriate set of gauge conditions. This allowed efficiently inspecting the influence of the different physical effects on the film's thermal profile by tracking the evolution of the temperature at the free surface and the solid wall. Notably, the overall temperature field can be reconstructed by projecting the ansatz chosen for the temperature correction using polynomial functions. Fig. 1 showcases simulations of the hydrothermal evolution of the liquid film using the simplest single-variable model and a more complex two-variable model, for two distinct cases: Fig. 1(a) presents a case where the radiation absorbed at the solid wall mostly enters into the liquid bulk resulting in elevated temperatures at both the solid wall and liquid interface, while Fig. 1(b) demonstrates the resulting evolution when the incoming radiation is mostly conducted into the solid wall and away from the liquid film.

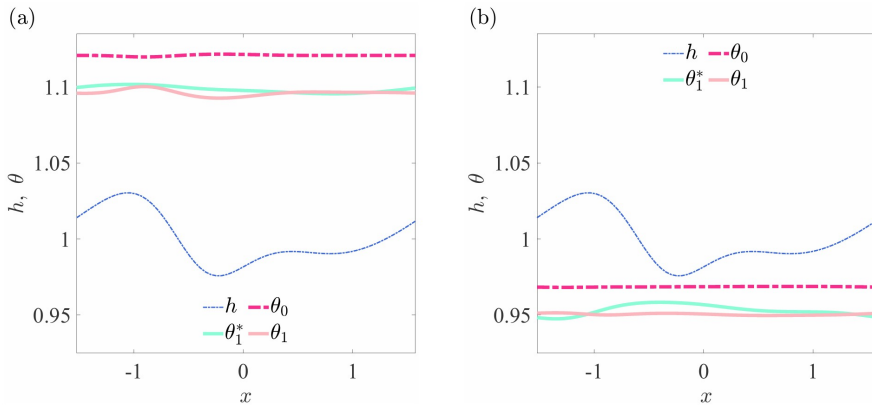


FIG. 1: Numerical simulations of the coupled liquid film interface height and temperature field where θ_1^* is the liquid interface temperature obtained from a single-variable model, and θ_0 and θ_1 are the liquid's wall and interface temperatures from a two-variable model, respectively. (a) The absorbed radiation at the solid wall mostly enters into the liquid bulk. (b) The absorbed radiation is mostly conducted into the solid wall.

-
- [1] S. Krauter, *Solar Energy Materials and Solar Cells*, vol. 82, no. 1, pp. 131–137, 2004. CANCUN 2003.
- [2] S. Kurtz, K. Whitfield, D. Miller, J. Joyce, J. Wohlgemuth, M. Kempe, N. Dhere, N. Bosco, and T. Zgonena, *2009 34th IEEE Photovoltaic Specialists Conference (PVSC)*, pp. 002399–002404, 2009.
- [3] P. Yoshimura, T. Nosoko, and T. Nagata, *Chemical Engineering Science*, vol. **51**, no. 8, p. 1231 – 1240, 1996.
- [4] C. Ruyer-Quil and P. Manneville, *Eur. Phys. J. B*, vol. **15**, pp. 357–369, May 2000.
- [5] N. Cellier and C. Ruyer-Quil, *Int. J. Heat Mass Transf.*, vol. **154**, p. 119700, June 2020.

Parasitic capillary ripples on finite amplitude surface waves

Ratul Dasgupta^{1,2}, Nikhil Yewale¹ and Vinod Kadari¹

¹*Department of Chemical Engineering, IIT Bombay, 400076, Powai, India*

²*dasgupta.ratul@iitb.ac.in*

I. INTRODUCTION AND MOTIVATION

Parasitic capillary ripples are easily observed on the forward face of finite amplitude travelling, surface wave trains [1], both in the lab and in the open ocean. Despite the theoretical modelling of this phenomena dating to 1887 [2], several fundamental questions remain open; particularly their role in micro-breaking of ocean surface waves (i.e. wave breaking without significant air entrainment) in the absence of wind (see recent studies with and without wind [3, 4] respectively). Here, we carefully study these ripples, as they develop on the forward face (only) of a travelling finite-amplitude Stokes wave. The theoretical model of these waves by [5], employed Rayleigh's theory computing the Green function for the effect of a travelling pressure forcing (delta function) on the free-surface of a stream moving with uniform velocity U . The steady-state free-surface shape as obtained by Rayleigh, has a marked asymmetry in the far-field (i.e. far from the delta function), being dominated by pure capillary and pure gravity waves respectively. It will be seen that for moderately steep Stokes wave, similar ripples preferentially develop only on its forward face. These ripples then extract energy from the primary wave. This extraction does not produce significant distortion of the primary waveform at moderate steepness. However, as the Stokes wave steepness increases, the extraction of energy is found to generate an $O(1)$ distortion of the Stokes wave shape (thereby justifying the adjective 'parasitic' for these ripples).

II. RESULTS AND OBSERVATIONS

In order to study this phenomena, we seed our computations (Basilisk) initially with an accurately computed Stokes wave (with only gravity and no surface tension). The simulations are then evolved in time including both gravity and surface tension. Figure 1 (see next page) represents a Stokes wave which has been evolved in time in simulations using Basilisk [6]. As the initial Stokes wave provided as input into Basilisk, does not have surface tension, there are no parasitic ripples initially. However these develop with time as is seen in the figure. For this case the steepness of the Stokes wave is chosen to be around 0.3. It is seen that a capillary wave train is formed on the forward face of the wave (the primary wave travels from right to left in this figure). Physically, these ripples appear due to the sharp crests which develop in the Stokes wave as its steepness increases. Around a sharp crest, a surface tension induced pressure jump is generated which acts as a source of distributed pressure, thereby generating the ripple pattern preferentially only on one side of the Stokes wave. In order to model our simulational observations, we calculate the surface displacement $\zeta(s)$ taking into account parasitic capillary ripples following the theoretical model of [5]. The distorted interface generated by distributed action of surface-tension ($T_\kappa(s)$) is given by following integral along the arc length s .

$$\zeta(s) = \int_s^\infty \frac{2T\kappa(s')}{D(\phi)D(\phi')} \frac{F(\phi)}{F(\phi')} \sin(\theta' - \theta) ds' \quad (5)$$

where $D(\phi) = (U^4 - 4g * T)^{\frac{1}{4}}$, $F = (\phi) = \exp\left(4\nu \int_0^\phi \frac{k^2}{D^2} d\phi\right)$, $\theta(\phi) = \int_0^\phi \frac{k}{U} d\phi$. In computing the integral in eqn. 1, we obtain as a input the fluid velocity at the surface (U), the effective gravity g^* and curvature k from the Stokes wave itself computed with only gravity. Here k is the capillary wave number. The effect of these ripples and conditions under which they can cause micro-breaking on the forward face of the Stokes wave will be discussed in the conference.

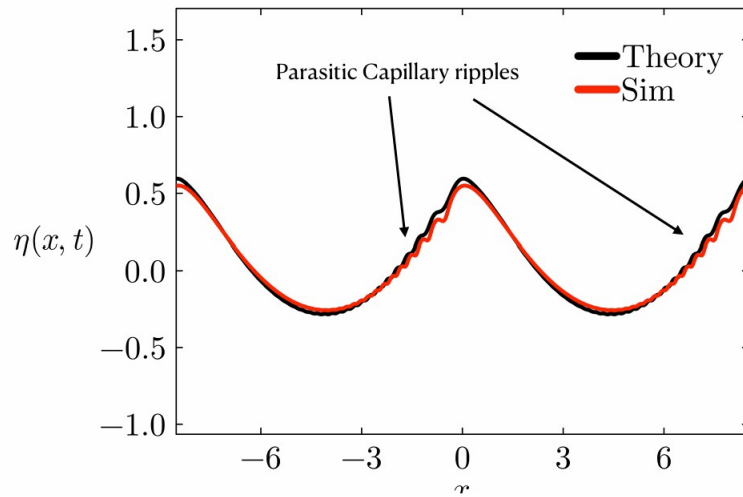


FIG. 1: Comparison of DNS with theory (eqn 1) of parasitic capillary ripples [5] on a (air-water) Stokes wave of steepness 0.3. Note the good agreement between theory and DNS.

-
- [1] Cox, Charles S. "Measurements of slopes of high-frequency wind waves." *J. Mar. Res.* **16** (1958): 199-225.
 - [2] Lord Rayleigh, The form of standing waves on the surface of running water, *Proc. London Math. Soc.* **15**, pp. 69, 1883.
 - [3] Xu, Chang, and Marc Perlin. "Parasitic waves and micro-breaking on highly nonlinear gravity-capillary waves in a convergent channel." *Journal of Fluid Mechanics* **962** (2023): A46.
 - [4] Dosaev, Alexander, Yuliya I. Troitskaya, and Victor I. Shrira. "On the physical mechanism of front-back asymmetry of non-breaking gravity-capillary waves." *Journal of Fluid Mechanics* **906** (2021): A11.
 - [5] M. S. Longuet-Higgins, Parasitic capillary waves : a direct calculation, *J. Fluid Mech.* (1995), vol. **301**, pp. 79-107
 - [6] basilisk.fr

Session 8 – Thermocapillarity and thermal effects

Tuesday June 10, 15:45–17:00

Manipulation of Particle Deposition of Inkjet-printed Droplets with the Combined Effects of Concentration and Temperature Marangoni Flows

Mengsen Zhang^{1,2} and Lu Qiu^{1,3}

¹School of Energy and Power Engineering, BUAA, 100191, Beijing, China

²zhangmengsen@buaa.edu.cn; ³qiulu@buaa.edu.cn

The deposition characteristics of inkjet-printed nanoparticle droplets directly impact the performance of device manufacturing. During the evaporation process of the droplets, the internal Marangoni flow is a critical factor determining the deposition characteristics of nanoparticles [1]. By adjusting the magnitude and direction of the Marangoni flow, the deposition behavior of the droplets can be significantly altered.

In this study, we employed a heated substrate method, setting the temperature at the droplet s three-phase contact line higher than that at the droplet s top. This results in a temperature-driven Marangoni flow moving from the center of the droplet towards the three-phase line, enhancing the coffee ring effect. Simultaneously, we utilized a binary solvent ink (ethylene glycol and isopropanol, with a mass fraction of 20% ITO nanoparticles), ensuring that the concentration of isopropanol at the three-phase line is higher than that at the top of the droplet. This generates a concentration-driven Marangoni flow moving from the three-phase line towards the center of the droplet, suppressing the coffee ring effect.

By adjusting the substrate temperature T_w and the ratio of the binary solvent in the droplet α , we can control the relative magnitudes of these two Marangoni flows, thereby influencing the direction and intensity of the total Marangoni flow. We calculated the strengths of the internal flows using the temperature Marangoni number $Ma_T = R(d\sigma/dT)\Delta T/\mu\alpha$, the concentration Marangoni number $Ma_C = R(d\sigma/dC)\Delta C/\mu D$, and the capillary number $La = \rho l\sigma_w/\mu^2$, as shown in fig. 1. Based on the dimensionless criterion number $M = Ma_C/(Ma_T + La)$, we can control and predict the magnitude and direction of the Marangoni effect. When ($M < 1$), the concentration Marangoni flow dominates over the temperature Marangoni flow, resulting in a uniform deposition pattern.

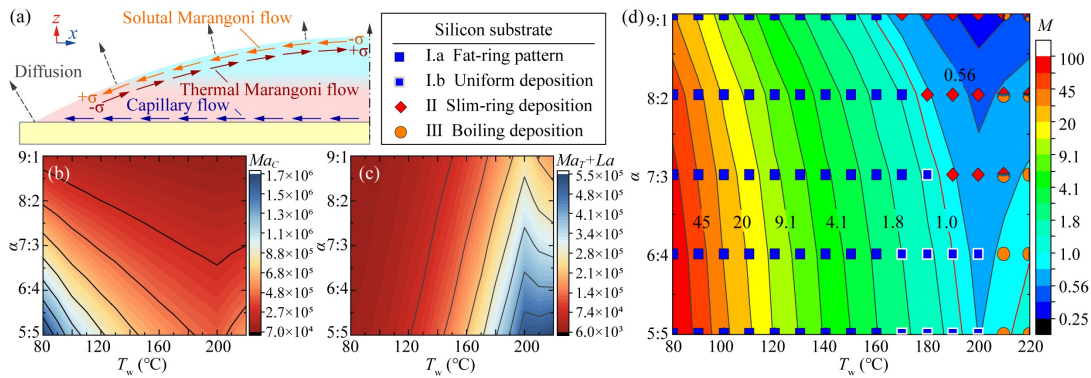


FIG. 1: (a) The internal flow of droplet evaporation. (b-c) The temperature Marangoni number and concentration Marangoni number contour. (d) Comparison of the dimensionless number M contour to the deposition pattern phase diagram.

[1] H. Zargartalebi, S. H. Hejazi and A. Sanati-Nezhad, Self-assembly of Highly Ordered Micro- and Nanoparticle Deposits, Nat. Commun. **13**, 3085 (2022).

Numerical study of Marangoni instability: effect of interface deformation

Hector Valdez¹, Jean Cousin¹ and Jorge César Brändle de Motta^{1,2}

¹Univ Rouen Normandie, INSA Rouen Normandie, CNRS, CORIA UMR 6614, F-76000 Rouen, France

²jorge.brandle@coria.fr

The Marangoni instability has been studied over the last century using theoretical, numerical and experimental approaches. This instability was found to be dependent on many physical parameters. In experiments, the effect of gravity cannot be suppressed without using extremely expensive studies in microgravity. Numerical simulations are a good alternative to understand this instability and have shown excellent agreement with experiments in the past. However, in most of the numerical studies performed in the past, the interface is assumed to be flat or slightly deformed. This study proposes to investigate a wide range set of parameters using direct numerical simulations to analyse the effect of interface deformations.

Within this work we develop a new numerical implementation of thermocapillary effects based on the Coupled Levelset-Volume of Fluid approach, [1, 2]. The new method is presented along with canonical validations. A series of simulations of the Marangoni instability are carried out. The reference case is the one proposed by Eckert et al. [3], which is also used as a cross-validation. The figure 1 shows the temperature and velocity field of this reference simulation.

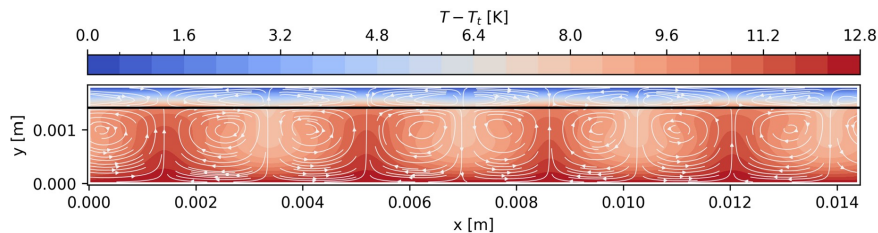


FIG. 1: Temperature field and velocity streamlines of the reference test case.

First, many 2D simulations are performed by varying the dimensionless numbers. The effect of thermal expansion and surface tension is studied by varying the Rayleigh (Ra) and Capillary (Ca) numbers respectively. The reference case shows small changes due to thermal expansion, which appear only when the Ra is increased. On the other hand, a large Ca shows larger deformations of the interface. However, due to the high density ratio, the interface remains almost flat. A diagram in the Ra Ca plane is proposed to show the different behaviours.

Then, some selected simulations are performed in 3D. Similar behaviour is observed, but with different region boundaries. The interface patterns are studied using classical metrics.

I. ACKNOWLEDGEMENTS

This work was supported by LabEx EMC3 through the HILIMBA project. This work was performed using HPC resources from GENCI (Grant A0132B1010) and CRIANN (201 704).

-
- [1] T. MÉnard, S. Tanguy and A. Berlemont, Coupling level set/VOF/ghost fluid methods: Validation and application to 3D simulation of the primary break-up of a liquid jet, *Int. J. Multiph. Flow*, **33**, 510–524 (2007).
 - [2] H. Valdez, Simulation of thermally driven two-phase flows, Ph.D. Rouen-Normandie University (2024).
 - [3] K. Eckert, M. Bestehorn and A. Thess, Square cells in surface-tension-driven Bénard convection: experiment and theory, *J. Fluid Mech.* **356**, 155–197 (1998).

Experimental study on the twisted patterns of coherent structure formed by low-Stokes-number particles in a concave liquid bridge

Shin Noguchi^{1,2,3} and Ichiro Ueno^{1,4}

¹*Dept. of Mech. Aerospace Eng., Faculty of Sci. and Tech., Tokyo Univ. Science, Japan*
²*7522703@ed.tus.ac.jp*; ³*7522703@alumni.tus.ac.jp*; ⁴*ich@rs.tus.ac.jp*

The inhomogeneous distribution of microscopic particles in convective systems within relatively closed spaces has been widely reported in various systems, such as lid-driven cavities [1, 2] and rotating drums [3, 4]. The confined environment investigated in our research is a half-zone liquid bridge (see FIG. 1). The thermocapillary-driven flow on the free surface is induced by a designated temperature difference, $\Delta T \equiv (T_H - T_C)$, imposed between the two end surfaces of the liquid bridge. Our focal point is on the coherent structures formed by low-Stokes-number particles moving within the closed-space thermocapillary convection field in the liquid bridge, so-called Particle Accumulation Structure (PAS) [5]. Since its discovery, an extensive body of research has been accumulated on this phenomenon. However, while most studies have focused on systems containing a single type of particle suspended in the liquid bridge, solid-liquid two-phase flows typically involve dispersed solid particles with varying diameters. The control of solid-particle dispersion in space is crucial, particularly in techniques for dispersing solids of different sizes and shapes. Recently, Noguchi and Ueno [6] reported that in a mixed systems of particles with different diameters, distinct coherent structures with similar structure are formed for each particle size, and these structures coexist. In this study, we reveal the twisted patterns (see FIG. 2) and quantitatively characterize their torsion of the KAM tori, which may emerge in the thermal flow field and act as particle attractors, by analyzing the envelope surfaces of particle trajectories that constitute distinct coherent structures, as reported in the previous study by Noguchi and Ueno [6]. We acknowledge financial support by Grant-in-Aid for Challenging Research (Exploratory) (grant number: 20K20977) from the JSPS.

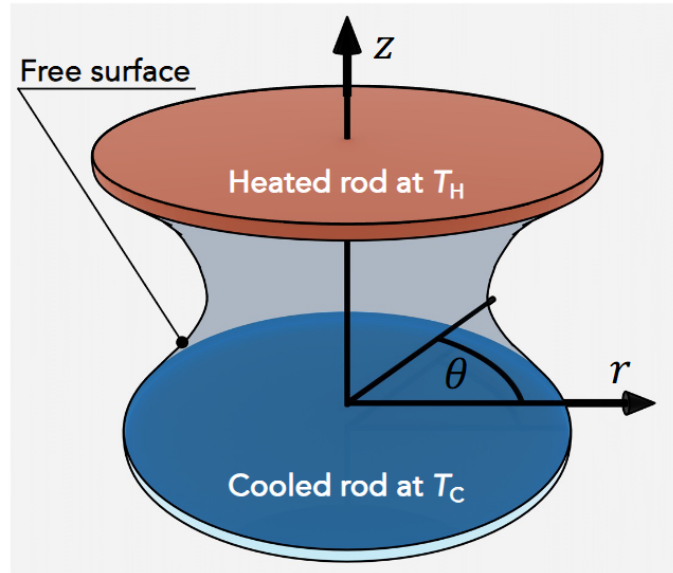


FIG. 1: Schematic of a half-zone liquid bridge.

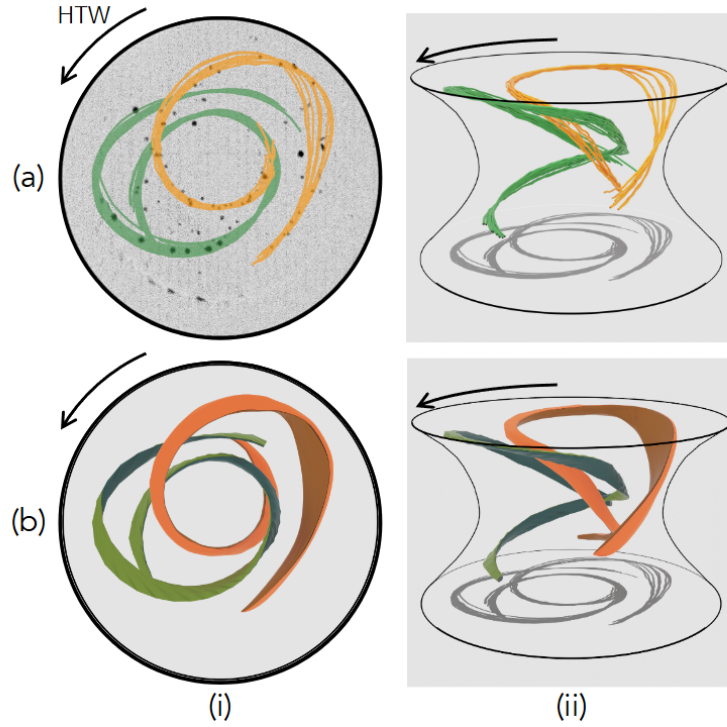


FIG. 2: Typical examples of (a) reconstructed particle trajectories and (b) envelope surfaces of particle trajectories, shown in (i) top view and (ii) bird's-eye view, under the conditions of $\Delta T = 22$ K or $Ma = 1.24 \times 10^4$ in a liquid bridge with $\Gamma = 1.2$ and $V/V_0 \approx 0.5$. In Panel (a), the orange and green lines represent particle trajectories for $d_p = 15 \mu m$ and $30 \mu m$, respectively, where both particle types are suspended simultaneously. In Panel (b), the envelope surfaces are color-coded for visibility: orange and brown for the orange particle trajectories, and light and dark green for the green particle trajectories.

-
- [1] H. Wu, F. Romanò, for the motion of finite-size particles in a two-sided lid-driven cavity, *PAMM* **17** (2017) 669–670.
 - [2] H. Wu, F. Romanò, H. C. Kuhlmann, Attractors for the motion of a finite-size particle in a cuboidal lid-driven cavity, *Journal of Fluid Mechanics* **955** (2023) A16.
 - [3] F. Romanò, 2016, Particle accumulation in incompressible laminar flows due to particle-boundary interaction.
 - [4] F. Romanò, A. Hajisharifi, H. C. Kuhlmann, Cellular flow in a partially filled rotating drum: regular and chaotic advection, *Journal of Fluid Mechanics* **825** (2017) 631 – 650.
 - [5] D. Schwabe, P. Hintz, S. Frank, New features of thermocapillary convection in floating zones revealed by tracer particle accumulation structure (PAS), *Microgravity Science and Technology* **9** (1996) 163–168.
 - [6] S. Noguchi and I. Ueno. Quantitative analysis of particle behavior constituting multiple coherent structures in liquid bridges. *Journal of Colloid and Interface Science*, **684**:29–42, 2025.

Thermocapillary Effects on the Migration, Reverse-Encapsulation, and Core-Release Dynamics of Compound Droplets

Yao Xiao^{1,2}, Liangqi Zhang^{1,3} and Zhong Zeng^{1,4}

¹College of Aerospace Engineering, Chongqing University, 400044, Chongqing, China

²xiaoyao79@cqu.edu.cn, ³zhangliangqi@cqu.edu.cn, ⁴zzeng@cqu.edu.cn

Multiphase flows are a crucial area of research in science and engineering, with broad applications spanning water evaporation, condensation, oil and gas production, inkjet printing[1], and microfluidics[2]. Droplet dynamics, in particular, have attracted significant attention due to their relevance in the development of advanced technologies, including targeted drug delivery, materials processing, and biomedical testing[2]. In practical scenarios, the size and internal morphology of three-phase droplets are influenced by factors such as microfluidic device geometry, flow rate ratios, viscosity ratios, and surface tension ratios[3]. Once formed, these droplets can be manipulated through external heat sources or temperature fields. This study addresses a gap in the literature by investigating the thermocapillary effects on the migration and release dynamics of compound droplets as shown in Fig. 1, a topic that has remained largely unexplored. While previous research has primarily focused on two-phase systems, this work expands the field by examining how the Marangoni number and Reynolds number influence the reverse-encapsulation and core-release processes in complex multi-fluid systems. The core-release process involves the separation of the inner droplet from its encapsulated state due to external forces, such as thermocapillary effects, transitioning the system from a core-shell structure to two separate droplets. Conversely, the reverse-encapsulation process involves the contraction of the outer fluid layer and the migration of the inner droplet to re-encapsulate the outer droplet, reforming the core-shell structure under thermocapillary effects. Using a reduction-consistent phase-field model for incompressible N-phase flows, this study provides a comprehensive analysis of these processes, highlighting the influence of dimensionless parameters such as the Marangoni number, Reynolds number, and the radius ratio of the inner-to-middle fluid in a core-shell structure. The findings show that while the Marangoni number has minimal impact on migration velocity, thermocapillary forces are the primary driver of the processes. The Reynolds number significantly affects encapsulation dynamics, with higher values resulting in slower, more turbulent processes. Furthermore, the radius ratio plays a critical role in determining the behaviors of reverse-encapsulation and core-release processes. These results enhance our understanding of multiphase fluid dynamics and offer important implications for applications in microfluidics, targeted drug delivery, and advanced materials synthesis.

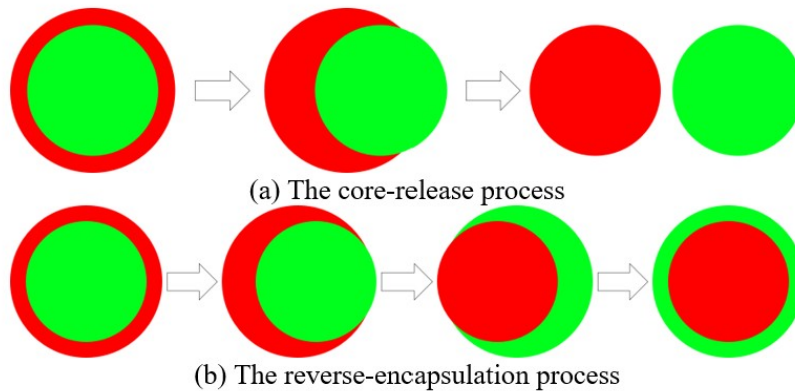


FIG. 1: Schematic representation of two processes in a compound droplet: (a) the core-release process; (b) the reverse-encapsulation process. (Red and green colors represent two different phase flows, and the background color represents the third phase flow) [4]

-
- [1] Basaran OA, Gao H, Bhat PP. Nonstandard Inkjets. *Annual Review of Fluid Mechanics*, 2013, 45(1): 85-113.
 - [2] Gérard A, Woolfe A, Mottet G, Reichen M, Castrillon C, Menrath V, et al. High-throughput single-cell activity-based screening and sequencing of antibodies using droplet microfluidics. *Nature biotechnology*, 2020, 38(6): 715-721.
 - [3] Pang Y, Du Y, Wang J, Liu ZM. Generation of single/double Janus emulsion droplets in co-flowing microtube. *International Journal of Multiphase Flow*, 2019, 113: 199-207.
 - [4] Yao X, Zhong Z, Liangqi Z, et al, The reverse-encapsulation and core-release process of a compound droplet under thermocapillary effects [J]. *International Journal of Heat and Mass Transfer*, 2025, 238: 126468

Solutal and Thermal Marangoni Convection at Growing Oxygen Bubbles during Water Electrolysis

Alexander Babich¹, Aleksandr Bashkatov³, Milad Eftekhari¹, Gerd Mutschke¹, Xuegeng Yang² and Kerstin Eckert^{1,2}

¹Institute of Fluid Dynamics, HZDR, 01328, Dresden, Germany

²Institute of Process Engineering and Environmental Technology, TU, Dresden, 01069, Dresden, Germany

³Max Planck Center for Complex Fluid Dynamics and J. M. Burgers Centre for Fluid Dynamics, University of Twente, 7522 NB, Enschede, Netherlands

In this study, we investigate the behavior of oxygen bubbles generated at a microelectrode in an acidic electrolyte (0.5 mol/L H_2SO_4) under high potentials. Using a three-electrode electrochemical cell, single oxygen bubbles were produced at the anode and monitored with high-speed shadowgraphy (up to 10 kHz frame rate). Concurrently, the velocity fields and refractive index variations around the bubble were measured using particle tracking velocimetry (PTV) and schlieren imaging, respectively.

Our experiments reveal distinct growth modes: the slow growth mode (sg) and the fast growth mode (fg). The sg mode is governed by solutal Marangoni convection, driven by proton production during oxygen evolution, which increases the sulfuric acid concentration and surface tension at the bubble base. Conversely, the fg mode is dominated by thermocapillary Marangoni convection, induced by localized heating at the bubble interface. Particle tracks obtained via PTV and schlieren images (Fig. 1) illustrate the contrasting vortex patterns generated during sg and fg modes. The transition between these modes is attributed to instabilities in the force equilibrium at the bubble interface.

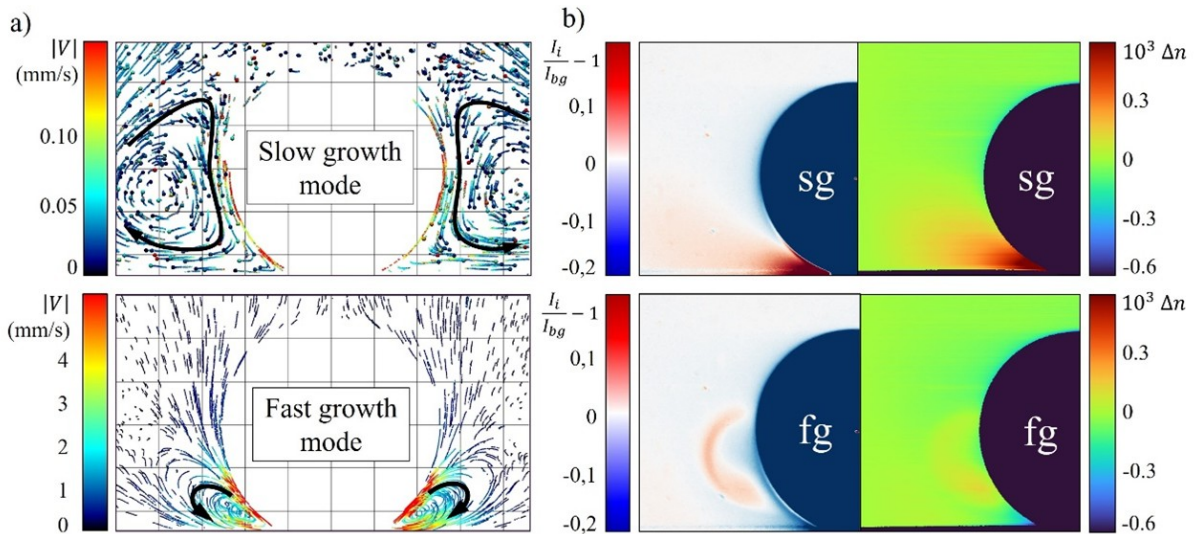


FIG. 2: a) Particle tracks obtained by PTV. The arrows in the figure show the direction of vortex motion. b) Dimensionless Schlieren images and refractive index fields.

For the first time, we experimentally confirm the existence of solutal Marangoni convection, corroborating predictions from theoretical studies [1, 2]. These findings offer new insights into the mechanisms governing bubble dynamics during electrolysis and have potential implications for optimizing gas evolution processes.

I. ACKNOWLEDGEMENTS

This project is supported by the German Space Agency (DLR), with funds provided by the Federal Ministry of Economics and Technology (BMWi) due to an enactment of the German Bundestag under Grant No. DLR 50WM2352 (project MADAGAS III), H2Giga (BMBF, 03HY123E) and the Hydrogen Lab of the School of Engineering of TU Dresden.

- [1] A. Meulenbroek, N. Deen, and A. Vreman, Marangoni forces on electrolytic bubbles on microelectrodes, *Electrochimica Acta*, 144510 (2024).
- [2] S. Park, L. Liu, Ç. Demirkır, O. van der Heijden, D. Lohse, D. Krug, and M. T. Koper, Solutal marangoni effect determines bubble dynamics during electrocatalytic hydrogen evolution, *Nature Chemistry* **15**, 1532 (2023).

Session 9 – Surfactants and particle suspensions II

Wednesday June 11, 9:00–10:00

Using light-actuated photosurfactants for liquid mixing and sculpting*

Demetrios T. Papageorgiou^{1,2}, Michael D. Mayer^{1,3} and Niall Oswald^{1,4}

¹Department of Mathematics, Imperial College London, London SW7 2AZ, United Kingdom

²d.papageorgiou@imperial.ac.uk; ³m.mayer@imperial.ac.uk;

⁴niall.oswald20@imperial.ac.uk

Photosurfactants are soluble surface active agents that can change conformation under illumination of different frequencies. When exposed to visible light they conform to the *trans state*. Illumination by shorter wavelength UV light transforms trans surfactants to the *cis state* by bending their hydrocarbon tails. The process is reversible. We introduce mathematical models that describe the two surfactant species, their exchange kinetics in the bulk due to light switching, their adsorption/desorption from interfaces (e.g. air-water), and the exchange between them at the interface (see also [1] for a study of liquid threads). In general, this leads to nonlinear coupled systems for the flow, surfactant concentrations (bulk and interfacial) and nonlinear interfacial deflections, to produce a challenging mathematical problem. We use the models to study the fundamental problem of harnessing non-uniform light gradients to induce mixing and interfacial non-uniformities in horizontal liquid layers wetting a solid substrate. This is carried out asymptotically for small spatially varying light gradients superimposed onto a background uniform illumination. We obtain analytical solutions and use them to reproduce experimental observations of light-actuated particle trapping by a local light pulse. Furthermore, we present light profiles that generically induce Marangoni flows with vortical structures - see figures 1a-1b. Finally, we use our analytical framework to show that inverse problems can be posed and solved to determine the required light gradients needed to produce a pre-determined interfacial amplitudes to achieve controlled sculpting.

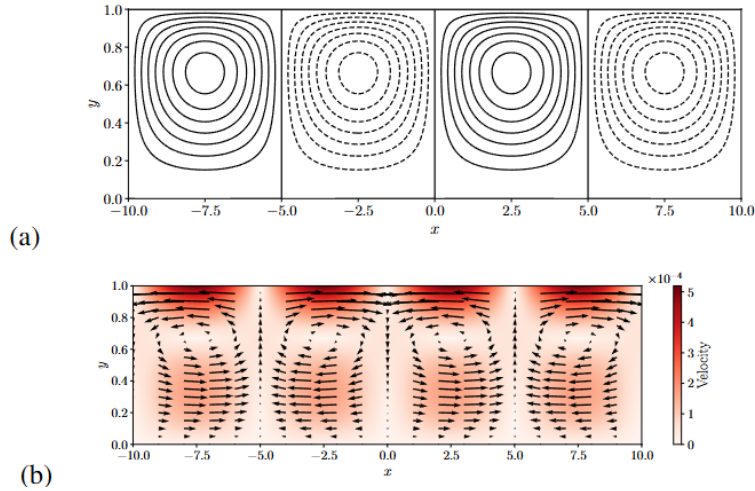


FIG. 1: Mixing due to a spatially periodic illumination superimposed on a uniform background light state: (a) Streamlines and corresponding (b) velocity field for the fluid flow at first order under.

I. ACKNOWLEDGEMENTS

Partly supported by supported by CBET-EPSRC Grant EP/V062298/1

[1] M. D. Mayer, T. L. Kirk and D. T. Papageorgiou, Stability of a photosurfactant-laden viscous liquid thread under illumination, J. Fluid Mech. 983 A10 (2024).

Modeling Marangoni flows induced by photo-responsive surfactants

Paolo Luzzatto-Fegiz¹, Xichen Liang², Kseniia M. Karnaukh³, Javier Read de Alaniz³ and Yangying Zhu¹

¹Mechanical Engineering Department, University of California, Santa Barbara, CA 93106 United States of America

²Chemical Engineering Department, University of California, Santa Barbara, CA 93106 United States of America

³Chemical Department, University of California, Santa Barbara, CA 93106 United States of America

Photo-responsive surfactants can reversibly change their molecular conformation when illuminated, thereby tuning interfacial tensions in a multi-phase flow, as shown in fig. 1a. These “photosurfactants” can therefore induce targeted and complex Marangoni flows (e.g.[1]), including droplet and bubble motion in the fluid interior or along interfaces (as sketched in fig.1b), and may enable new avenues for enhancing the performance of microfluidic, thermal, and water harvesting devices. However, to the best of our knowledge, there are currently no general models for predicting the resulting flows from a given combination of photosurfactant type, geometry, illumination and fluid properties. As a consequence, the potential capabilities and benefits that could be derived from photosurfactants remain largely unknown.

In this conference contribution, we examine several photosurfactants, and leverage experimental data that we gather from nuclear magnetic resonance, time-dependent tensiometry, as well as photosurfactant-driven flows of increasing complexity, both on Earth and in microgravity [2, 3]. We deduce models for the photo-switch mechanism and the attendant tension change, which we use to implement numerical simulations, as well as to derive scaling relations for several key flows of fundamental and technological importance (see [3]; an example is shown in fig.1c).

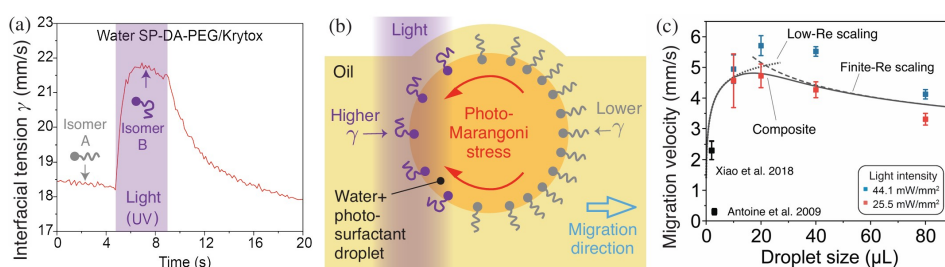


FIG. 1: (a) Interfacial tension between an aqueous solution of SP-DA-PEG photosurfactant and Krytox oil [3]. UV light triggers a change in molecular conformation, leading to an increase in interfacial tension. (b) Schematic of photo-Marangoni-driven motion of an aqueous droplet in Krytox oil. The drop migrates to the right. (c) Experimental and scaling results for the migration velocity of the droplet [3]

I. ACKNOWLEDGEMENTS

Supported by Grant #2025655 from NSF and the Center for the Advancement of Science in Space.

- [1] Y. Xiao, S. Zarghami, K. Wagner, P. Wagner, K.C. Gordon, L. Florea, D. Diamond, and D.L. Officer, Moving Droplets in 3D Using Light, *Adv. Mater.* 30(35), e1801821 (2018).
- [2] L. Zhao, S. Seshadri, X. Liang, S.J. Bailey, M. Haggmark, M. Gordon, M.E. Helgeson, J. Read de Alaniz, P. Luzzatto-Fegiz, and Y. Zhu, Depinning of Multiphase Fluid Using Light and Photo-Responsive Surfactants, *ACS Cent. Sci.* 8(2), 235–245 (2022).
- [3] X. Liang, K.M. Karnaukh, L. Zhao, S. Seshadri, A.J. DuBose, S.J. Bailey, Q. Cao, M. Cooper, H. Xu, M. Haggmark, M.E. Helgeson, M. Gordon, P. Luzzatto-Fegiz, J. Read de Alaniz, and Y. Zhu, Dynamic Manipulation of Droplets on Liquid-Infused Surfaces Using Photoresponsive Surfactant, *ACS Cent. Sci.* 10(3), 684–694 (2024).

Shear-induced particles migration in multi-disperse concentrated suspensions

Olga Lavrenteva^{1,2} and Avionoam Nir^{1,3}

¹Department of Chemical Engineering, Technion, 3200003, Haifa, Israel

²ceolga@technion.ac.il

³avinir@technion.ac.il

The shear-induced diffusion of particles in multi-dispersed suspension is considered. The diffusion model considers migration fluxes resulting from gradients of particle interaction, suspension viscosity, and variation of streamline curvature (Shauly *et al.* [1]). The viscosity of a suspension is assumed to depend on the ratio of local concentration and the close-packing concentration that, in its turn, is a function of particle size distribution. Models of suspension viscosity and of the close-packing concentration, for φ_{max} , are available in the literature. Several works propose various expressions for φ_{max} as a function of the first three statistical moments of a particle size distribution. In this contribution, the dependence suggested in Santos *et al.* [2] is adopted and applied to solve stationary flow pattern and the particle concentration distributions in multi-disperse suspensions in various viscometric flows (parallel plates, cone and plate, and Couette devices). The total migration of the particles and the size segregation of the various fractions are predicted for various total concentration and particle size distribution in the suspension. The similarity and difference from cases of mono-dispersed suspensions is discussed.

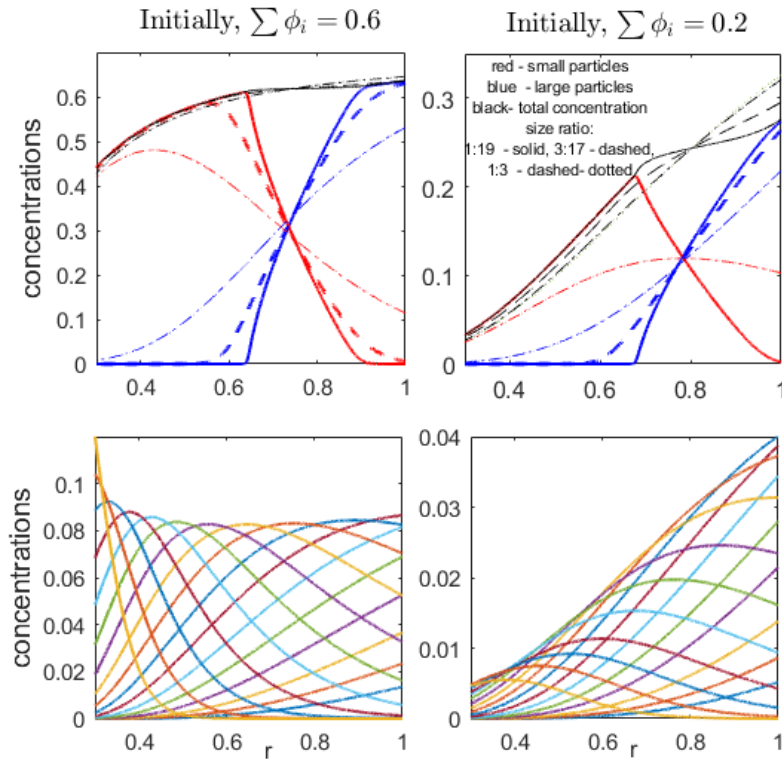


FIG. 1: Stationary concentrations of fractions of bi-modal (upper plots) and multi-modal suspensions sheared in a wide gap Couette device. The ratio between inner and outer cylinders equals 0.3.

Sample results on the stationary concentrations of individual fractions of suspensions sheared in a Couette device are presented in Fig.1 for high, 0.6, and low, 0.2, initial concentrations. The upper plots correspond to bi-modal suspension, with various particle size ratio, having initially equal volume concentrations of large and small particles. The lower plots address a suspension with particles of 17

different sizes. Initial concentrations mimic a normal distribution. Obviously, large and small particles migrate to the outer and inner cylinders, respectively, while those with intermediate sizes are pushed from both sides and exhibit maximum inside flow domain. Domains free from the large particles are seen near the inner cylinder. For higher concentration, also region free of smaller particles appear near the outer cylinder.

-
- [1] A. Shauly, A. Wachs and A. Nir, Shear-induced particle migration in a polydisperse concentrated suspension, *J. Rheol.* **42**, 1329 - 1348 (1998).
 - [2] A. Santos, S. B. Yuste, M. Lopez de Haro, G. Odriozola & Ogarko, Simple effective rule to estimate the jamming packing fraction of polydisperse hard spheres, *Phys. Rev. E* **89** 040302(R) (2014).

Particle-particle Interaction against Stable Formation of Coherent Structures in a Stable Travelling Flow

Sho Shidomi^{1,3}, Shin Noguchi^{1,4} and Ichiro Ueno²

¹Div. Mechanical & Aerospace Eng., Tokyo Univ. Science, Chiba 278-8510, Japan

³7524527@ed.tus.ac.jp ⁴7522703@ed.tus.ac.jp

²Dept. Mechanical & Aerospace Eng., Tokyo Univ. Science, Chiba 278-8510, Japan *ich@rs.tus.ac.jp*

As awareness of environmental impact increases, the aggregation and separation of solid particles and immiscible droplets in multiphase flows, such as wastewater, have been becoming more important. This study focuses on the behavior of small particles introduced into a closed system known as a half-zone liquid bridge (FIG. 1). A liquid bridge is formed by injecting a test liquid between two coaxially positioned rods. By imposing a designated temperature difference between the rods, Marangoni convection is induced by occurring surface tension difference on the free surface of the liquid bridge due to the temperature dependence of surface tension. When the temperature difference exceeds the critical value, the flow exhibits a transition from a steady two-dimensional flow to a three-dimensional oscillatory flow due to hydrothermal-wave (HTW) instability [1,2]. Under specific conditions in oscillatory flow, it has been observed that low-Stokes-number particles accumulate and form coherent structures, known as particle accumulation structure (PAS) [3]. The spatial characteristics of PAS exhibit a strong correlation with Kolmogorov-Arnold-Moser (KAM) tori, which are ordered structures formed within the thermal convection field [4,5]. Additionally, in a thermal convection field with an azimuthal wavenumber of $m_{HTW} = 3$, a phenomenon has been reported in which particles change their motion to exhibit transitions between different coherent structures [6]. In this study, we focus on the behavior of single type of particles forming a coherent structure in a high-aspect-ratio liquid bridge with an azimuthal wavenumber of $m_{HTW} = 1$. Under the condition where the interparticle distance near the free surface decreases, we firstly demonstrate experimentally the structure-to-structure transition of particle (FIG. 2). The transition takes place right after the direct interaction with neighboring particle in the vicinity of free surface. In the presentation, we will discuss the temporal-spatial four-dimensional behavior of interacting particles, to unveil the scenario of particle transition between structures by illustrating the spatial distance between adjacent particles

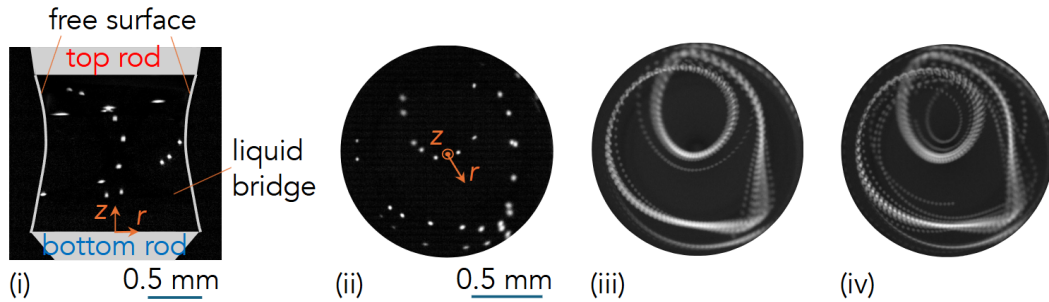


FIG. 1: (i) and (ii): Side- and top views of snapshots of the particle image, respectively; (iii) and (iv): Particle images stacked in a rotating frame of reference for cases with minimal and significant particle-particle interactions, respectively. White dots represent the particles of $40 \mu m$ in diameter (corresponding Stokes number $St = \rho d_p^2 / 18H^2 = 7.5 \times 10^{-5}$, where $\rho = \rho_p / \rho_l$ is the ratio of particle and liquid densities, d_p is the particle diameter, and H is the liquid bridge height). Images in (iii) and (iv) are obtained by stacking images for a period of $2\tau_{HTW}$, where τ_{HTW} is the fundamental period for travelling flow in azimuthal direction. Common experimental condition for all frames: $\Gamma = 1.93$, $V/V_0 = 0.837$, and $Re = |\gamma_T| \Delta T H / \rho_l \nu^2 = 8.1 \times 10^2$ ($\Delta T = 28K$). Here γ_T is the temperature coefficient of surface tension and ν is the kinematic viscosity of liquid.

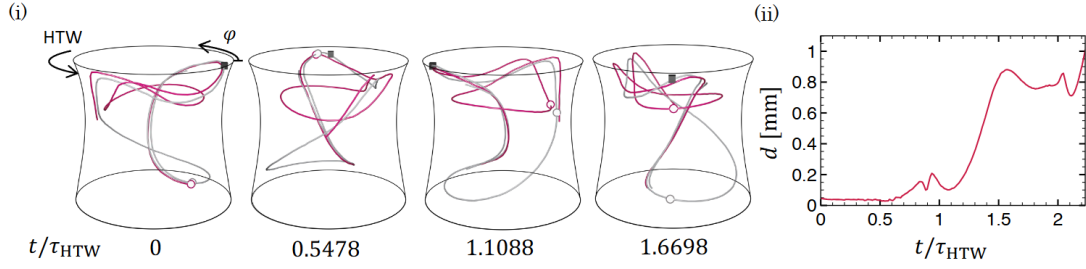


FIG. 2: Time series of (i) positions of particles interacting in liquid bridge in rotating frame of reference and (ii) evaluated their distance, d . In Panel (i), Circle (\circ) indicates position of the particles. The trajectories within the whole period of reconstruction are illustrated for the sake of visibility. Square (\blacksquare) indicates the maximum radial position in the gray trajectory and is set to $\varphi = 0$. The view point is varied for each frame to distinguish the mutual positions of particles (Frames from left to right represents the trajectories observed at the azimuthal position of $\varphi = 270$ degree, 180 degree, 90 degree and 0 degree)

Acknowledgements : This work was partially supported from the Japan Society for the Promotion of Science (JSPS) by Grant-in-Aid for Challenging Research (Exploratory) (grant number: 20K20977).

-
- [1] M.K. Smith and S.H. Davis, Instabilities of dynamic thermocapillary liquid layer. Part 1. Convective instabilities, *J. Fluid Mech.* **132**, 119 - 144 (1983)
 - [2] C.H. Chun and W. Wuest, Experiments on the transition from the steady to the oscillatory Marangoni-convection of a floating zone under reduced gravity effect, *Acta Astronaut.* **6**, 1073 - 1082 (1979).
 - [3] D. Schwabe, P. Hints and S. Frank, New features of thermocapillary convection in floating zones revealed by tracer particle accumulation structures (PAS), *Microgravity Sci. Technol.* **9**, 163 - 168 (1996).
 - [4] R.V. Mukin and H.C. Kuhlmann, Topology of hydrothermal waves in liquid bridges and dissipative structures of transported particles, *Phys. Rev. E* **88**, 053016 (2013).
 - [5] F. Romano and H.C. Kuhlmann, Finite-size Lagrangian coherent structures in thermocapillary liquid bridges, *Phys. Rev. Fluids* **3**, 094302 (2018).
 - [6] K. Yamaguchi, T. Hori and I. Ueno, Long-term Behaviors of a Single Particle Forming a Coherent Structure in Thermocapillary-driven Convection in Half-zone Liquid Bridge of High Prandtl-number Fluid, *Int. J. Microgravity Sci. Appl.* **36**, 360203, (2019)

Session 10 – Poster session

Wednesday June 11, 10:00–10:30

Rayleigh-Taylor instability in an elastic slab bounded by a rigid wall

S. A. Piriz,^{1,4} A. R. Piriz,^{2,5} and N. A. Tahir^{3,6}

¹*Instituto de Investigaciones Energéticas (INEI), E.I.I.A., and CYTEMA, Universidad de Castilla-La Mancha, 45071 Toledo, Spain* ⁴*sofiaayelen.piriz@uclm.es*

²*Instituto de Investigaciones Energéticas (INEI), E.T.S.I.I., and CYTEMA, Universidad de Castilla-La Mancha, 13071 Ciudad Real, Spain* ⁵*roberto.piriz@uclm.es*

³*GSI Helmholtzzentrum für Schwerionenforschung Darmstadt, Planckstrasse 1, 64291 Darmstadt, Germany*

⁶*n.tahir@gsi.de*

A quasi-irrotational approximation for the linear Rayleigh-Taylor instability in elastic solids with finite thickness has been developed for the case in which the slab is in contact with a rigid wall. The approximation yields simple but still reasonably accurate expressions for the instability growth rate. They have the same character than the completely irrotational approximations already developed for semi-infinite media, and recover its results in the limit for very thick slabs. The model is applied to the analysis of the boundary of stability and the boundary for the elastic to plastic transition in elastic-plastic media. The approach allows for considering the presence of a viscous fluid beneath the elastic-plastic slab, extending previous results for ideal fluids.

Modeling surfactant flow and surface tension modulations in foam dynamics

Chaima Nasri^{1,2}, and Christophe Oguey^{1,3}

¹LPTM, CY Cergy Paris University, 95302, Cergy-Pontoise, France

²chaima.nasri@cyu.fr; ³christophe.oguey@cyu.fr

Surface tension modulation by surfactant flow plays an important role in soap film dynamics. This effect is especially manifest in the fast motion implied by topological changes in soap froths. The T1 process, whereby four bubbles exchange contacts, is a paradigmatic example [1][4].

This study aims to decompose and reconstruct the phenomena influenced by the Marangoni effect through numerical simulations. Dealing with larger systems is a challenge, even in two dimensions. Our method combines two approaches:

First, at the scale of a few bubbles or a single film junction [1], the film motion coupled to the surfactant transfer along the interfaces are found by solving the flow and balance equations in a discretization scheme [4].

Second, a numerical model, previously developed [3] to investigate bubble deformations and foam dynamics, will be revisited and adapted to incorporate both surfactant flow and the implied surface tension variations.

An important feature of foam rheology is the interplay of different time scales: the slow overall deformation of the flowing foam, and the rapid movements triggered by local topological transformations (T1 and T2 processes) involving dissipation and surfactant transport.

Viscous dissipation also occurs at the contact with solid walls. We consider two different setup: bubble rafts with nearly free interfaces and quasi 2D foams confined between two rigid plates (Hele-Shaw cell).

The results should provide the foundations for a more accurate numerical representation of foam flow, including Marangoni-driven effects essential for foam stability and dynamics.

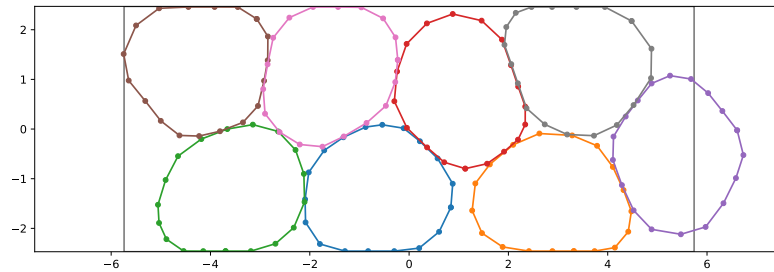


FIG. 1: Confined foam with interfaces subdivided into segments

[1] R. Satomi, P. Grassia, and Ch. Oguey, *Col. Surf. A*, 2013, **438**, 1016. , DOI: 10.1016/j.colsurfa.2013.08.021.

[2] S. Cox and T. Davies, *Phys. Rev. E*, 2021, **53**, 101440.

[3] T. Kähärä, T. Tallinen, and J. Timonen, *Phys. Rev. E*, 2014, **90**, 032307.

[4] F. Zaccagnino, A. Audebert, and S.J. Cox, *Phys. Rev. E*, 2018, **98**, 022801.

Visualization of thermocapillary flows in water sessile droplets under different heating conditions

G. Lorite Méndez¹, S. Fusco¹, M.Á. Cabrerizo Vílchez¹ and M. Á. Rodríguez Valverde^{1,2}

¹Lab of Surface and Interface Physics, Department of Applied Physics, University of Granada, 18071, Granada, Spain ²marodri@ugr.es

Marangoni thermal flows at fluid interfaces are induced by interfacial temperature gradients. These flows significantly affect the internal fluid dynamics of droplets [1]. Understanding thermocapillary flows is crucial for microfluidics, heat transfer and interfacial science. In this work, we investigate the behavior of Marangoni-driven flows in water sessile droplets deposited on non-wetting surfaces under different heating conditions. A temperature gradient can be introduced either by directly illuminating the droplet apex with a CW laser or by heating the substrate using a Peltier plate. In the first case, the laser can generate temperature gradients at the liquid-vapor interface, which, due to the intrinsic properties of a 2D laser sheet, may not be homogeneous across the entire drop surface. This can result in anisotropic heating, potentially inducing asymmetric Marangoni flows. Conversely, by thermal conduction, the entire solid-liquid interface reaches a uniform temperature, creating a well-defined temperature gradient between the top and bottom of the droplet. These different heating configurations can give rise to distinct thermally induced flow patterns, where the competition between surface and bulk temperature effects may lead to complex and non-trivial circulation dynamics. The combination of both heating mechanisms may offer new insights into the resulting flow patterns. To visualize and analyze these thermally induced flows, we introduce fluorescent tracers into a water sessile droplet, enabling real-time tracking of flow structures via particle image velocimetry. By systematically varying heating conditions, we aim to explore the fundamental mechanisms governing these flows. This study provides a general framework for understanding thermally-induced flows in confined liquid systems and contributes to the broader field of interfacial fluid dynamics.

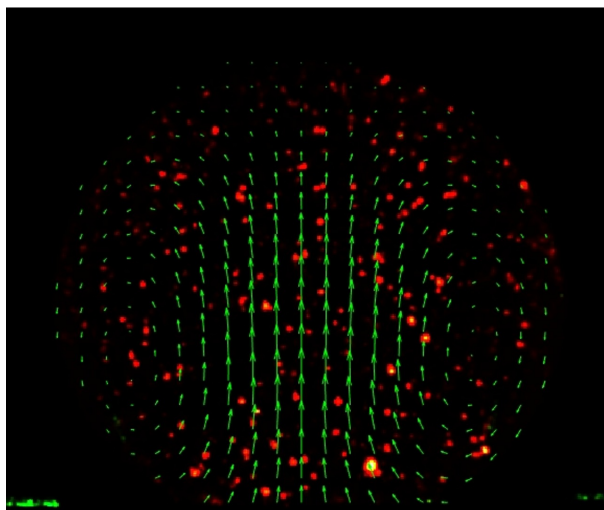


FIG. 1: Representative PIV visualization of internal flow patterns in a 10 μL water sessile droplet evaporating on a superhydrophobic surface

[1] X. Xu, J. Luo, Marangoni flow in an evaporating water droplet. *Appl. Phys. Lett.* 17 September 2007; 91 (12): 124102. <https://doi.org/10.1063/1.2789402>

Concrete lightweight materials: Global Engineering Challenges

Abhay Ghuge¹, Fouzan Ameer¹ and Dominika Zabiega^{1,2}

¹Smart Materials and Surfaces Laboratory, Faculty of Engineering and Environment, Northumbria University, NE1 8ST Newcastle upon Tyne, United Kingdom ²dominika.zabiegaj@northumbria.ac.uk

Global warming is an important issue now a days and the major driver for this phenomenon is CO2 emissions [1]. To tackle this issue both the thermal management system and CO2 reduction are important tasks to develop. Moreover, due to the ageing nuclear power plants and the hazardous effect of radiation leads to the importance of having radiation shielding materials. It is important to develop novel composites that can withstand CO2 emission under the thermal management system for radiation shielding material.

Concrete has been a widely accepted material for a variety of applications including thermal storage material, radiation shielding material, building structure materials etc. However, it has faced several challenges due to its density and weight, workability, cost, thermal insulation, maintenance and environmental impacts [2]. To tackle those issues, several researchers tried to develop novel concrete utilizing several the natural or industrial waste, fibres, minerals, nanoparticles so that it can help to reduce the CO2 reduction to align with the net zero emission. However, there is still concern about the sustainability of those concrete and its effectiveness of the concrete, as there is still under review.

Incorporating porous structure to the concrete can be solution of the many issues towards its drawbacks. Porous structures help to reduce the weight of the structure having the larger surface area and high absorption capacity [3]. Moreover, it can be eco-friendly through utilizing the plants, soil, natural minerals which helps to reduce the CO2 emissions to align with the net zero emissions [4].

To tackle all the concern, this research is focusing on two distinctive area. It will contribute a hol-low review about the effectiveness of the novel concrete for radiation shielding material and its impact towards CO2 reduction to maintain the net zero emissions. Moreover, this research also contributed towards developing a novel porous concrete composite utilizing the natural clay mineral to meet towards the sustainability and CO2 reduction for radiation shielding applications.

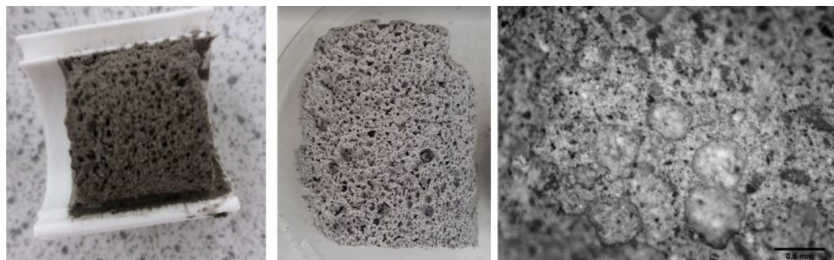


FIG. 1: Freestanding foamed concrete samples.

-
- [1] O. Osman Gencel, "Properties of eco-friendly foam concrete containing PCM impregnated rice husk ash for thermal management of buildings," *Journal of Building Engineering*, vol. **58**, no. 104961, 2022.
 - [2] B. B. D. P. N. Q. Salim Barbhuiya, "A comprehensive review of radiation shielding concrete," *Structural Concrete*, 2024.
 - [3] C. Z. Zipeng Guo, "Recent advances in ink-based additive manufacturing for porous structures," *Additive Manufacturing*, vol. **48**, no. B, 2021.

Characterization of the compressible phase in Richtmyer-Meshkov Instability

F. Cobos^{1,5}, M. Napieralski², T. Sano³, C. Matsuoka⁴ and C. Huete²

¹*Instituto de Investigaciones Energéticas (INEI), Universidad de Castilla-La Mancha, 13005, Ciudad Real, Spain. ⁵Francisco.Cobos@uclm.es*

²*Departamento de Ingeniería Térmica y de Fluidos, Universidad Carlos III de Madrid, 28911, Leganés, Spain.*

³*Institute of Laser Engineering (ILE), Osaka University, Suita, Osaka 565-0871, Japan.*

⁴*Laboratory of Applied Mathematics, Graduate School of Engineering, Osaka City University, Suita, Osaka 565-0871, Japan.*

A study of the linear phase of the Richtmyer-Meshkov Instability (RMI) is presented for both reflected shock/rarefaction wave configurations. The type of reflected wave and the subsequent time evolution of the problem are determined by four initial pre-shock parameters: two quantities that characterize the fluids compressibility (for an ideal gas equation of state, their specific heat ratios), the initial density ratio across the interface, and the incident shock strength. Due to the front corrugation, hydrodynamic perturbations are generated in the compressed or expanded fluids. There are three types of perturbations: evanescent sound waves, vorticity, and entropy fluctuations. The two latter are frozen to the fluid elements for inviscid flow. The initial contact surface ripple begins to grow in time, driven by the perturbation fields and the initial velocity shear deposited by the fronts just after they separate from it. In the linear growth phase, two distinct phases can be distinguished: the first is a transient compressible stage in which oscillations due to evanescent sound waves are observed; and the second is a linear incompressible phase when the ripple growth reaches its asymptotic velocity. A comparative analysis has been conducted among compressible linear theory [1, 2], hydrodynamic simulations, the vortex sheet model [3], and classical RMI experiments. The analysis revealed a high degree of agreement among these methods in cases where the initial ripple amplitude is sufficiently small to induce linear growth. It has been demonstrated that incompressible nonlinear models must consider the compressible effects that occur during the linear transient phase to ensure accurate predictions in later stages of the instability. The duration of this linear transient phase has been estimated and compared with previous prescriptions.

The authors acknowledge support by ILE Collaborative Research 2023B2-013, and grants PID2022-139082NB-C51, PID2021-125550OB-I00 and TED2021-129446B-C41 funded by MCIN/AEI and project H2SFE-CM-UC3M funded by Madrid Government-UC3M Multiannual Agreement.

[1]] F. Cobos Campos, and J. G. Wouchuk, Phys. Rev. E **93**, 053111 (2016).

[2]] F. Cobos Campos, and J. G. Wouchuk, Phys. Rev. E **96**, 013102 (2017)

[3]] C. Matsuoka and N. Nishihara, Phys. Rev. E **73**, 026304 (2006).

Reduced-order modeling of heated falling films

I. B. Ignatius^{1,2}, F. Giraud^{1,3}, and C. Ruyer-Quil^{1,4}

¹*Laboratoire LOCIE, Université Savoie Mont Blanc, 73000, Chambéry, France*

²*iginbenny@gmail.com,*

³*florine.giraud@univ-savoie.fr,*⁴*christian.ruyer-quil@univ-savoie.fr*

I. ABSTRACT

A thin film flowing down a vertical wall develops large solitary waves at its free surface due to Kapitza instability, enhancing heat transport across the film. Modeling this phenomenon is important due to its relevance in waste heat recovery in industrial processes using falling films.

In this work, two families of robust reduced-order models, single and two-variable models, are developed to predict temperature profile and heat transfer in falling films at low to high Reynolds (Re) and Prandtl (Pr) numbers. First, single-variable models are formulated in terms of the interface temperature using Galerkin projections of temperature profiles onto polynomial eigenfunctions [1]. These models perform well for low to moderate Re and high Pr, but deviate at high Re or large interface deflections due to the dependence of interface temperature on interface deflections. To address this, two-variable models incorporating both interface temperature and its curvature are developed. These models effectively capture thermal convective circulations near solitary wave crests formed at high Re and Pr, a feature missed by single-variable models. While the two variable models enhance the accuracy in this range, the simpler single-variable model remain effective for low to moderate Re.

This work distinguishes itself from existing works in two key ways. First, it develops robust reduced-order models by employing higher-degree polynomial projections of the temperature profile. Second, it incorporates Robin boundary conditions at both the wall and the free surface, facilitating effortless integration of the model with various thermophysical problems.

II. ACKNOWLEDGEMENTS

The authors gratefully acknowledge funding from ANR via grant ANR-23-CE05-0001.

Analysis of Phase Change Materials for passenger comfort in car vehicles

C. Martinez Martínez^{1,2} and D. Gomez-Lendinez^{1,3}

¹Polytechnic School, Nebrija University, 28015, Madrid, Spain, ²cmartinezml14@alumnos.nebrija.es, ³dgomezle@nebrija.es

I. INTRODUCTION

Nowadays, sustainability and energy efficiency are key factors in vehicle design and development. In this context, the integration of phase change materials (PCMs) in the automotive industry emerges as a promising approach to enhance passenger comfort. PCMs can absorb and store large amounts of thermal energy during phase transitions and release that energy when the temperature drops, helping to reduce peak cabin temperatures. This, in turn, decreases the use of air conditioning systems, which consume significant energy and negatively affect both fuel efficiency in combustion vehicles and driving range in electric vehicles [1-6].

This work involves selecting PCMs from the literature with optimal thermal properties for automotive applications, followed by thermal simulations to evaluate their performance when integrated into the vehicle roof. The study aims to assess the PCM's ability to regulate interior temperatures and release heat in a controlled manner [1-6].

II. METHODOLOGY

This study analyses the thermal behavior of Phase Change Materials (PCMs) in a vehicle roof considering both summer and winter scenarios with the vehicle in motion. Simulations were conducted modeling heat transfer and phase change phenomena. Madrid's climate served as the reference, chosen for its representative hot summers (34.03 Celsius ave. max. temp.) and moderately cold winters (2.54 Celsius ave. min. temp.), with theoretical foundations based on literature. The conceptual design involved a simplified multi-layer model of the vehicle roof, including the steel exterior, insulation, PCM layer, and interior lining, focusing on vertical heat flow driven by external radiation/forced convection and internal natural convection.

The simulation setup utilized a reduced-scale geometry (20mm x 10mm x 0.5mm) to manage computational constraints. Realistic boundary conditions were applied: a mixed condition of radiation and external forced convection on the top surface (exterior) and natural convection on the bottom surface (cabin interior), with coupled surfaces between layers to allow heat transfer. Data for these simulations were compiled from various sources, including PCM dimensions (4mm thickness based on a Segment C vehicle roof, see figure 1), typical Madrid travel time (23 minutes), thermophysical conditions for Madrid in 2024 (temperatures, wind, solar irradiation, heat flux for warm/cold months), air properties for heat transfer calculations, and properties of selected PCMs (including commercial and literaturesourced materials with varied melting ranges, i.e. RT18HC, n-Heptadecane, HS22P, Coconut oil, RT25HC, n-Octadecane + Al₂O₃ nanoparticles) [7-10].

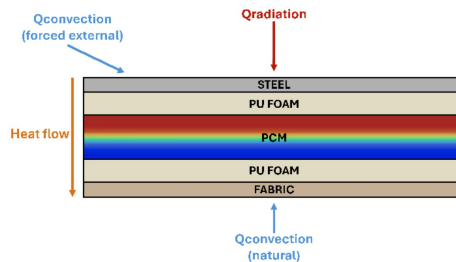


FIG. 1: Roof PCM-integrated cross-section.

III. RESULTS

PCMs act as thermal insulation, absorbing and releasing heat in a controlled manner. Specific PCMs like n-heptadecane, HS22P, and RT25HC were particularly effective in warm conditions, keeping the temperature of the roof's lower surface (near the cabin) almost constant, with increases of less than 0.5 K during the simulated trip. This is a significant improvement compared to the air cavity (7.5 K increase) or PU foam (8.2 K increase) reference cases. The internal convection during melting helps distribute heat more uniformly within the PCM. See figure 2.

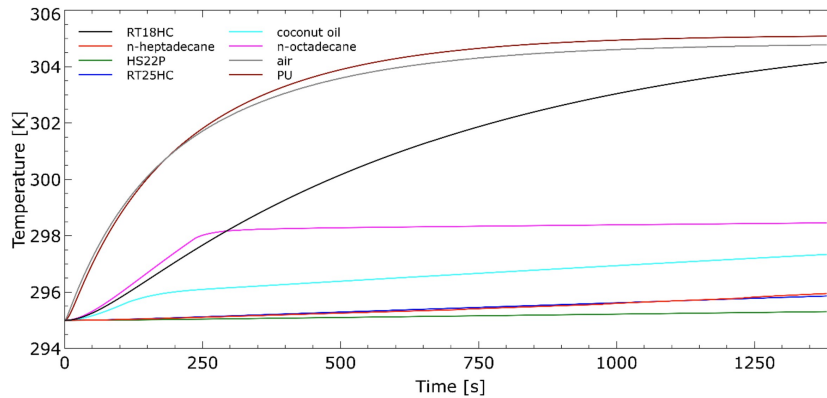


FIG. 2: PCM Average Temperature summer case

IV. CONCLUSIONS

Preliminary results indicate that incorporating PCM in the vehicle roof can reduce the dependence on the HVAC system and enhance thermal comfort in the cabin, key factors for energy efficiency in both electric and conventional vehicles.

-
- [1] International Energy Agency, Global EV Outlook 2024, 2024.
 - [2] Jaguemont, J., Omar, N., Van den Bossche, P., & Mierlo, J. (2018). Phase-change materials (PCM) for automotive applications: A review. *Applied thermal engineering*, 132, 308-320. 2018, 1359-4311, <https://doi.org/10.1016/j.applthermaleng.2017.12.097>.
 - [3] Oró, E., de Jong, E., & Cabeza, L. F. (2016). Experimental analysis of a car incorporating phase change material. *Journal of Energy Storage*, 7, 131-135. 2352-152X, <https://doi.org/10.1016/j.est.2016.05.003>.
 - [4] Nicolalde, J. F., Cabrera, M., Martínez-Gómez, J., Salazar, R. B., & Reyes, E. (2022). Selection of a phase change material for energy storage by multi-criteria decision method regarding the thermal comfort in a vehicle. *Journal of Energy Storage*, 51, 104437. <https://doi.org/10.1016/j.est.2022.104437>.
 - [5] Afzal, A., Saleel, C. A., Badruddin, I. A., Khan, T. Y., Kamangar, S., Mallick, Z., ... & Soudagar, M. E. M. (2020). Human thermal comfort in passenger vehicles using an organic phase change material—an experimental investigation, neural network modelling, and optimization. *Building and Environment*, 180, 107012, 0360-1323, <https://doi.org/10.1016/j.buildenv.2020.107012>.
 - [6] Consorcio Regional de Transportes de Madrid, “Encuesta de movilidad de la Comunidad de Madrid 2018: Documento síntesis,” Deloitte e IPD, 2019.
 - [7] Madrid, spain weather history. <https://www.wunderground.com/history/monthly/es/madrid/LEMD/date/2024-12>. Accessed: 2025-04-24.
 - [8] Madruga, S., & Mendoza, C. (2021). Heat transfer performance and thermal energy storage in nano-enhanced phase change materials driven by thermocapillarity. *International Communications in Heat and Mass Transfer*, 129, 105672. <https://doi.org/10.1016/j.icheatmasstransfer.2021.105672>.
 - [9] Pcm rt-line, versatile organic pcm for your application. <https://www.rubitherm.eu/en/productcategory/organische-pcm-rt>. Accessed: 2025-04-24.
 - [10] Phase change material. <https://pcmpacks.com/>. Accessed: 2025-04-24.

Numerical Study of Polylactic Acid Extrusion in FDM 3D Printing

D. Gomez-Lendinez^{1,2}, R. Rodriguez Larios^{1,3}, J. Garcia-Moreno Caraballo^{1,4} and R. Barea^{1,5}

¹*Polytechnic School, Nebrija University, 28015, Madrid, Spain* ²*dgomezle@nebrija.es*,
³*rrodriguez14@alumnos.nebrija.es*, ⁴*jgarciamoreno@nebrija.es*,
⁵*rbarea@nebrija.es*

I. INTRODUCTION

Additive manufacturing, specifically Fused Deposition Modeling (FDM), has gained popularity due to its versatility and ease of use. Polylactic acid (PLA) is one of the most widely used filaments in FDM because of its biodegradability, low melting temperature, and favorable mechanical properties. Understanding the flow behavior of PLA during extrusion is crucial for enhancing print quality and optimizing the manufacturing process. [1-9] FDM printing involves heating and extruding thermoplastic filaments through a nozzle, where factors such as temperature, extrusion speed, and layer height significantly affect print quality. Previous studies have explored the rheology and thermal properties of PLA. However, a detailed computational analysis of its extrusion dynamics remains underdeveloped. Advanced simulations using computational fluid dynamics (CFD) provide deeper insights into material behavior during printing. The present work is an extension of the study presented in [2].

II. METHODOLOGY

The study focuses on the extrusion of polylactic acid (PLA) in Fused Deposition Modeling (FDM) through a computational approach using. A computational fluid dynamics (CFD) model was developed to simulate the behavior of PLA during extrusion, considering its rheological properties and heat transfer characteristics. The Volume of Fluid (VOF) model was employed to track the interface between the molten PLA and surrounding air. To ensure accuracy, a refined and optimized mesh was used, particularly in regions with high thermal gradients and complex flow dynamics.

The geometry of the extrusion system, including the nozzle and filament path, was modeled based on standard FDM printer specifications (see Figure 1). Boundary conditions were defined, with the nozzle temperature set at 190°C as standard PLA fusion temperature and different extrusion velocities ranging from 0.01 m/s to 0.04 m/s. The bed velocity was varied between 0.02 m/s and 0.08 m/s to analyze its impact on filament deposition. The time step was set to 0.0005 s to capture transient effects during the extrusion process, ensuring precise modeling of flow stability and thermal diffusion. The surface tension is assumed constant, and the density of PLA is modeled according to Witzke [9].

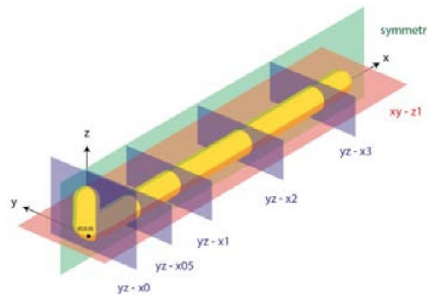


FIG. 1: Plane representation with respect flow extrusion.

III. RESULTS

The simulations revealed that extrusion height significantly influences the final print quality. Lower layer heights (0.05 mm) resulted in a flatter and more compressed filament distribution, which increased processing time and caused instabilities during extrusion at flow borders. In contrast, higher layer heights

(0.4 mm) reduced printing time for the same deposited volume but led to inconsistencies in material deposition and weaker inter-layer bonding due to a smaller contact area.

Density contour plots showed variations in filament deposition, with higher layer heights resulting in a more uniform flow. Temperature contour analyses indicated that rapid cooling at lower layer heights contributed to better adhesion and could potentially affect mechanical properties.

The following figure 2 shows density profiles at $h = 0.4$ mm, $V_{\text{extrusion}} = 0.03$ m/s and $V_{\text{bed}} = 0.04$ m/s with a Carreau viscous model at symmetry plane.

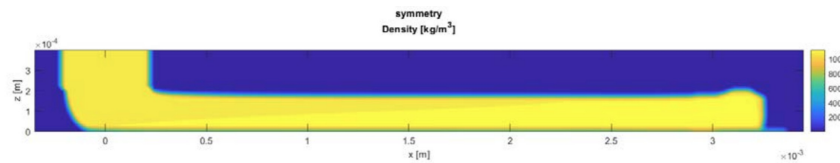


FIG. 2: Density contour at symmetry plane.

IV. CONCLUSIONS

The computational analysis successfully simulated the extrusion behavior of PLA in FDM 3D printing, providing valuable insights into flow dynamics, temperature distribution, and filament deposition. Moreover, results demonstrated that lower layer heights (0.05 mm) improve resolution but increase processing time, while higher layer heights (0.4 mm) reduce print time but may lead to defects such as poor adhesion and warping.

Future enhancements in simulation accuracy could lead to better control of extrusion parameters, reducing defects and improving the overall mechanical strength of printed objects. In addition, simulations are expected to be expanded to include multi-material extrusion processes and/or dynamic speeds along the printing paths.

-
- [1] Bikas, H., Stavropoulos, P. & Chryssolouris, G. Additive manufacturing methods and modelling approaches: a critical review. *Int J Adv Manuf Technol* 83, 389–405 (2016). <https://doi.org/10.1007/s00170-015-7576-2>
 - [2] Gomez Lendinez, D.; Rodriguez Larios, R.; Barea del Cerro, R. Computational Analysis and Simulation of Polylactic Acid Extrusion in 3D Printing, in *Proceedings of the 5th International Electronic Conference on Applied Sciences*, 4–6 December 2024, MDPI: Basel, Switzerland
 - [3] Farah S, Anderson DG, Langer R. Physical and mechanical properties of PLA, and their functions in widespread applications - A comprehensive review. *Adv Drug Deliv Rev.* 2016 Dec 15;107:367-392. doi: 10.1016/j.addr.2016.06.012. Epub 2016 Jun 26. PMID: 27356150.
 - [4] Gosset, A., Barreiro-Villaverde, D., Becerra Permy, J. C., Lema, M., Ares-Pernas, A., & Abad López, M. J. (2020). Experimental and Numerical Investigation of the Extrusion and Deposition Process of a Poly(lactic Acid) Strand with Fused Deposition Modeling. *Polymers*, 12(12), 2885. <https://doi.org/10.3390/polym12122885>
 - [5] Serdeczny, M. P., Comminal, R. B., Pedersen, D. B., & Spangenberg, J. (2018). Experimental validation of a numerical model for the strand shape in material extrusion additive manufacturing. *Additive Manufacturing*, 24, 145-153. <https://doi.org/10.1016/j.addma.2018.09.022>
 - [6] Serdeczny, M. P., Comminal, R., Pedersen, D. B., & Spangenberg, J. (2019). Numerical simulations of the mesostructure formation in material extrusion additive manufacturing. *Additive Manufacturing*, 28, 419-429. <https://doi.org/10.1016/j.addma.2019.05.024>
 - [7] Serdeczny, M. P., Comminal, R., Mollah, M. T., Pedersen, D. B., & Spangenberg, J. (2020). Numerical modeling of the polymer flow through the hot-end in filament-based material extrusion additive manufacturing. *Additive Manufacturing*, 36, Article 101454. <https://doi.org/10.1016/j.addma.2020.101454>
 - [8] Serdeczny, M. P., Comminal, R., Pedersen, D. B., & Spangenberg, J. (2020). Experimental and analytical study of the polymer melt flow through the hot-end in material extrusion additive manufacturing. *Additive Manufacturing*, 32, Article 100997. <https://doi.org/10.1016/j.addma.2019.100997>.
 - [9] Witzke, D.R. (1997) Introduction to properties, engineering and prospects of polylactide polymers. PhD Thesis, Michigan State University, East Lansing, 389.

Session 11 – Droplet dynamics and wetting

Wednesday June 11, 11:00–12:30

Pinning–depinning transition of droplets on inclined substrates with a three-dimensional topographical defect

Ninad V. Mhatre¹ and Satish Kumar^{1,2}

¹*Department of Chemical Engineering and Materials Science, University of Minnesota, MN 55455, Minneapolis, United States of America* ²*kumar030@umn.edu*

Droplets on inclined substrates can depin and slide freely above a critical substrate inclination angle. Pinning can be caused by topographical defects on the substrate, and understanding the influence of defect geometry on the pinning–depinning transition is important for diverse applications such as fog harvesting, droplet-based microfluidic devices, self-cleaning surfaces, and inkjet printing. Here, we develop a lubrication-theory-based model to investigate the motion of droplets on inclined substrates with a single three-dimensional Gaussian-shaped defect that can be in the form of a bump or a dent. A precursor-film/disjoining-pressure approach is used to capture contact-line motion, and a nonlinear evolution equation is derived which describes droplet thickness as a function of the position along the substrate and time. The evolution equation is solved numerically using an alternating direction implicit finite-difference scheme to study how the defect geometry influences the critical inclination angle and the shape of a pinned droplet. It is found that the critical substrate inclination angle increases as the defect becomes taller/deeper or wider along the direction lateral to the droplet-sliding direction. However, the critical inclination angle decreases as the defect becomes wider along the sliding direction. Below the critical inclination angle, the advancing contact line of the droplet at the droplet centerline is pinned to the defect at the point having maximum negative slope. Simple scaling relations that reflect the influence of defect geometry on the droplet retention force arising from surface tension are able to account for many of the trends observed in the numerical simulations [1].

[1] N. V. Mhatre and S. Kumar, *Soft Matter* **20**, 3529-3540 (2024).

Chemo-mechanical coupling in sessile drops covered by reactive surfactants- from simple self-propulsion to irregular motion

Florian Voss¹ and Uwe Thiele^{1,2}

¹*Institute for Theoretical Physics, University of Münster, Wilhelm-Klemm-Str. 9, 48149, Münster, Germany*

²*Center for Nonlinear Science (CeNoS), University of Münster, Corrensstr. 2, 48149 Münster, Germany*

Wetting and dewetting dynamics of simple and complex liquids is described by kinetic equations in gradient dynamic form incorporating the various coupled dissipative processes in a thermodynamically consistent way. After reviewing recent advances for sessile shallow drops on various substrates, we also review how chemical reactions can be captured by a related gradient dynamics description. Then, we bring both aspects together and discuss mesoscopic reactive thin-film hydrodynamics illustrated by two examples, namely, models for reactive wetting and reactive surfactants where the interplay of an autocatalytic reaction of surfactant-like chemical species on the free surface, the resulting solutal Marangoni effect and the physics of wetting is of central importance. In all cases, these models can describe the approach to equilibrium. However, in the presence of chemical fuel they may also be employed to study out-of-equilibrium chemo-mechanical dynamics [1]. Then, one breaks detailed balance by chemostating and obtains active (non-gradient) systems.

In the case of reactive wetting we recover the well-known running drops driven by chemically sustained wettability gradients [2, 3]. In the case of drops covered by autocatalytic reactive surfactants we describe the positive feedback loop between the local reactions and the Marangoni effect that allows for self-oscillating and self-propelled drops. Besides simple directional motion, we discuss crawling drops (periodic stick-slip motion) and shuttling drops (periodic back-and-forth motion) as well as drops performing random walks, thus exploring the entire substrate. We study the occurring dynamics and show how the observed states emerge from local and global bifurcations. Due to the underlying generic thermodynamic structure, we expect that our results are relevant not only to directly related biomimetic drop systems [3, 4] but also to systems of similar structure like reactive phase-separating mixtures [5].

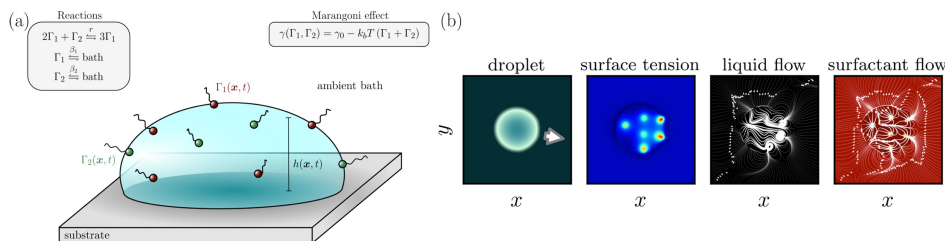


FIG. 1: (a) Sketch of a droplet on a flat, rigid and chemically homogeneous substrate covered by two autocatalytically reacting species of surfactant. The system is driven by an exchange of surfactant with an ambient bath (chemostat). (b) Snapshot from a corresponding time simulation. Large drops perform a self-organized random walk by nucleation of localized surface tension structures. The arrow indicates the momentary direction of motion.

-
- [1] Voss, F., Thiele, U., *J. Eng. Math.* 149, 2 (2024). doi: 10.1007/s10665-024-10402-x
[2] Dos Santos, F. D., Ondarcuhu, T., *Phys. Rev. Lett.* 75, 2972 (1995). doi: 10.1103/PhysRevLett.75.2972
[3] Sumino, Y., Magome, N., Hamada, T., Yoshikawa, K., *Phys. Rev. Lett.* 94, 068301 (2005), doi: 10.1103/PhysRevLett.94.068301
[4] Satoh, Y., Sogabe, Y., Kayahara, K., Tanaka, S., Nagayama, M., Nakata, S., *Soft Matter* 13, 3422 (2017), doi: 10.1039/c7sm00252a
[5] Demarchi, L., Goychuk, A., Maryshev, I., Frey, E., *Phys. Rev. Lett.* 130, 128401 (2023), doi: 10.1103/PhysRevLett.130.128401

The partial wetting problem revisited to account for large Bond numbers

Marc Medale^{1,3} and Bruno Cochelin^{2,4}

¹Aix-Marseille Université, IUSTI UMR CNRS 7343, Marseille, France ³marc.medale@univ-amu.fr

²Aix-Marseille Université, Centrale Méditerranée, LMA UMR CNRS 7031, Marseille, France

⁴bruno.cochelin@centrale-med.fr

This work concerns the modeling at macroscopic scale of a sessile drop, whose size is on the scale of its capillary length or above it. Indeed, almost all works dealing with Axisymmetric Drop Shape Analysis (ADSA) are based on solving Laplace's equation along the liquid–fluid interface together with Young's equation [1] as a boundary condition at contact line. Despite this widespread practice one can wonder how legitimate is this approach if one wants to model real life experiments for which many conditions significantly deviate from those involved in the formal derivation of Young's equation [2].

The present work presents the governing equations to deal with cases with a body force that induces large Bond number and accounts for horizontal but non-ideal solid substrates. Although it is assumed at thermodynamical equilibrium the sessile drop is not an isolated system. It exchanges some mechanical work with the solid substrate and surrounding fluid until it reaches an equilibrium shape that satisfies the total energy conservation. Meanwhile the main part of the involved mechanical work is reversible, the part associated with the pinning at contact line is not. This irreversible part is responsible for the differential behavior experienced for advancing or receding contact line, that results in the hysteresis of macroscopic contact angle. The outcomes of the proposed approach are: i) the energy associated with the three-phase-zone influences the macroscopic contact angle in a $1/r$ trend (r being the dimensionless wetted radius), so this contribution becomes negligible for sizes of sessile drop on macroscopic scale. The macroscopic contact angle asymptotically tends towards the value of advancing contact angle; ii) the macroscopic contact angle also depends on the Bond number over a broad range of values, cf. Fig. 1 for seven dimensionless ratios of surface free energies ($\mathcal{S} = \frac{\gamma_{sf} - \gamma_{sl}}{\gamma_{lf}}$). Solid lines refers to the solution with no line energy, short and long dashed lines refer to advancing and receding contact lines, respectively. Thus, it follows that in many situations where earth gravity is no longer negligible at macroscopic scale,

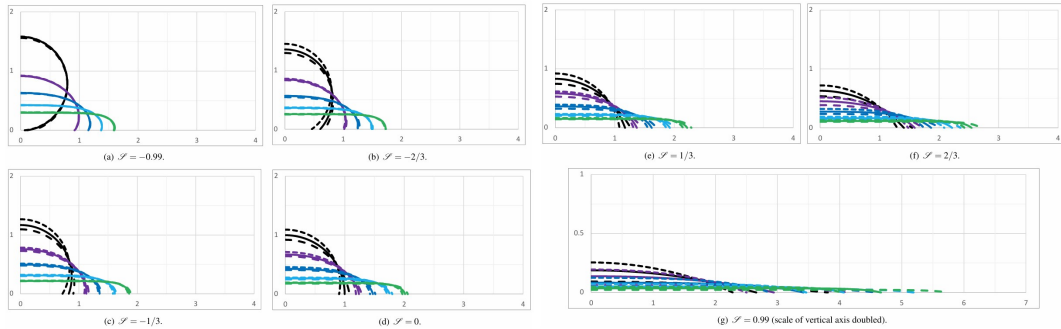


FIG. 1: Sessile drops in a gravity field for Bond number ranging from 0-4 (step of 1).

interfacial free energies deduced from Young's equation could be incorrectly evaluated. So, in a gravity field once the size of a sessile drop is on the scale of its capillary length or above it, Young's equation is only an approximate relationship for the macroscopic contact angle.

[1] Young, T. An Essay on the Cohesion of Fluids. Philos. Transactions, Roy. Soc. Lond. 95, 65-87 (1805).

[2] Medale, M., Brutin, D. Sessile drops in weightlessness: an ideal playground for challenging Young's equation. npj Microgravity 7, 30, DOI: 10.1038/s41526-021-00153-9 (2021)

Emergence of run-and-tumble-like swimming in self-propelling active droplets in soft microchannels

Ranabir Dey^{1,3}, Smita S. Sontakke^{1,4}, Aneesha Kajampady^{1,5} and Mohd Suhail Rizvi^{2,6}

¹Department of Mechanical and Aerospace Engineering, Indian Institute of Technology Hyderabad, 502285, Kandi, Sangareddy, India ³ranabir@mae.iith.ac.in; ⁴me21resch11008@iith.ac.in; ⁵me22mtech12001@iith.ac.in

²Department of Biomedical Engineering, Indian Institute of Technology Hyderabad, 502285, Kandi, Sangareddy, India ⁶suhailr@bme.iith.ac.in

The dynamic response of self-propelling microswimmers, e.g. flagellated bacteria, to alterations in the stiffness/softness of confining walls remains ambiguous despite their biophysical significance [1, 2]. Here, we experimentally investigate the effects of increasing softness of the walls of a micro-confinement on the swimming dynamics of self-propelling microswimmers, considering active droplets in microchannels as a synthetic model system. Active droplets spontaneously develop self-sustaining gradients in interfacial surfactant coverage in supramicellar aqueous surfactant solutions, resulting in Marangoni stress driven self-propulsion [3]. We use a combination of double-channel fluorescence microscopy, and micro-PIV analyses to reveal the microswimmer dynamics in soft microchannels. Fascinatingly, in a soft microchannel, the self-propelling droplet microswimmers exhibit a run-and-tumble-like swimming, in contrast to unidirectional, wall-hugging swimming in a rigid microchannel (Fig.1(a)). Specifically, the former dynamics is characterized by frequent sharp reorientations ('tumbles') in the swimming direction, which are preceded and followed respectively by local deceleration and acceleration of the microswimmer (Fig.1(b), (c)). We connect such emergent swimming dynamics in a soft microchannel to the alterations in chemo-hydrodynamics using numerical simulations based on boundary integral method and the experimentally evaluated evolution of the chemical trail ejected by the droplet microswimmers.

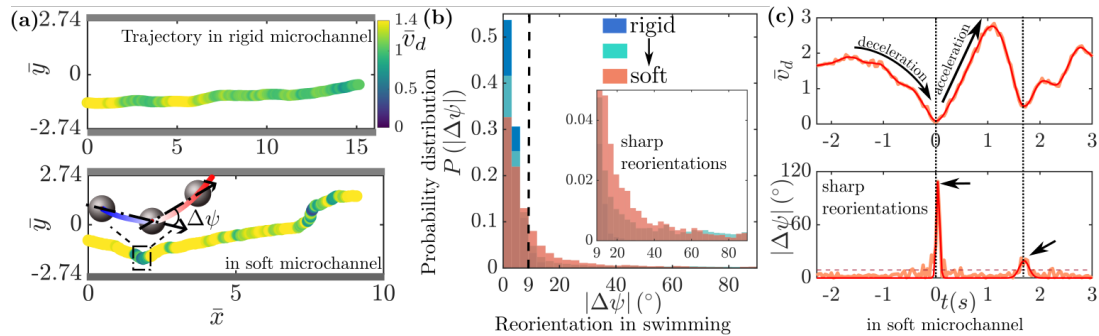


FIG. 1: (a) Trajectories of active droplets in rigid and soft microchannels. (b) Increase in reorientation events with microchannel softness. (c) Correlation between sharp reorientation and variation in local swimming velocity.

-
- [1] F. Song, and D. Ren, Stiffness of cross-linked poly(dimethylsiloxane) affects bacterial adhesion and antibiotic susceptibility of attached cells, *Langmuir* **30**, 10354-10362, (2014).
 [2] Q. Peng *et al.*, Three-dimensional bacterial motions near a surface investigated by digital holographic microscopy: Effect of surface stiffness, *Langmuir* **35**, 12257-12263, (2019).
 [3] S. Michelin, Self-propulsion of chemically active droplets, *Ann. Rev. Fluid Mech.* **55**, 77-101, (2023).

Characterizing Droplet Evolution in Liquid-Liquid Systems: A Quantitative Approach

Lokendra Mohan Sharma¹, Harish N. Dixit¹ and Lakshmana Dora Chandrala^{1,2}

¹*Department of Mechanical & Aerospace Engineering, Indian Institute of Technology Hyderabad, 502284, Telangana, India*

²*lchandrala@mae.iith.ac.in*

We experimentally investigate the ejection of liquid from a nozzle into a quiescent, immiscible fluid. Measuring velocity fields in such liquid-in-liquid systems presents significant challenges due to optical aberrations caused by refractive index gradients. To overcome this, we utilize a refractive index-matched liquid pair, specifically silicon oil injected into a sugar-water mixture. This index matching enables simultaneous measurements of velocity and volume fraction using Particle Image Velocimetry (PIV) and Planar Laser-Induced Fluorescence (PLIF), respectively. As the flow rate increases, we observe a transition from a dripping regime to a jetting regime [1]. At low flow rates, surface tension outweighs inertia, causing the liquid bridge (stem) between the main drop and the nozzle to curve more prominently. This curvature promotes the formation of satellite droplets, as illustrated in fig. 2(a). However, as the inlet velocity increases, the stem exhibits lower curvature, leading to the formation of only a primary drop. Once detached, the droplet propagates vertically under buoyancy. Velocity field analysis (insets in fig. 2 (a) and (b)) reveals a recirculating zone at the droplet tip, with maximum vorticity (not shown here) observed at higher flow rates. Additionally, the wake region expands with increasing ejection velocity. Ongoing work focuses on analyzing velocity patterns within the droplet at different stages of its propagation.

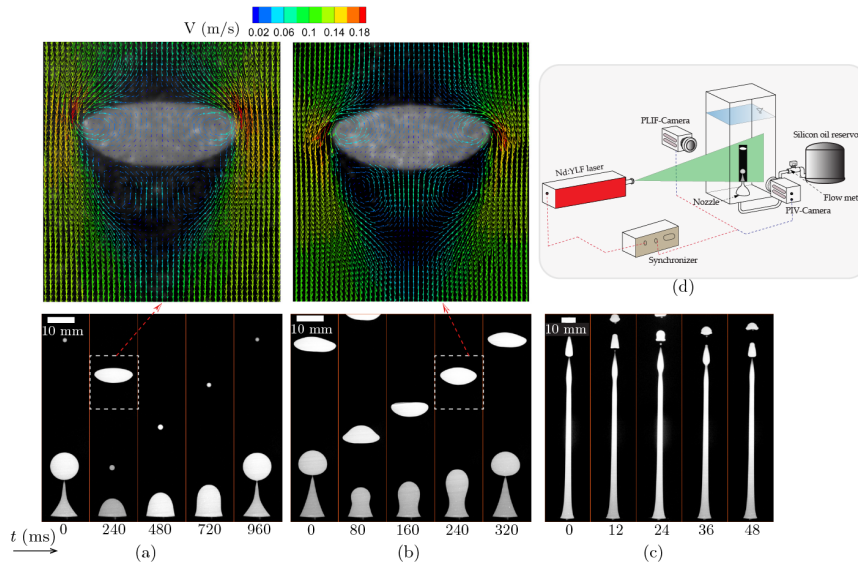


FIG. 2: Dynamics of silicon oil ejected into a sugar-water solution. PLIF images are presented for different Reynolds numbers: (a) $Re = 7$, (b) $Re = 20$, and (c) $Re = 45$. The Reynolds number is defined as $Re = \rho_i U D / \mu_i$, where U is the mean ejection (exit) velocity, D is the nozzle diameter, and ρ_i and μ_i represent the density and viscosity of silicon oil, respectively. The kinematic viscosities of silicon oil and the sugar-water mixture are 10 cSt and 5.6 cSt, while their densities are 960 kg/m^3 and 1150 kg/m^3 , respectively. The nozzle diameter is 10 mm, and the interfacial tension is 0.027 N/m. Insets in (a) and (b) illustrate the velocity field in the frame of reference of the droplet. Subfigure (d) provides an overview of the experimental setup.

[1] A. S. Utada and A. Fernandez-Nieves, H. A. Stone and D. A. Weitz, Dripping to Jetting Transitions in Coflowing Liquid Streams, *Phys. Rev. Lett.* **99**, 094502-4 (2007).

Dynamics of compound polymeric droplet in viscoelastic extensional flow

Malay Vyas^{1,2} and Uddipta Ghosh^{1,3}

¹Department of Mechanical Engineering, Indian Institute of Technology Gandhinagar, 382055, Gujarat, India
²vyas_malay@iitgn.ac.in, ³uddipta.ghosh@iitgn.ac.in

Complex fluid behavior is omnipresent in the processing industry and in bio-medical applications. The intricate phenomena arising due to the interplay between fluid complexity and interfacial effects are hitherto unexplored in detail. To this end, the present work explores the steady-state and transient behavior of compound viscoelastic droplets suspended in another immiscible viscoelastic medium. The Giesekus constitutive equation is used to characterize the viscoelasticity for all three phases, as it captures not only shear-dependent viscosity but also predicts non-zero first and second normal stress coefficients. The initially spherical compound droplet (comprising a spherical inner droplet encased in a spherical shell) is placed in an axisymmetric Stokesian extensional flow and is allowed to deform.

We first utilize an asymptotic framework to solve the problem analytically in small Deborah and Capillary number limits. Using a combination of regular and domain perturbations [1], we achieve asymptotic solutions for steady-state deformation which gives us fundamental insights into the physical interplay between interfacial forces and viscoelastic effects. The primary analytical results are shown in Figure 1(a).

We then use a numerical framework developed on the COMSOL FEA package to probe the transient regime and to go beyond the small Ca and De limits. We are currently in the last stages of validating [2,3] the numerical framework, which utilizes Phase-Field method to capture the interface and a custom PDE solver to account for the viscoelastic stresses. We expect to obtain the results for our parametric space shortly. The representative result for primary transient simulations is shown in Figure 1(b).

The parametric dependence on viscosity ratios, mobility terms, relaxation times, and deformability is being investigated in depth. The preliminary findings show significant non-monotonous behavior and a strong dependence on the properties of the shell, which can inhibit deformation and delay breakup. The complete findings will have implications for several applications like polymer processing, medical and pharmaceutical fields such as targeted drug delivery, etc.

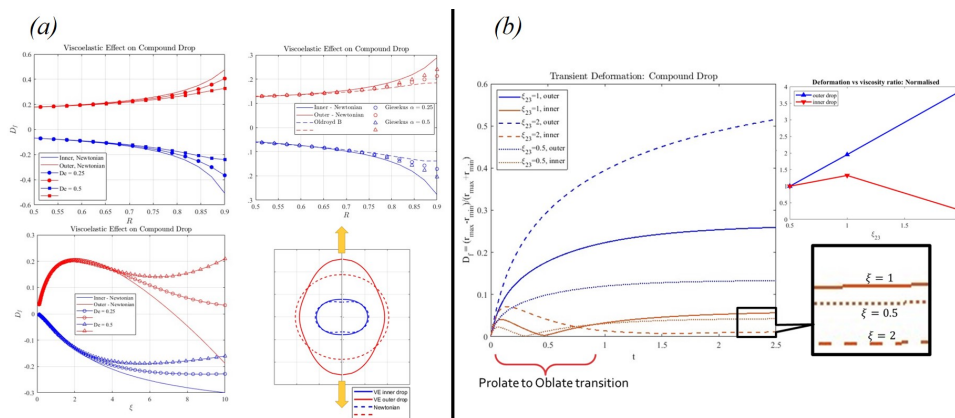


FIG. 1: (a) Analytical steady state results: different parameters, and pictorial representation of the deformed drop (b) Representative numerical transient result: non-monotonous behavior with viscosity ratios

-
- [1] M. Vyas and U. Ghosh, Thermocapillary effects on viscoelastic drops suspended in axisymmetric pressure driven flows, *Phys. Fluids*, **33**, 123103 (2021).
 - [2] R. W. Hooper et al., Transient polymeric drop extension and retraction in uniaxial extensional flows, *J. Non-Newtonian Fluid Mech.*, **98**, 141–168 (2001).
 - [3] T. Chinyoka et al., Two-dimensional study of drop deformation under simple shear for Oldroyd-B liquids, *J. Non-Newtonian Fluid Mech.*, **130**, 45–56 (2005).

Session 12 – Microgravity

Thursday June 12, 9:00–10:15

Study of Binary Water Droplet Coalescence in Microgravity

Mihai Boni^{1,6}, J. Benedikt Schmidt², Ionut R. Andrei¹, Ionut P. Ungureanu¹, Mugurel Balan³, Sebastien-Vincent Bonnieu⁴, Jeanette Hussong², Ilia V. Roisman², Mihail L. Pascu¹ and Stephen Garoff⁵

¹National Institute for Laser, Plasma and Radiation Physics, Magurele, 077125, Ilfov, Romania

⁶*mihai.boni@inflpr.ro*

²Institute for Fluid Mechanics and Aerodynamics, TU Darmstadt, 64287, Darmstadt, Germany

³Romanian InSpace Engineering S.R.L, Magurele, 077125, Ilfov, Romania

⁴European Space Research and Technology Centre, European Space Agency, 2201, AZ Noordwijk, Netherlands

⁵Department of Physics, Carnegie Mellon University, Wean Hall, Pittsburgh, PA, 15213, United States of America

Studying droplet coalescence and mixing in microgravity conditions provides insights into fluid mechanical phenomena that are otherwise masked by the dominance of gravity on Earth [1]. This study investigates the coalescence of two water droplets in a gaseous environment under microgravity conditions aboard the Columbus Module on the International Space Station (ISS). The research is conducted as part of a European Space Agency (ESA) project. In the experiments, droplets are generated at the ends of two needles, which are moved along a common axis to facilitate collision. The droplet diameters and velocities are systematically varied to analyze their impact on coalescence dynamics. High-resolution, high-speed video recordings capture key processes, including droplet deformation, coalescence, and mixing. To visualize mixing, one droplet is marked with Methylene Blue dye. The microgravity level at which the experiments are performed is between $10^{-4}g$ and $10^{-6}g$.

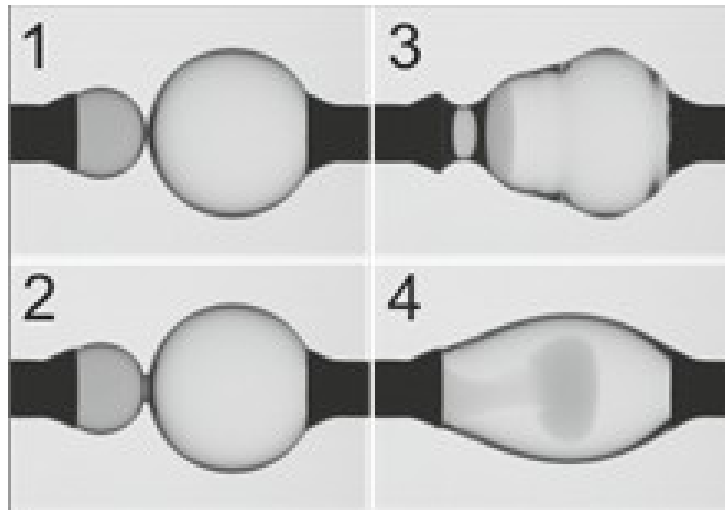


FIG. 1: Asymmetrical case of binary water droplet coalescence in microgravity. 1 Before coalescence; 2. Bridge healing; 3. Capillary wave propagation; 4. Mixing.

A coalescence experiment is presented in Fig. 1, and highlights stages such as bridge formation and healing, capillary wave generation, and mixing dynamics between the droplets. The experiments are designed to systematically assess the effects of symmetrical and asymmetrical droplet diameter combinations, impact velocities, on coalescence and mixing behavior. The velocities were chosen to maintain a small Weber number to minimize the risk of the formation of stray, free-floating droplets inside the interaction chamber. In some cases, the newly formed liquid column is pinched off from the tips of the needles. Depending on the experimental parameters, small or large free-floating droplets are generated. Currently, this observed behavior of the coalescence process is being investigated, with focus on the influence of capillary waves on the individual parts of the process [2].

I. ACKNOWLEDGEMENTS

The authors gratefully acknowledge the European Space Agency for funding the instrument “Drop Coalescence”. This work was supported by a grant of the Deutsches Zentrum für Luft- und Raumfahrt in the framework of project ‘interDropCoal’, project number 50WM2149; the Ministry of Research, Innovation, and Digitization, CNCS - UEFISCDI, project number PN-IV-P7-7.1-PED-2024-1995, within PNCDI IV, and Romanian National Nucleu Program LAPLAS VII, project number 30N/2023.

- [1] McCraney, J. Ludwicki, J. Bostwick, S. Daniel, and P. Steen,” Coalescence-induced droplet spreading: Experiments aboard the International Space Station,” *Physics of Fluids*, vol. **34**, no. 12, 2022
- [2] K. Kirar, S. D. Pokale, K. C. Sahu, B. Ray, and G. Biswas,” Influence of the interaction of capillary waves on the dynamics of two drops falling side-by-side on a liquid pool,” *Physics of Fluids*, vol. **34**, no. 11, 2022.

Controlling the dynamics of a free surface in microgravity via thermocapillary flows

Pablo Salgado Sánchez^{1,2}, Dan Gligor¹, Ignacio Jiménez¹, Úrsula Martínez¹, Jose Miguel Ezquerro¹
and Ana Laverón Simavilla¹

¹*E-USOC, Center for Computational Simulation, E. T. S. de Ingeniería Aeronáutica y del Espacio, Universidad Politécnica de Madrid, 28223, Madrid, Spain* ²*pablo.salgado@upm.es*

Fluid manipulation and control is crucial for space exploration. The “Thermocapillary-based control of a free surface in microgravity” (ThermoSlosh) microgravity experiment [1] proposes the use of thermocapillary flows for controlling the dynamics of a free surface in circular or slightly elliptical cells, half-filled with different silicone oils or a fluorinert; see Fig. 1(left). Here, we conduct a detailed numerical analysis of the associated dynamics when subjected to thermal forcing. The effect on the free surface dynamics of the applied temperature difference ΔT , fluid and contact properties, and ellipticity δ is analyzed. Results strongly suggest that thermocapillary flows can be used to control the interface orientation within the cell. In particular, the steady, thermally-driven position of the interface — perpendicular to applied ΔT — undergoes a pitchfork bifurcation at a critical ellipticity δ_{cr} that breaks the symmetry of the system [2]; see Fig. 1(right). This control can be further improved by using classical PID feedback to adjust the cell boundary temperatures in real-time. The proportional and derivative gains can be selected to optimize the stabilization time and/or energy cost, while the integral contribution is ineffective in reducing the steady-state error [3].

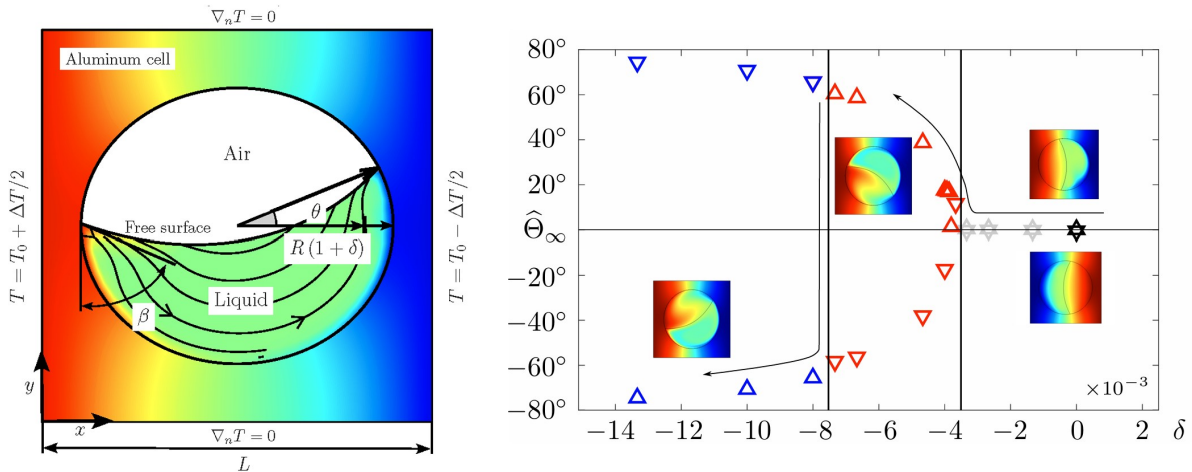


FIG. 1: (left) Sketch of the 2D numerical model. (right) Steady free surface orientation $\hat{\Theta}_\infty$ as a function of the ellipticity δ .

-
- [1] P. Salgado Sánchez, U. Martínez, D. Gligor, I. Torres, J. Plaza and J. M. Ezquerro, The “Thermocapillary based control of a free surface in microgravity” experiment, *Acta Astron.* **205**, 57–67 (2023).
[2] I. Jiménez, P. Salgado Sánchez, D. Gligor, A. Borshchak Kachalov and A. Arshadi, Microgravity control of a free surface in elliptical containers via thermocapillary flows, *Microg. Sci. Technol.* (submitted).
[3] J. Plaza, D. Gligor, P. Salgado Sánchez, J. Rodríguez and K. Olfe, Controlling a free surface with thermocapillary flows and vibrations in microgravity, *Microg. Sci. Technol.* **36**, 13 (2024)

Tomographic Reconstruction of $m = 1$ PAS in a Thermocapillary Liquid Bridge Formed in Space Experiment

Taishi Yano^{1,2} and Yuji Nakanishi¹

¹Department of Mechanical Engineering, Kanagawa University, 221-8686, Yokohama, Japan

²t-yano@kanagawa-u.ac.jp

The particle accumulation structure (PAS) is a unique feature that appears in a liquid bridge associated with oscillatory thermocapillary convection and is attracting much attention from many researchers [1, 2]. When the oscillation mode is the rotating type and conditions, e.g., temperature, shape of the liquid bridge, are set to proper values, particles seeded in a liquid bridge accumulate along specific orbits, resulting in the formation of PAS. A series of space experiments on thermocapillary convection in a liquid bridge, called *Dynamic Surf* project, were conducted aboard the International Space Station from 2013 to 2016 [3]. One of the main objectives of this project was to observe the PAS in a large-scale liquid bridge, and this was achieved, as reported by Sakata et al. [2], who identified the PAS with the azimuthal mode number of $m = 1$. The present study also focuses on this PAS, but in the sense of visualizing its spatial structure through the optical tomographic reconstruction technique [4]. The typical result is shown in Fig. 1. In the present space experiment, the liquid bridge was formed between the aluminum disk at a lower temperature and the transparent sapphire disk at a higher temperature. As shown in Fig. 1(a), three top-view cameras mounted above the sapphire disk observed the spatiotemporal behavior of tracer particles from different perspectives, and the particles can be reconstructed using these images. Figure 1(b) shows the distribution of tracer particles represented by a green, fog-like region, with the dark green line illustrating the orbit. We notice that the tomographic reconstruction technique used here has been customized by the authors to suit flow visualization in a cylindrical system. The spirally ascending PAS with $m = 1$ can be recognized, and by using this result, one can make qualitative and quantitative evaluations of the PAS in a more precise sense, e.g., the degree of accumulation [1]

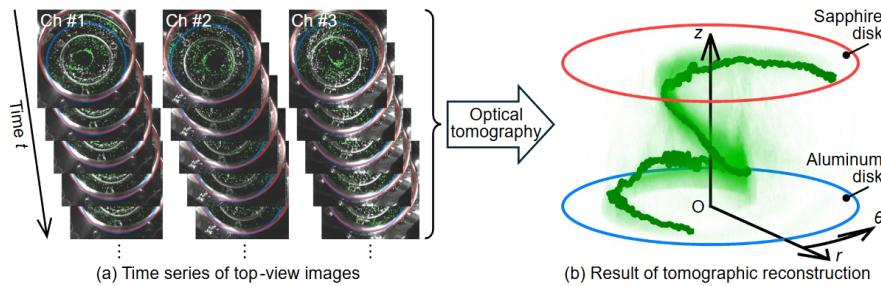


FIG. 1: (a) Top views of PAS observed in the space experiment and (b) its tomographic reconstruction.

-
- [1] H. C. Kuhlmann and F. H. Muldoon, Particle-accumulation structures in periodic free-surface flows: Inertia versus collisions, *Phys. Rev. E* **85**, 046310 (2012).
 - [2] T. Sakata et al., Coherent structures of $m = 1$ by low-Stokes-number particles suspended in a half-zone liquid bridge of high aspect ratio: Microgravity and terrestrial experiments, *Phys. Rev. Fluids* **7**, 014005 (2022).
 - [3] T. Yano et al., Report on microgravity experiments of dynamic surface deformation effects on Marangoni instability in high-Prandtl-number liquid bridges, *Microgravity Sci. Technol.* **30**, 599–610 (2018).
 - [4] G. E. Elsinga et al., Tomographic particle image velocimetry, *Exp. Fluids* **41**, 933–947 (2006).

Interplay between Marangoni effect and buoyancy in absorption process

P.F. Arroiabe^{1,3}, M. Martinez-Agirre², M.M. Bou-Ali¹ and V. Shetsova^{1,2,4}

¹Fluid Mechanics Group, Faculty of Engineering, Mondragon University, Loramendi 4, 20500, Mondragon, Spain, ³, parroaiabe@mondragon.edu

²IKERBASQUE, Basque Foundation for Science, Plaza Euskadi 5, 48009, Bilbao, Spain

⁴x.vshevtsova@mondragon.edu

I. INTRODUCTION

Absorption technology is attracting significant attention due to its potential for sustainable and energy efficient heating and cooling. More broadly, gas absorption by fluids plays a critical role in a wide range of applications, including environmental control, chemical engineering, and space technology. A small perturbation in absorption on the free surface of a fluid causes variations in surface tension, which result from changes in concentration and temperature. These variations create shear stress that drives the fluid along the interface toward regions of higher surface tension, a phenomenon known as Marangoni flow. The use of Marangoni convection to enhance heat and mass transfer at absorbing interfaces has attracted considerable interest, particularly in heat exchanger applications[1]. The absorbing liquid typically has a large interface, with its thickness depending on the specific application. Three processes interact in this context: absorption, Marangoni effects (both solutal and thermal), and buoyancy. The interplay between the Marangoni force and buoyancy can lead to oscillatory regimes. In practice, surfactants are often used to enhance Marangoni convection, altering the balance between Marangoni and buoyancy effects. We suggest a different approach to study this competition, specifically by reducing gravity. To realistically simulate gravity variations, we consider levels corresponding to Earth, Mars, the Moon, and the Space Station (microgravity).

II. PROBLEM FORMULATION

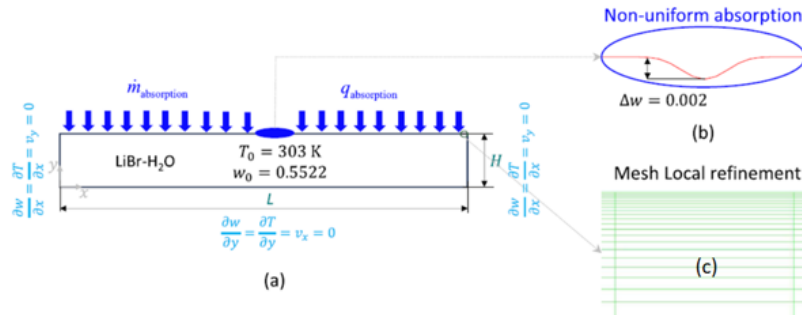


FIG. 1: (a) Geometry of the problem and boundary conditions of the model $L = 75$ mm, $h = 10$ mm; (b) Local perturbation of mass fraction; (c) Mesh refinement near the interface.

The $LiBr - H_2O$ mixture is confined in a cavity of length L and height H , as shown in Fig.1a. This study examines convective instability in a $LiBr$ -water binary mixture that absorbs water vapor. During the process, the water is absorbed from the gaseous medium in contact with the solution, while $LiBr$ neither consumed nor added to the solution. Thus, the phase boundary remains impermeable to $LiBr$, displaced by the entry of the absorbate into the solution. During entire absorption process, the temperature and concentration at the interface are continuously related by equilibrium conditions[2].

$$T_e = A_1 + A_2 w_e \quad (6)$$

Here T is the temperature, w is the mass fraction, A_1 and A_2 are the coefficients depending on the mixture and the subscript e means equilibrium. The absorption problem is described by the Navier–Stokes, heat, and mass transfer equations which can be found in our recent publication[3][4][5], here we indicate that first ten seconds we leave for uniform absorption and then introduce a perturbation. To do this, the mass fraction distribution within the localized perturbed region is modelled as a cosine function.

III. RESULTS

This study investigates the dynamics of absorption under varying gravitational conditions: Earth, Mars, Lunar, and Microgravity. The Marangoni and buoyant (in the presence of gravity) flows were initiated by small perturbations in the composition at the center of the cell. The development of the flow and its propagation from the center to the side walls occurred more rapidly with decreasing gravity.

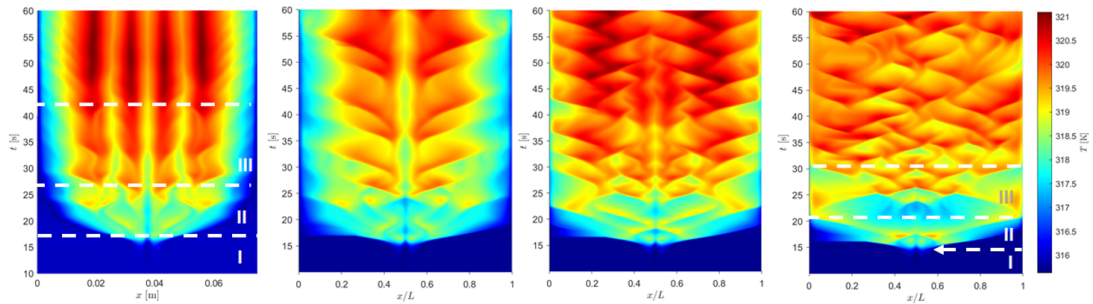


FIG. 2: The time–space map presenting the evolution of the mass fraction at the interface at Earth, Mars, Moon and zero gravity during 60 s. The white dashed lines in the case of Earth and zero gravity indicate the intermediate regimes that have recently been studied in detail[3][4].

In the presence of gravity, the coupling between solutal, thermal, and buoyant convection exhibited both competing and cooperative effects, most visibly manifesting in the space–time maps of mass fraction. These maps revealed how gravitational forces influence flow patterns, showing well-defined, periodic behavior in Earth gravity. As gravity decreased, the patterns became increasingly complex and less regular. The strength of the periodicity in the flow patterns is highly gravity-dependent. Earth gravity displayed the most regular periodic behavior, while Lunar gravity showed near-periodic oscillations, and Martian gravity exhibited quasi-periodic behavior which is still questionable. In micro-gravity, the absence of buoyancy forces led to irregular patterns with no clear periodicity.

-
- [1] H. Daiguji, E. Hihara, and T. Saito, “Mechanism of absorption enhancement by surfactant,” *Int. J. Heat Mass Transfer* **40**, 1743–1752 (1997).
 - [2] N. Grigoreva and V. Nakoryakov, “Exact solution of combined heat- and mass transfer problem during film absorptions,” *J. Eng. Phys.* **33**, 1349–1353 (1997).
 - [3] P. F. Arroiabe, M. Martinez-Agirre, A. Nepomnyashchy, M. M. Bou-Ali, and V. Shevtsova, “The effect of small perturbation on dynamics of absorptive LiBr–water solution,” *Phys. Fluids* **36**, 022119 (2024).
 - [4] P. Arroiabe, M. Martinez-Agirre, and M. M. Bou-Ali, “Numerical analysis of different mass transfer models for falling film absorbers,” *Int. J. Heat Mass Transfer* **182**, 121892 (2022)
 - [5] P.F. Arroiabe, M. Martinez-Agirre, M.M. Bou-Ali, V. Shevtsova, Influence of gravity on dynamics of absorbing binary mixture, *Acta Astronautica*, **229**, 270-276 (2025)

Sloshing reduction in microgravity using thermocapillary flows and passive baffles

Pablo Salgado Sánchez^{1,2}, Dan Gligor¹, Carlos Peromingo¹, Álvaro Bello¹, Karl Olfe¹ and Victoria Lapuerta¹

¹E-USOC, Center for Computational Simulation, E. T. S. de Ingeniería Aeronáutica y del Espacio, Universidad Politécnica de Madrid, 28223, Madrid, Spain ²pablo.salgado@upm.es

Numerical simulations are used to analyze the potential of thermocapillary flows for sloshing reduction in microgravity. The dynamics of a free surface, excited by thermal modulations at the lateral boundaries, are analyzed first [1] and characterized by the displacement of the contact points [2]; see Fig. 1(left). A frequency sweep is used to obtain a Bode-type diagram that reveals a resonance peak in the vicinity of the first sloshing mode. The ability of thermocapillary flows to excite this sloshing mode suggests a control strategy that uses thermal modulations to dampen sloshing motion. A classical PID controller is implemented, which produces an output signal ΔT that is applied anti-symmetrically at the lateral walls of the container. Its performance is characterized via the functional $\mathcal{P} = (1 - \lambda)\tau + \lambda\kappa$, which allows for a trade-off (by varying $\lambda \in [0, 1]$) between the damping of sloshing, measured via decay time τ , and the cost of implementing the control κ . We minimize \mathcal{P} and determine the associated Pareto front; see Fig. 1(right). Results show that thermocapillary controllers are generally able to reduce τ by a 50% factor, with reasonable cost and $\Delta\tau$. A novel strategy combining thermocapillary control and passive baffles is further assessed, where baffles play a key role and significantly alleviate the thermal requirements associated with the control; see the lower curve of the right panel. Finally, the aforementioned strategies are tested against a reboosting maneuver of the ISS, showing their potential for sloshing reduction in microgravity.

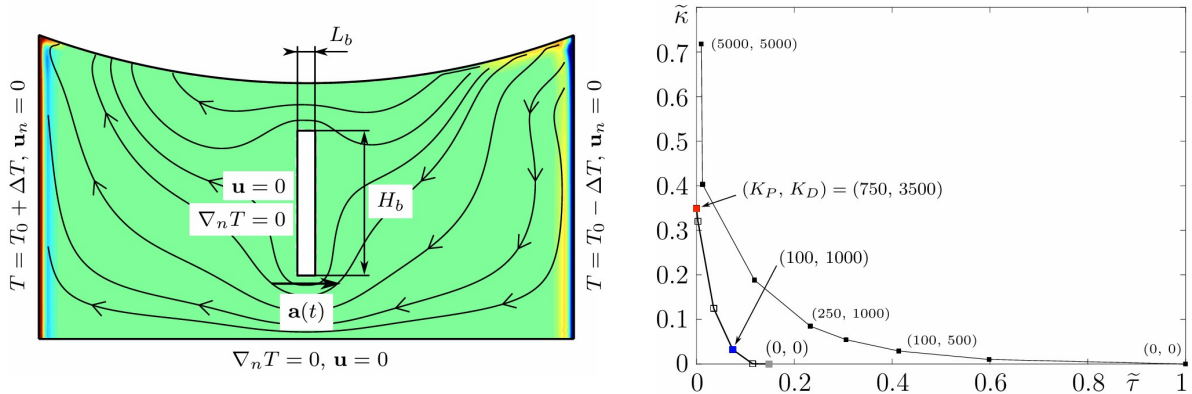


FIG. 1: (left) Sketch of the 2D numerical model including a centered vertical baffle.(right) Pareto front of the thermocapillary-based controller with (lower curve) and without (upper curve) baffle.

-
- [1] D.Gligor, P. Salgado Sánchez, J. Porter and J. M. Ezquerro, Thermocapillary-driven dynamics of a free surface in microgravity: control of sloshing, *Phys. Fluids* **34**, 072109 (2022).
 - [2] D. Gligor, P. Salgado Sánchez, J. Porter and I. Tinao, Thermocapillary-driven dynamics of a free surface in microgravity: response to steady and oscillatory thermal excitation, *Phys. Fluids* **34**, 042116 (2022).
 - [3] C. Peromingo, D. Gligor, P. Salgado Sánchez, A. Bello and K. Olfe, Sloshing reduction in microgravity: Thermocapillary-based control and passive baffles, *Phys. Fluids* **35**, 102114 (2023).

Session 13 – Solid-liquid phase change II

Thursday June 12, 10:45–11:30

Accelerating the melting of PCMs via convective flows and optimal container design

Andriy Borshchak Kachalov¹, Pablo Salgado Sánchez¹, Jeff Porter^{1,2}, Ali Arshadi¹ and Karl Olfe¹

¹*E-USOC, Center for Computational Simulation, E. T. S. de Ingeniería Aeronáutica y del Espacio, Universidad Politécnica de Madrid, 28040, Madrid, Spain* ²*jeff.porter@upm.es*

Various strategies for enhancing the melting rate of phase change materials (PCMs) are analyzed numerically. First, we investigate melting dynamics in trapezoidal and triangular containers that incorporate a free surface supporting thermocapillary flow [1]; see Fig. 1(left). The analysis is then extended to consider the additional effects of natural convection and variations in container geometry motivated by the natural shape of the advancing solid/liquid front [3]; see Fig. 1(right). This final analysis evaluates melting dynamics for both individual and combined enhancement strategies. The efficacy of each strategy is quantified using the associated melting time τ , which is compared to τ_0 for the reference case: a rectangular PCM domain with heat transferred purely by conduction [3]. The inverse ratio $\mathcal{G} = \tau_0/\tau$ defines the enhancement factor. Comparisons are made for small and large values of the applied thermal forcing and for different (aspect) ratios between the vertical and horizontal lengthscales of the PCM domain.

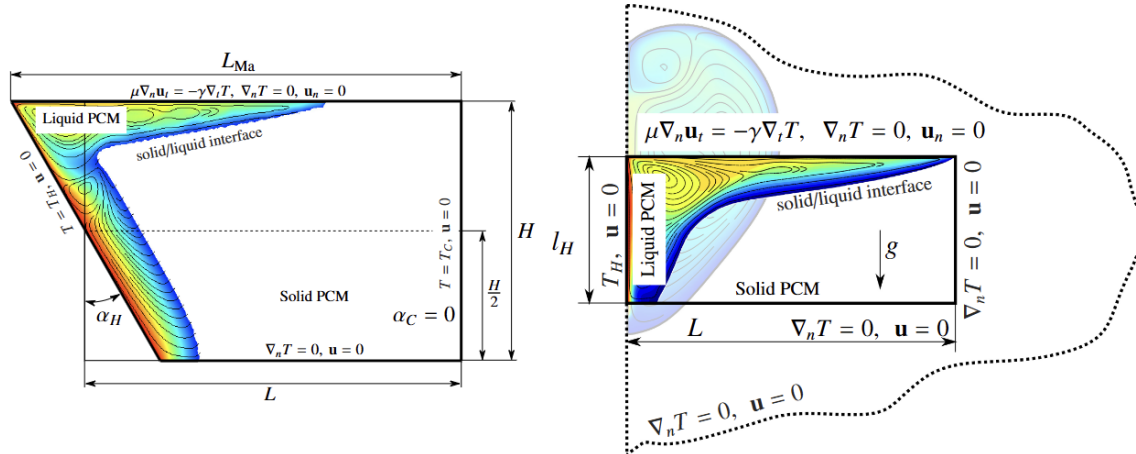


FIG. 1: Sketches of the setups used in numerical models: (left) trapezoidal container, (right) rectangular and optimal containers. This optimal container is suggested by the natural shape of the advancing solid/liquid front in a semi-infinite domain.

-
- [1] A. Borshchak Kachalov, P. Salgado Sánchez, U. Martínez, J. Fernández and J. M. Ezquerro, Optimization of thermocapillary-driven melting in trapezoidal and triangular geometry in microgravity, *Int. J. Heat Mass Transf.* **185**, 122427 (2022).
 - [2] A. Borshchak Kachalov, P. Salgado Sánchez, J. Fernández and K. Olfe, Enhancing the melting of phase change materials via convective flows and container geometry, *Int. Comm. Heat Mass Transf.* **158**, 107922 (2024).
 - [3] P. Salgado Sánchez, J. M. Ezquerro, J. Fernández and J. Rodríguez, Thermocapillary effects during the melting of phase change materials in microgravity: Heat transport enhancement, *Int. J. Heat Mass Transf.* **163**, 120478 (2020).

On the Gravity and Orientation Driven Thermal Convection Dynamics During the Melting of Phase Change Material

Keyur Kansara¹, Shobhana Singh^{1,2}, Navin Kumar Dwivedi³ and Maxim L. Khodachenko⁴

¹Dept. of Mechanical Engineering, Indian Institute of Technology Jodhpur, 342030 Jodhpur, India

²Center of Emerging Technologies for Sustainable Development, Indian Institute of Technology Jodhpur, 342030 Jodhpur, India

³HUN-REN Institute of Earth Physics and Space Science, 9400 Sopron, Csatkai E.-6-8, Hungary

⁴Space Research Institute, Austrian Academy of Sciences, 8042 Graz, Austria

Phase Change Materials (PCMs) have gained significant attention for their potential in effective thermal management of space systems. PCM based heat accumulators are widely used in electronic payloads in Spacecraft, Orbiters, and Landers, for the temperature control ensuring reliable operation under stringent environmental conditions. In this study, we investigate the effect of variable gravity and its relative orientation with the global temperature gradient on the performance of the PCM-based heat accumulator. The results reveal the effect of orientation ($\alpha \in [0^\circ, 180^\circ]$) on the flow dynamics of melted PCM and therefore, on the prevailing mode of thermal convection. For $\alpha = 0^\circ$, the flow dynamics are governed by thermal plumes and chaotic fluid motion, which evolves to the formation of a single, clockwise-rotating large-scale circulation due to shear effects at higher orientation, (*i.e.*, $\alpha > 0^\circ$). A strong dependence of heat transfer on orientation is shown in Fig. 1, where the Nusselt number increases with α due to enhanced convective heat transfer and reaches its highest at $\alpha = 60^\circ$. At higher angles $\alpha > 90^\circ$, the convection is suppressed by conduction, leading to decreased Nusselt number and inefficient melting. The reduction in gravity creates a destabilizing effect on the evolution of the flow structures and reduces the melting rate of PCM significantly. For instance, the slower melting rate under low gravity ‘0.1g’ requires approximately three times the duration 3000 s to achieve 75% of PCM melting, which is attained in just 1000 s under standard gravity (‘g’). These insights are crucial in ensuring maximum heat accumulation and efficient phase transition in PCM-based applications.

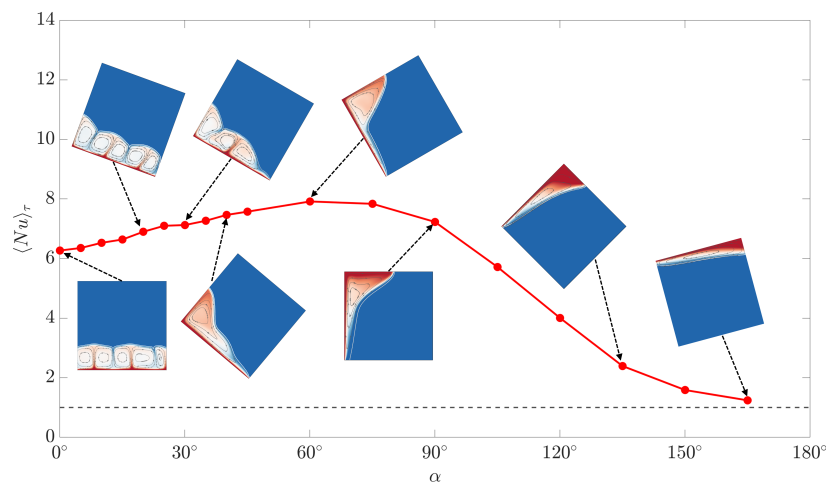


FIG. 1: Volume-time-averaged Nusselt number $\langle Nu \rangle_\tau$ as a function of the orientation angle (α). Inset contour plots show temperature (Θ) superimposed with velocity streamlines at $\tau = 0.066(300 \text{ s})$, illustrating the convection evolution phase under the standard gravity.

Innovative Dual-Thermocapillary-Enhanced-PCM Strategy for Energy Storage in Space Applications

Keyur Kansara¹, Pablo Salgado Sánchez², Shobhana Singh^{1,3} and Andriy Borshchak Kachalov²

¹Dept. of Mechanical Engineering, Indian Institute of Technology Jodhpur, 342030 Jodhpur, India

²E-USOC, Center for Computational Simulation, Universidad Politécnica de Madrid, 28223, Madrid, Spain

³Center of Emerging Technologies for Sustainable Development, Indian Institute of Technology Jodhpur, 342030 Jodhpur, India

Recent research has shown the potential of thermocapillary convection for enhancing heat transfer within PCMs, making it a promising alternative to improve their performance as thermal control devices in space applications [1]. In this work, a novel dual-PCM approach is proposed that combines a primary, thermocapillary-enhanced PCM, with a secondary, highly conductive PCM. The underlying idea is that the secondary PCM substitutes the primary one over portions of the domain where thermocapillary convection is less effective. We explore the rectangular containers filled with n-Octadecane and gallium in trapezoidal and triangular partitions, respectively; see Fig. 1 (left). A detailed assessment of the improvement achieved in the overall heat transfer rate and energy storage capacity is provided. Compared to rectangular containers holding solely n-Octadecane [2], melting times are reduced up to 88% and 71% for short and large containers. Further, the total energy storage capacity exhibits up to a 44% increase [3]]. These results demonstrate that the proposed dual-thermocapillary-enhanced-PCM approach presents a promising alternative for space missions as well as terrestrial applications.

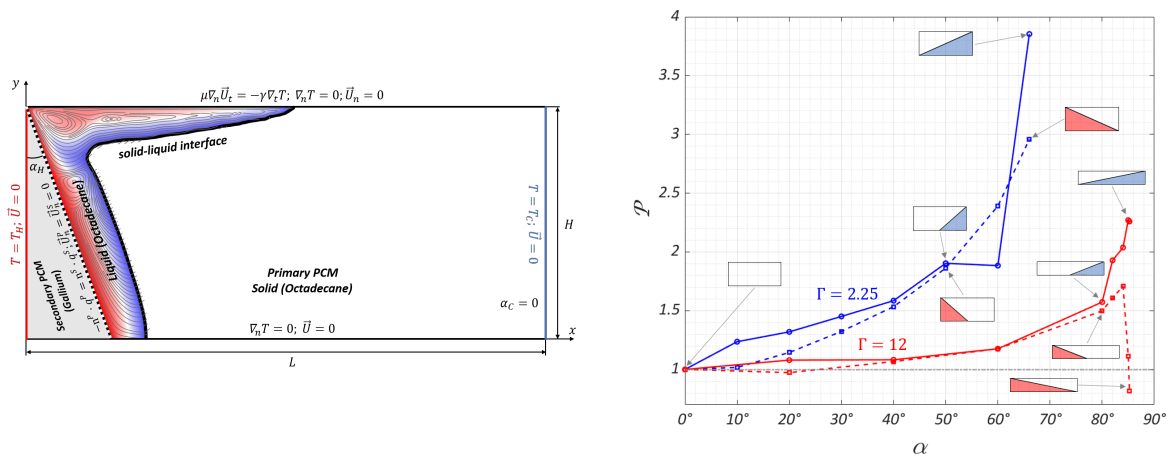


FIG. 1: (left) Sketch of the dual-thermocapillary-enhanced PCM approach. (right) Storage enhancement (\mathcal{P}) as a function of the dual-PCM geometry for small (blue) and large (red) containers.

-
- [1] J. Porter et al., The ‘Effect of Marangoni Convection on Heat Transfer in Phase Change Materials’ experiment, *Acta Astron.* **210**, 212–223 (2023).
- [2] P. Salgado Sánchez, J. M. Ezquerro, J. Fernández and J. Rodríguez, Thermocapillary effects during the melting of phase change materials in microgravity: Heat transport enhancement, *Int. J. Heat Mass Transf.* **163**, 120478 (2020).
- [3] K. Kansara, P. Salgado Sánchez, S. Singh and A. Borshchak Kachalov, Innovative Dual-PCM approach for energy storage enhancement during thermocapillary-driven PCM melting in microgravity, *Int. J. Heat Mass Transf.*, under review.

Session 14 – Surfactants and drops II

Thursday June 12, 11:30–12:00

Analytical study of hydrodynamic flows: heat and mass transfer in a sessile hemispherical evaporating droplet

Peter Lebedev-Stepanov¹

¹*Shubnikov Institute of Crystallography, Kurchatov Complex of Crystallography and Photonics, Leninskiy Prospekt, 59, 119333, Moscow, Russia* lebstep.p@crys.ras.ru

As many studies show, convective instability in a small evaporating sessile droplet is a complex and multifactorial phenomenon, the description of which is not reduced to simply calculating the Marangoni number and comparing it with some critical value [1]. The development of analytical approaches makes it possible to clarify the theoretical description of these processes by appealing to "first principles".

We used an alternative form of the general solution of the linearized stationary axisymmetric Navier-Stokes equations for an incompressible fluid in spherical coordinates [2] to describe heat and mass transfer in a sessile evaporating droplet ($Re \ll 1$, $Pe \ll 1$). An analytical calculation of the temperature profile for a hemispherical water drop corresponding to a constant substrate temperature is carried out [Fig. 1 a-b]. It has been established that the temperature difference does not depend on the droplet size. The temperature profile that presented here corresponds to a relative humidity of 50%). Analytical calculation of the radial flow [3] that is responsible for the coffee ring effect [Fig.1 c], and the Marangoni flows corresponding to a given evaporation rate and heat-absorbing properties of the substrate [Fig.1.d] are carried out.

Also, solutal Marangoni convection in a small hemispherical drop of binary solvent was investigated. Evaporation was assumed to be slow enough for the quasi-stationary approximation to be valid. The smallness of the Peclet number was also accepted, which corresponds to relatively small velocity of convective flow in relation to the velocity of diffusion transfer of the impurity. In this case, the Marangoni number can have a value in the range from 1 to several tens. The model was tested on water-ethanol and ethanol-hydrogen peroxide systems. The streamlines of convective flows were visualized, and the conditions for their occurrence were considered [4].

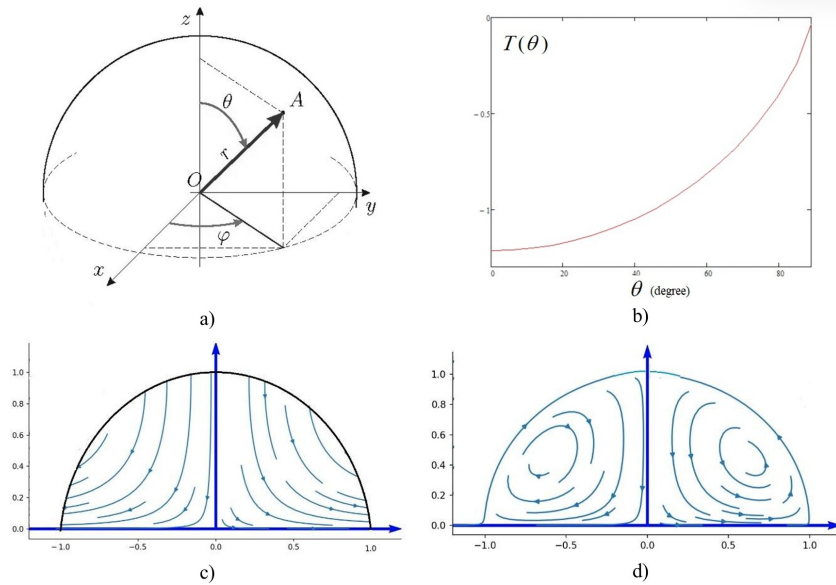


FIG. 1: See description in text

[1] A.M.J. Edwards et al. Phys. Rev. Lett. 121 (2018), 184501.

- [2] P. Lebedev-Stepanov. Appendix in: ArXiv:2411.15853 [physics.flu-dyn].
- [3] R.D. Deegan et al. *Nature* 389, 1997, pp. 827–831.
- [4] P. Lebedev-Stepanov. *Colloid Journal*. 2025 (4), in print.

Thermosolutal instabilities in a moderately dense nanoparticle suspension: Effect of thermal conductivity stratification

Alexander Oron,¹ Alexander Nepomnyashchy,^{2,3} and Raj Gandhi^{2,4}

¹Department of Mechanical Engineering, Technion-Israel Institute of Technology, 3200003, Haifa, Israel
meroron@technion.ac.il

²Department of Mathematics, Technion- Israel Institute of Technology, 3200003, Haifa, Israel

³nepom@technion.ac.il, ⁴raj.gandhi@campus.technion.ac.il

Nanofluids are colloidal dispersions made of nanoparticles of diameter 1-100 nm in a base liquid. Nanoparticle suspension with moderately dense concentration naturally exhibits the dependence of all thermophysical properties on the local particle concentration. In fact, in heat transfer applications they are purposefully employed to enhance the thermal conductivity of the carrier liquid. We investigate the thermocapillary instability in a layer of nanofluid heated at the substrate and exposed to the gas phase at its interface when the thermal conductivity of the layer varies linearly with the volume concentration of nanoparticles with the factor a and in the presence of the Soret effect. The left panel of Figure 1 displays the threshold values of the monotonic and oscillatory thermocapillary instability. We note that the nanofluid with a relatively small a displays monotonic thermocapillary instability. However, an oscillatory thermocapillary instability emerges for higher values of the parameter a . We infer that the onset of oscillatory instability takes place due to the disparity of the diffusional timescale of the nanoparticle concentration and that of thermal diffusion measured by the Lewis number L . Interestingly enough, we observe that the critical value of the parameter $a = a_c$ where the instability switches from one kind to another varies with the Lewis number as $a_c \sim L^2$, as shown in the right panel of Figure 1. Hence, suspensions with a fast concentration diffusion require larger values of a to exhibit the oscillatory thermocapillary instability.

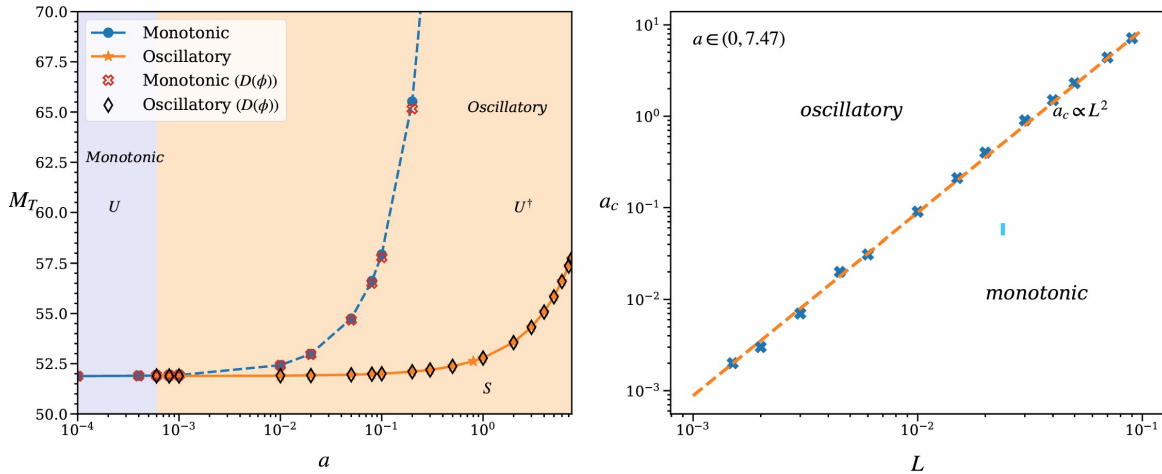


FIG. 1: Left panel: Variation of the critical thermal Marangoni number M_T with the thermal conductivity stratification parameter a for $L = 10^{-3}$. The symbols U , U^\dagger , and S denote the domains with one real positive eigenvalue, with two leading complex conjugate eigenvalues with a positive real part, and that of stability, respectively; Right panel: Variation of the critical thermal conductivity stratification parameter a_c with the Lewis number L in the case of heating at the substrate for a certain parameter set. The dashed line represents the data fit $a_c \propto L^2$ with the factor of 8.80×10^2 .

This work is supported by the grant from the European Union's Horizon 2020 research and innovation program under the Marie Skłodowska-Curie Grant # 955612(NanoPaInt).

Index of Authors

- A. Kerem Uğuz 36
Abdallah Daddi-Moussa-Ider 19
Abhay Ghuge 76
Adam Chafai 10
Adrie Bruneton 30
Aleksandr Bashkatov 63
Alexander A. Mikishev 35
Alexander Babich 63
Alexander Nepomnyashchy 21,24,35,106
Alexander Oron 24,106
Alexandra J. Hardy 19
Alexey Rednikov 10
Ali Arshadi 100, 44
Álvaro Bello 44, 98
Amir H. Hirsa 22
Ana Laverón Simavilla 94
Andriy Borshchak Kachalov 41,44,100,102
Aneesha Kajampady 87
Antonio Roberto Piriz 28, 73
Anubhab Roy 25
Anubhav Dubey 29
Arnaud Erriguible 13
Avionoam Nir 68
B. Dinesh 39
Benoît Mathieu 30
Bruno Cochelin 86
C. Huete 77
C. Matsuoka 77
C. Ruyer-Quil 78
Carlos Martinez Martínez 79
Carlos Peromingo 98
Chaima Nasri 74
Christian Ruyer-Quil 52
Christophe Oguey 74
Constantin Habes 29
Dan Gligor 45, 94, 98
Daniel Gomez-Lendinez 79, 81
Daniela Placha 16
Deewakar Sharma 13,17
Demetrios T. Papageorgiou 66
Dominika Zabiega 16, 76
Elie Saikali 30
Linda J. Cummings 47
Lokendra Mohan Sharma 88
Lou Kondic 47
Lu Qiu 57
Luca Biancofiore 52
M. Martinez-Agirre 96
M. Napieralsk 77
M.M. Bou-Ali 96
M.Á. Cabrerizo Vílchez 75
Mahesh Pachagnula 25
Malay Vyas 89
Marc Medale 86
Marcos Levi Cazaes 16
Matthieu Rykner 30
Maxim L. Khodachenko 101
Mengsen Zhang 57
Michael Bestehorn 17,34,38
Michael D. Mayer 66
Mihai Boni 92
Mihail L. Pascu 92
Milad Eftekhari 63
Mohd Suhail Rizvi 87
Mugurel Balan 92
N. A. Tahir 28,73
Navin Kumar Dwivedi 101
Niall Oswald 66
Nikhil Yewale 54
Ninad V. Mhatre 84
Ofer Manor 33,37
Olga Lavrenteva 68
Omair A. A. Mohamed 52
Pablo Salgado Sánchez 41,44, 94,98,100,102
Paolo Luzzatto-Fegiz 67
Peru F. Arroiabe 96
Peter Lebedev-Stepanov 104
Phillipe Beltrame 51
Pierre Colinet 10
Prabhash Kumar 25
Prahallada Jutur 25
Rafael Barea 81
Rafael Tadmor 26
Raj Gandhi 24, 106
Ranabir Dey 87

Index of Authors

- Elsen Tjhung 19
Fabio Dias de Sousa 16
Fei Duan 7
Fernando Temprano-Coleto 23
Fikret Alic 42
Florian Cajo 51
Florian Voss 85
Florine Giraud 73
Fouzan Ameer 76
Francisco Cobos 77
Franz-Theo Schön 38
Gabriel Meletti 48
Georg Dietze 30, 39
Gerd Mutschke 63
Gideon Onuh 33
Greg Paris 49
Guillermo Lorite Méndez 75
Harish N. Dixit 88
Hector Valdez 58
Holger Marschall 29
Howard A. Stone 23
Ichiro Ueno 59,70
Igin B. Ignatius 39, 78
Ignacio Jiménez 94
Ignacio Tinao 45
Ilia V. Roisman 92
Ion Dan Borcia 34, 38
Ionut P. Ungureanu 92
Ionut R. Andrei 92
Isabelle Raspo 48
J. Benedikt Schmidt 92
Jacobo Rodríguez 41
Jason Yalim 22
Javier Read de Alaniz 67
Jean Cousin 58
Jean-Pierre Delville 8
Jeanette Hussong 92
Jeff Porter 41, 100
Jesus Garcia-Moreno Caraballo 81
Jinan P 37
Joe A. Adam 22
Jorge César Brändle de Motta 58
Jose Fernández 45
Ranga Narayanan 39
Ratul Dasgupta 54
Robin Maximilian Behle 10
Rodica Borcia 17, 34,38
Rodrigo Rodriguez Larios 81
Roiy Sayag 26
Roni Kroll 18
Ryan H. Allaire 47
Sakir Amiroudine 13,17,29
Samantha A. McBride 49
Samuel Cameron 19
Satish Kumar 84
Schon Fusco 75
Sebastien-Vincent Bonnieu 92
Senthil Kumar Parimalanathan 10
Seymen İlke Kaykanat 36
Shin Noguchi 59,70
Sho Shidomi 70
Shobhana Singh 102, 101
Smita S. Sontakke 87
Sofía Piriz 28, 73
Stefan Karpitschka 9
Stephen Garoff 92
Steven McDonald 19
Stéphane Abide 48
Stéphane Viazzo 48
Sudeepti Aremanda 33
T. Sano 77
Taishi Yano 95
Tatiana Gambaryan-Roisman 10
Tatyana Lyubimova 21
Tyler J. Mucci 22
Uddipta Ghosh 89
Ulysse Delabre 8
Úrsula Martínez 44, 45,94,
Uwe Harlander 38, 48
Uwe Thiele 85
Vadim Nikolayev 30
Valentina Shetsova 96
Victor Multanen 26
Victoria Lapuerta 98
Vinod Kadari 54
Xichen Liang 67
Xuegeng Yang 63

Index of Authors

Jose Miguel Ezquerro 41,44,45,94
Juan M. Lopez 22
Karl Olfe 98, 100
Kerstin Eckert 63
Keyur Kansara 101,102
Kripa K. Varanasi 49
Kseniia M. Karnaukh 67
Lakshmana Dora Chandrala 88

Yangying Zhu 67
Yao Xiao 61
Yifan Li 33
Yoav Tsori 18
Yotam Stern 26
Yuji Nakanish 95
Ze Xu 9
Zhong Zeng 61